

# **Neutron Reflector Reflooding Confirmatory Test**

**Non-Proprietary Version**

**August 2008**

**© 2008 Mitsubishi Heavy Industries, Ltd.  
All Rights Reserved**

**Revision History**

Revision	Page	Description
0	All	Original issue

© 2008

**MITSUBISHI HEAVY INDUSTRIES, LTD.**

All Rights Reserved

This document has been prepared by Mitsubishi Heavy Industries, Ltd. (“MHI”) in connection with the U.S. Nuclear Regulatory Commission’s (“NRC”) licensing review of MHI’s US-APWR nuclear power plant design. No right to disclose, use or copy any of the information in this document, other than by the NRC and its contractors in support of the licensing review of the US-APWR, is authorized without the express written permission of MHI.

This document contains technology information and intellectual property relating to the US-APWR and it is delivered to the NRC on the express condition that it not be disclosed, copied or reproduced in whole or in part, or used for the benefit of anyone other than MHI without the express written permission of MHI, except as set forth in the previous paragraph.

This document is protected by the laws of Japan, U.S. copyright law, international treaties and conventions, and the applicable laws of any country where it is being used.

Mitsubishi Heavy Industries, Ltd.  
16-5, Konan 2-chome, Minato-ku  
Tokyo 108-8215 Japan

## **Abstract**

In order to confirm the applicability of the WCOBRA/TRAC(M1.0) code to the thermal-hydraulic analysis of the US-APWR neutron reflector during the LBLOCA reflooding phase, a series of reflooding tests and the confirmatory analyses using WCOBRA/TRAC(M1.0) were performed and their results have been evaluated. The tests were performed using the test section of the same length, hydraulic diameter, heat capacity, and material as those of the US-APWR neutron reflector. The key parameters measured in the tests include: the outlet flow rates of the steam and water; and the temperatures of the coolant and structure at different axial locations along the test section. The test conditions were determined from the results of the thermal-hydraulic analysis of the US-APWR neutron reflector by using WCOBRA/TRAC(M1.0). For each test condition, the thermal-hydraulic analysis was performed using WCOBRA/TRAC (M1.0) and the key parameters predicted by the code were compared with the measured test data. [

], it has been confirmed that the WCOBRA/TRAC(M1.0) code can be applied to the analysis of the thermal-hydraulic behavior in the neutron reflector of the US-APWR during the reflooding phase in the LBLOCA scenario.





## **List of Tables**

Table 3-1	Configurations of Test Section and NR for US-APWR.....	3-7
Table 5-1	Test Conditions .....	5-2
Table 7-1	Conditions Used in Confirmatory Analyses Using WCOBRA/TRAC(M1.0) .....	7-10
Table 7-2	Uncertainty in Released Metal Energy Predicted by WCOBRA/TRAC(M1.0) .....	7-11
Table A-1	Calibration and Confirmation of Soundness of Measurement System Throughout Test Period .....	A-4
Table A-2	Calibration Results.....	A-5
Table B-1	Uncertainties of Measurement Systems .....	B-6
Table C-1	Channel Descriptions for US-APWR Vessel Model .....	C-8
Table C-2	Gap Connections for US-APWR Vessel Model .....	C-11
Table C-3	Conditions for Sensitivity Analysis .....	C-13
Table C-4	PCTs Calculated by WCOBRA/TRAC(M1.0) for Sensitivity Analysis (DECLG).....	C-14
Table C-5	PCTs Calculated by WCOBRA/TRAC(M1.0) for Sensitivity Analysis (SPLIT) .....	C-14
Table C-6	Summary of Conditions for NR Reflooding Test .....	C-15











**List of Figures (Continued)**

Figure C-4	US-APWR Vessel Sections 3 to 4 (Horizontal View) .....	C-19
Figure C-5	US-APWR Vessel Sections 5 to 6 (Horizontal View) .....	C-20
Figure C-6	US-APWR Vessel Sections 7 to 8 (Horizontal View) .....	C-21
Figure C-7	US-APWR Vessel Sections 9 to 10 (Horizontal View) .....	C-22
Figure C-8	US-APWR WCOBRA/TRAC(M1.0) Model Vessel/Loop Layout .....	C-23
Figure C-9	Power Shape for Sensitivity Analysis.....	C-24
Figure C-10	Reflood PCT versus Equivalent Break Size .....	C-25
Figure C-11	Peak Cladding Temperature of Hot Rod (DECLG) .....	C-26
Figure C-12	Peak Cladding Temperature of Hot Rod (SPLIT).....	C-26
Figure C-13	Hot Assembly and NR Liquid Level (Cd*Abreak/ACL=2.4 DECLG) .....	C-27
Figure C-14	Downcomer Liquid Level (Cd*Abreak/ACL=2.4 DECLG) .....	C-27
Figure C-15	Integral of Vapor Mass Flow Rate at Core and NR Outlet (Cd*Abreak/ACL=2.4 DECLG).....	C-28
Figure C-16	Integral of Entrainment and Liquid Mass Flow Rate at Core and NR Outlet (Cd*Abreak/ACL=2.4 DECLG).....	C-28
Figure C-17	Integral of Velocity at Inlet of NR .....	C-29
Figure C-18	NR Wall Temperature.....	C-30
Figure C-19	Lower Plenum Water Temperature (DECLG) .....	C-31
Figure C-20	Lower Plenum Water Temperature (SPLIT).....	C-31
Figure C-21	NR Outlet Pressure (DECLG).....	C-32
Figure C-22	NR Outlet Pressure (SPLIT) .....	C-32

---

## List of Acronyms

APWR	Advanced Pressurized Water Reactor
BE	Best Estimate
BOCREC	Bottom of Core Recovery
CCFL	Counter-Current Flow Limitation
Cd	Coefficient of Discharge
CFR	Code of Federal Regulation
DECLG	Double-Ended Cold-Leg Guillotine
DVI	Direct Vessel Injection
ECCS	Emergency Core Cooling System
GT	Guide Tube
GUM	Guide to the Expression of Uncertainty in Measurement
HA	Hot Assembly
LBLOCA	Large-Break Loss-of-Coolant Accident
MHI	Mitsubishi Heavy Industries, Ltd.
NR	Neutron Reflector
NRC	Nuclear Regulatory Commission
OLM	On-Line Maintenance
PC	Personal Computer
PCT	Peak Cladding Temperature
PIA	Particle Image Analyzer
PIRT	Phenomena Identification and Ranking Table
PWR	Pressurized Water Reactor
PZR	Pressurizer
RCP	Reactor Coolant Pump
RV	Reactor Vessel
SCR	Silicon-Controlled Rectifier
SG	Steam Generator
SMD	Sauter Mean Diameter
TF	Temperature of the Fluid
TMI	Temperature of the Metal Structure (Inside)
TMM	Temperature of the Metal Structure (Middle)
TMO	Temperature of the Metal Structure (Outside)
TRAC	Transient Reactor Analysis Code

**List of Acronyms (Continued)**

US United States

WCOBRA Westinghouse Coolant Boiling in Rod Arrays

## 1.0 INTRODUCTION

The application of the WCOBRA/TRAC code to the Best-Estimate (BE) analysis of the Large-Break Loss-of-Coolant Accident (LBLOCA) in conventional Pressurized Water Reactors (PWRs) was approved by the United States Nuclear Regulatory Commission (USNRC) (Ref. 1). For the BE analysis of the LBLOCA in the US Advanced PWR (US-APWR), the WCOBRA/TRAC code was modified with the implementation of appropriate models for the new or improved design features specific to the US-APWR and has been named WCOBRA/TRAC(M1.0) (Ref. 1). The applicability of WCOBRA/TRAC(M1.0) to the LBLOCA analysis for the US-APWR is now under the review by the NRC.

In order to confirm the applicability of WCOBRA/TRAC(M1.0) to the thermal-hydraulic analysis of the Neutron Reflector (NR), which is one of the improved design features of the US-APWR, during the reflooding phase in the LBLOCA scenario, a series of reflooding tests and the confirmatory analyses using WCOBRA/TRAC(M1.0) were performed and the results are evaluated in this report.

Chapter 2.0 of this report describes the background and purpose for performing the NR reflooding tests and the confirmatory analyses by WCOBRA/TRAC(M1.0). The test facility, procedure, and conditions are described in Chapters 3.0, 4.0, and 5.0, respectively. In Chapter 6.0 are described some of the NR reflooding test results, which are compared with the results of the confirmatory analyses by WCOBRA/TRAC(M1.0), which are described and discussed in Chapter 7.0. Finally, Chapter 8.0 concludes the report with the summary of the evaluation of the results.

## 2.0 BACKGROUND AND PURPOSE

An NR surrounding the core is used in the US-APWR to improve neutron utilization by reflecting neutrons back into the core, thereby reducing neutron leakage and thus the fuel cycle cost, to reduce neutron irradiation of the reactor vessel, and to increase structural reliability by eliminating bolts in the high neutron flux region. The NR assembly in the US-APWR, as shown in Figure 2-1, is located between the core barrel and core, and consists of thick stainless steel blocks. The NR is cooled by the coolant flowing upward through the cooling holes in the blocks to prevent excessive stress and thermal deflections of the blocks due to the gamma heating.

During the reflooding phase in the LBLOCA, the NR would reflood in a similar way as the core.

Meanwhile, the WCOBRA/TRAC(M1.0) code to be used in the LBLOCA analysis for the US-APWR is a three-dimensional analysis code simulating the thermal-hydraulic behavior in the reactor vessel in detail. The applicability of the code to the analysis of the reflooding phenomena in the PWR fuel bundles has already been reviewed and approved by the NRC (Ref. 1). The WCOBRA/TRAC(M1.0) code is capable of modeling the NR as a separate channel with a heat structure. The physical models for the NR in the US-APWR implemented in the WCOBRA/TRAC(M1.0) code are described in the topical report on the LBLOCA code applicability for the US-APWR (Ref. 1) for the NRC's review.

Although the effect of the thermal-hydraulic behavior in the NR on the reflood PCT is considered to be relatively small and the WCOBRA/TRAC(M1.0) code includes the model to

simulate a two-phase thermal-hydraulic behavior in the NR, a series of reflooding tests and the confirmatory analyses using WCOBRA/TRAC(M1.0) were performed in order to confirm the applicability of the WCOBRA/TRAC(M1.0) code to the thermal-hydraulic analysis of the NR in the US-APWR during the LBLOCA reflooding phase.

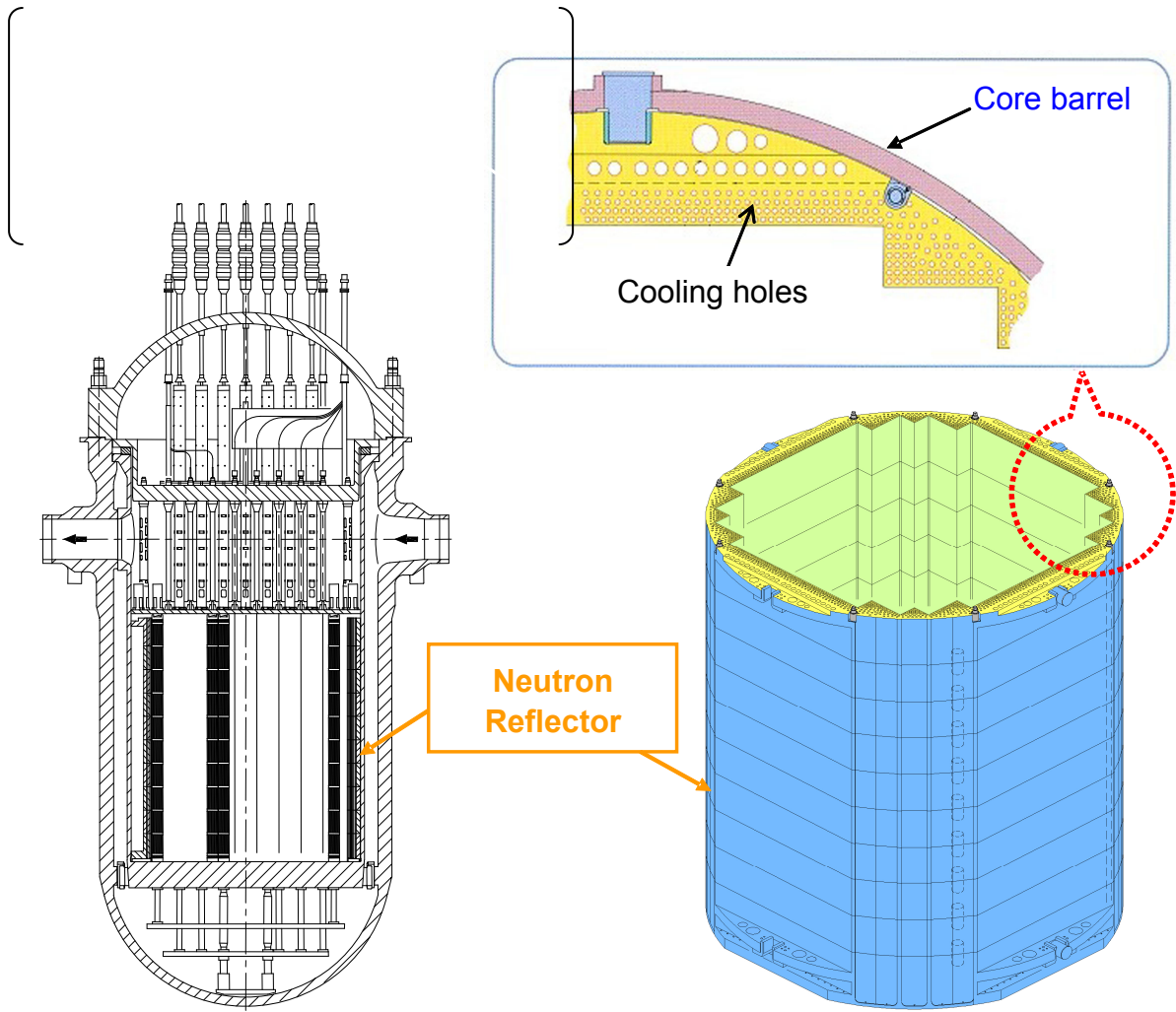


Figure 2-1 Neutron Reflector in US-APWR

### 3.0 TEST FACILITY

An overview of the test facility used in the NR reflooding tests is shown in Figure 3-1. A schematic diagram of the test loop is shown in Figure 3-2. Reflooding water was supplied to the test section through the lower plenum from the reflooding water feed line and was boiled by the heated metal in the test section, which is shown in Figure 3-3. The steam-water two-phase mixture flowed out of the test section into the upper plenum, where the water film and lump were separated and drained into the liquid storage tank. The water droplets in the mist flow discharged from the upper plenum were separated from the steam by the separator and were stored in the gas-liquid separation tank. The steam separated by the separator flowed into the steam line through a steam flow meter measuring the steam flow rate.

#### 3.1 Test Section

Figure 3-3 shows a schematic diagram of the test section with the locations of various measuring instruments. The key dimensions of the test section are compared with those of the NR for the US-APWR in Table 3-1. The test section was of the same length, hydraulic diameter, heat capacity, and material as those of the NR in the US-APWR. The outer diameter of the NR metal in the test section was determined from the average heat capacity of the NR metal per cooling hole in the US-APWR, which was intended to model the NR so as to be consistent with its modeling in the Emergency Core Cooling System (ECCS) analysis for the US-APWR using WCOBRA/TRAC(M1.0). A single cooling hole and the surrounding metal in the test section simulated the entire NR in the US-APWR.

The NR for the US-APWR has more than [ ] cooling holes. The test section simulated only one cooling hole representative of the performance of the entire NR in the US-APWR, and the results could be scaled up conservatively. The scaled-up effect was evaluated by the preliminary analysis with several cooling holes and metal thicknesses by WCOBRA/TRAC (M1.0).

The metal in the test section was wrapped in thinner thermo-cement and sheath heater, which were then wrapped in some insulation material in order to warm it up and to maintain its initial temperature, which simulated the metal temperature at the beginning of the reflooding. The heater was turned off simultaneously with the beginning of the reflooding in order to simulate the effect of the heat released from the metal to the fluid in the cooling hole.



through the return line and did not flow into the cooling hole of the test section by controlling the water level in the lower plenum.

The test loop was pressurized by supplying steam from the boiler and the system pressure was controlled to the specified constant value with the pressure control valve on the steam line.

The NR metal was heated to the specified temperature by the heater installed between the outer surface of the NR metal and the thermal insulator.

### **3.2.2 Reflooding Period**

The reflooding was started with supplying the water into the cooling hole in the test section by closing the solenoid-operated valve on the return line. The reflooding water received the heat released from the NR metal and boiled in the cooling hole. The thermal-hydraulic behaviors in the cooling hole and NR metal in the test section were measured by thermocouples, void sensors, and liquid film sensors installed along the test section.

The steam-water two-phase mixture flowed out of the test section into the upper plenum. The steam entrained a part of the water droplets and flowed out of the upper plenum into the gas-liquid separation tank, and the entrained water droplets were separated from the steam by the cyclone-type separator in the gas-liquid separation tank. The separated steam flowed through an orifice-type steam flow meter installed inside the line connecting the gas-liquid separation tank and steam line, and was discharged into the atmosphere together with the steam from the boiler. The separated water droplets remained in the gas-liquid separation tank, and the integrated water droplet outlet flow was obtained by measuring the water level change in the tank. The water film and lump that were not entrained by the steam in the upper plenum flowed into the liquid storage tank from the bottom of the upper plenum. The integrated water film and lump outlet flow was obtained by measuring the water level change in the liquid storage tank. Furthermore, the flow regime such as water droplets' behavior was observed through an observation port mounted on the upper plenum wall.

During the reflooding period, the system pressure was maintained constantly by controlling the rate of the steam discharged into the atmosphere via the pressure control valve, even though the steam generated in the cooling hole was added to the steam supplied from the boiler in the steam line.

### **3.3 Measurement and Calibration**

#### **3.3.1 Measurement**

The main measurement items are shown in Figures 3-2 and 3-3 and are described in the following.

##### **3.3.1.1 Measurement Items Inside Test Section**

###### (1) Fluid temperature in NR cooling hole

The temperatures of the fluid in the cooling hole near the inner surface of the NR metal were measured by thermocouples at a pitch of [ ] along the test section as shown in Figure 3-3.

###### (2) NR metal temperature

The temperatures inside the NR metal were measured at a pitch of [ ] along the test section at the same axial locations as those for the fluid temperature measurement as shown in Figure 3-3. To confirm the symmetry of the radial temperature distribution, on the opposite sides of the cooling hole were mounted two metal blocks, on either of which thermocouples were embedded near the inner and outer surfaces of the NR metal and at some intermediate position between them as well.

###### (3) Liquid fraction in NR cooling hole

The liquid fractions (accordingly void fractions) in the cooling hole near the inner surface of the NR metal were measured by void sensors at a pitch of [ ] along the test section at the same axial locations as those for the temperature measurements as shown in Figure 3-3. A void sensor consisted of two electrodes, one of which had a tip displaced a few millimeters inside the cooling hole from the inner surface of the NR metal as shown in Figure 3-4.

###### (4) Liquid film existence in NR cooling hole

The liquid film existences on the inner surface of the NR metal were measured by liquid film sensors at a pitch of [ ] along the test section at the same axial locations as those for the

temperature measurements as shown in Figure 3-3. A liquid film sensor consisted of two electrodes, both of which were flush with the inner surface of the NR metal as shown in Figure 3-5.

(5) Differential pressure in NR cooling hole

The differential pressures were measured in the flow direction as shown in Figure 3-3. The measurements were performed over [ ] lengths of the test section.

### 3.3.1.2 Measurement Items Outside Test Section

(1) Steam flow rate out of NR cooling hole

The outlet steam flow rate was measured by an orifice-type steam flow meter installed inside the line connecting the gas-liquid separation tank and steam line as shown in Figure 3-2.

(2) Water flow rate out of NR cooling hole

The outlet water flow rate was obtained by measuring the water level changes in the liquid storage tank and gas-liquid separation tank as shown in Figure 3-2.

(3) Reflooding water flow rate into NR cooling hole

The reflooding water flow rate was measured by a liquid flow meter on the reflooding water feed line as shown in Figure 3-2.

(4) Pressures

The pressures were measured in the lower and upper plenums as shown in Figure 3-2.

(5) Flow regime at outlet of NR cooling hole

The behavior of the water droplets ejected out of the cooling hole was observed by using a video camera through the observation port glass mounted on the upper plenum wall.

(6) Temperatures in other components (feed water line and so on)

Temperatures are measured with thermocouples as shown in Figure 3-2.

(7) Water droplet diameters at outlet of NR cooling hole

The diameters of the water droplets and water lumps were measured by a background light particle image analyzer system.

### **3.3.2 Calibration**

Calibrations of the measurement systems were carried out as described in the following. The details of the procedure are described in Appendices A and B.

(1) Before installation

Only the measuring instruments that had been calibrated were used in the test. The calibration should be performed prior to the installation in order to comprehend the measurement errors.

(2) In use check for data reliability

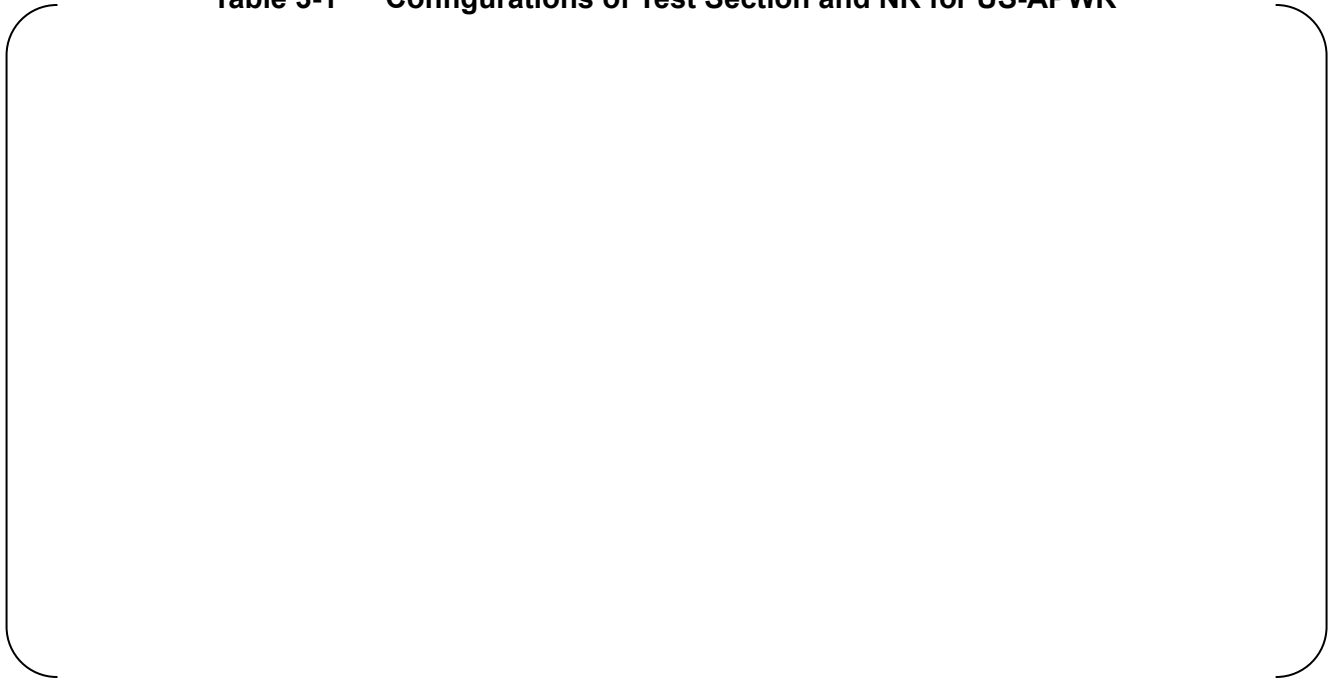
The data reliability was checked periodically by the following manner.

- Mass balance at a specific time
- Consistency between saturated pressure and saturated temperature for pressure and temperature
- Consistency between several in-kind measuring instruments such as pressure and temperature

(3) After final test

It was difficult to detach the measuring instruments from the test section because the metal block with thermocouples for metal and fluid temperature measurements as shown in Figure 3-3 was welded directly to the NR metal. Therefore a specific test with the known state as fluid condition was performed to obtain thermal-hydraulic data by using the measuring instruments and the test loop. It was confirmed that the last data reproduced its original data.

**Table 3-1 Configurations of Test Section and NR for US-APWR**



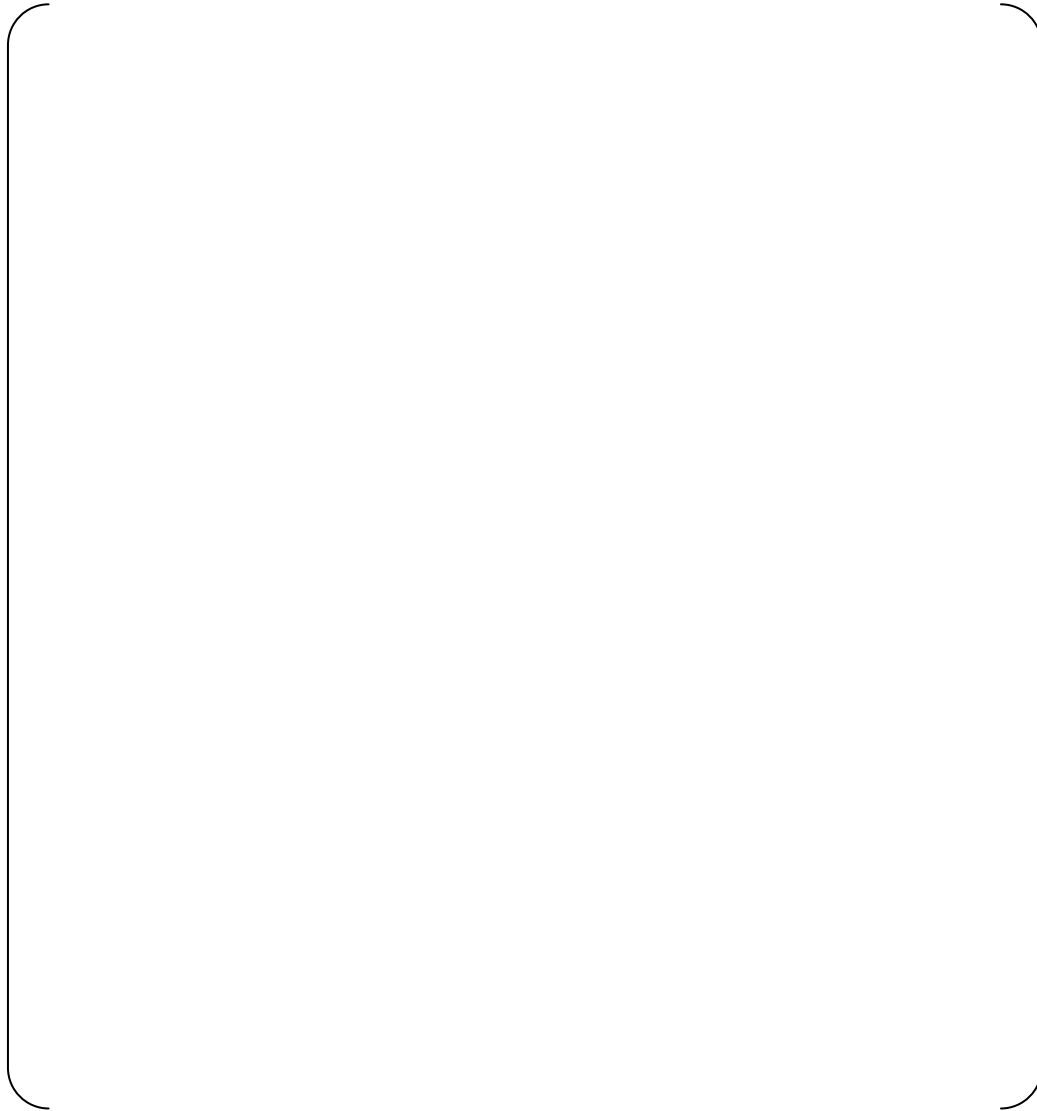
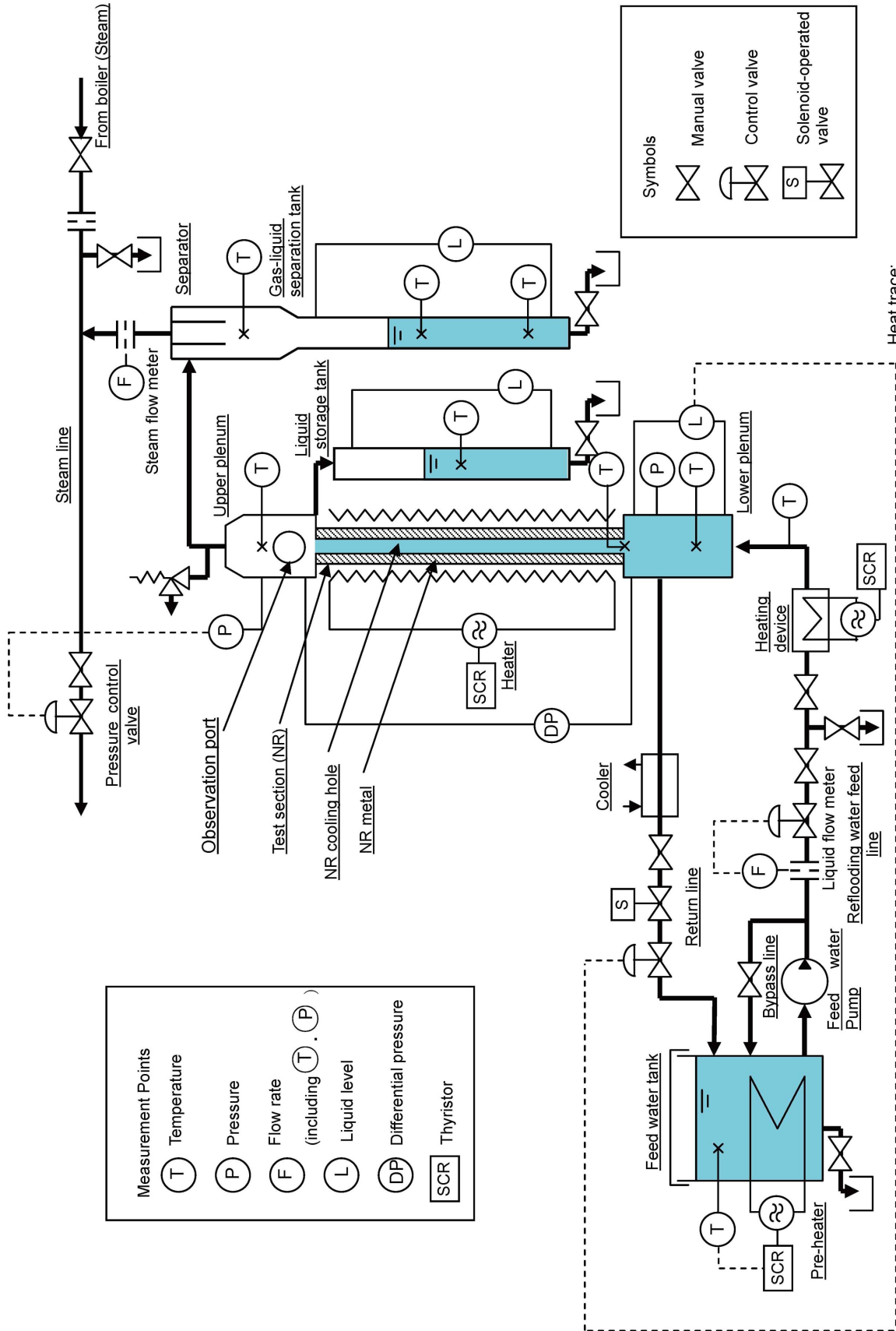


**Figure 3-1 Overview of Test Facility**



Heat trace:  
liquid storage tank, gas-liquid separation tank and component from outlet of the test section to outlet of steam flow meter.

**Figure 3-2 Schematic of Test Loop**

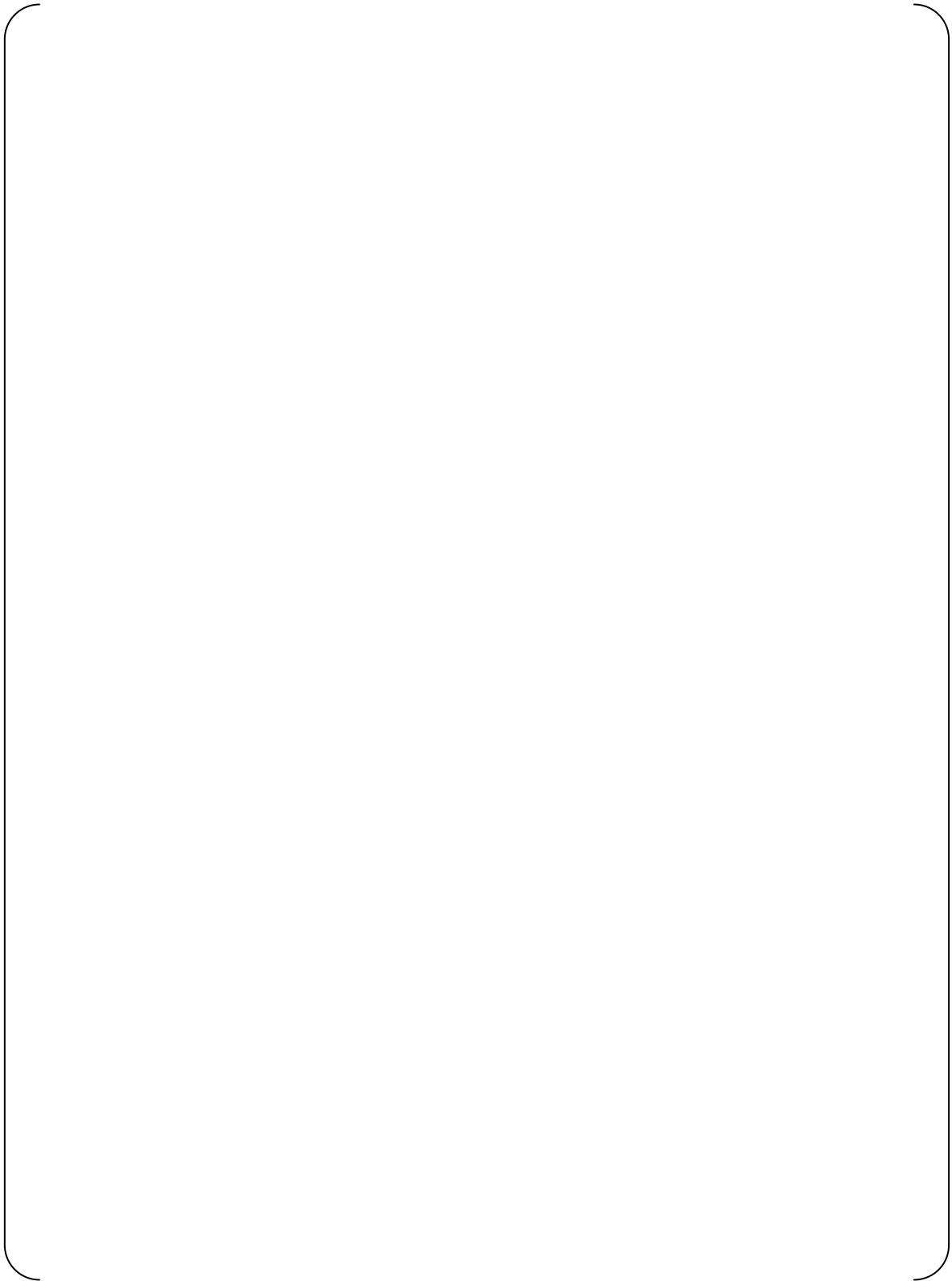


**Figure 3-3 Test Section and Instrumentation**



**Figure 3-4 Void Sensor**

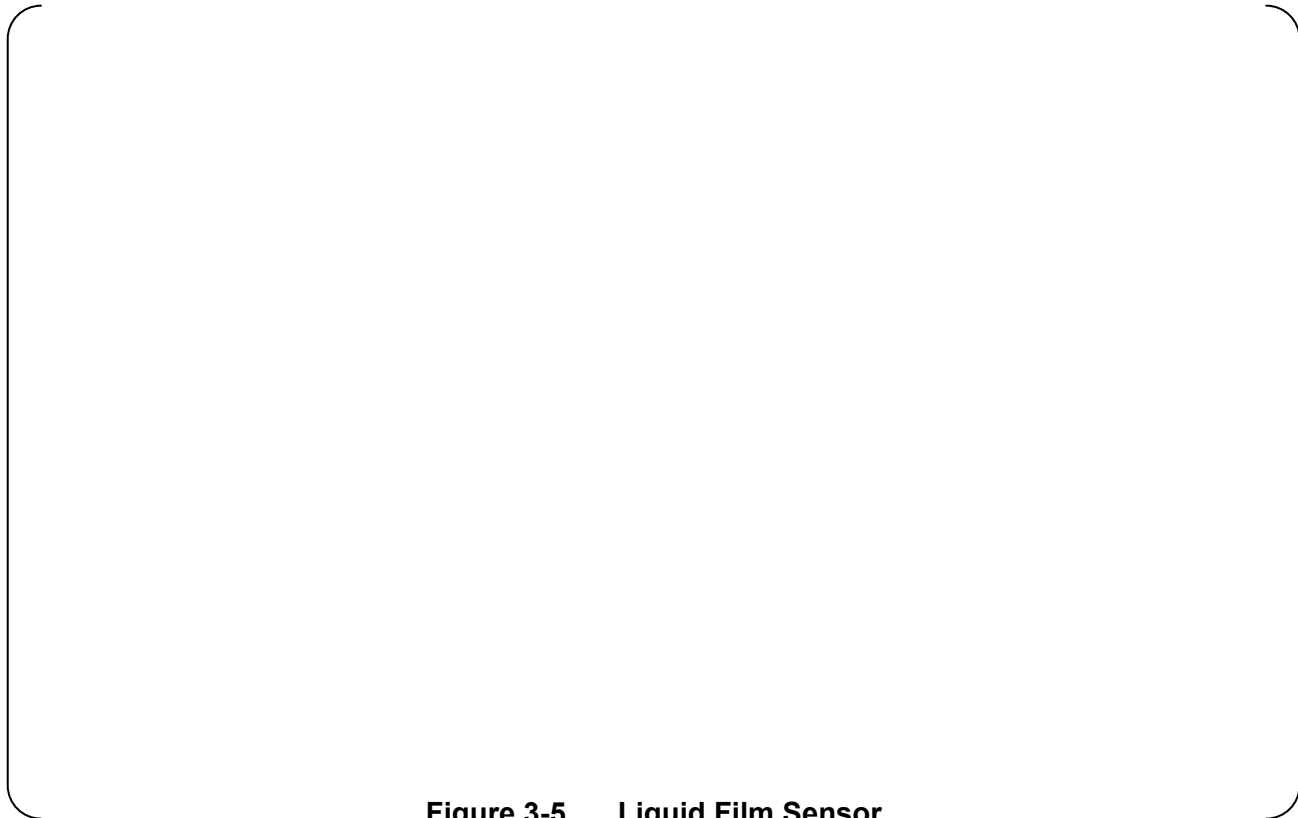


**Figure 3-5 Liquid Film Sensor**

## 4.0 TEST PROCEDURE

The tests were performed under the quality assurance program of the Takasago Research and Development Center that satisfies “10 CFR Part 50 Appendix B” and have been approved by the Nuclear Energy Systems Quality and Safety Management Department of MHI.

The test procedure is described in the following.

### 4.1 Preparation of Reflooding System

#### (1) Filling of feed water tank with water

Fill pure water from the water purifying device into the feed water tank.

#### (2) Start of feed water pump

Start the feed water pump and begin the control with the feed water control valve to obtain the specified flow rate of the reflooding water. Set the bypass manual valve to achieve circulation with the pump bypass line, because the reflooding flow rate is low in comparison with the rated flow rate of the pump.

#### (3) Control of water level in lower plenum

Start the control with the control valve on the return line so that the reflooding water that has entered in the lower plenum can not flow into the cooling hole and the water that has flowed into the lower plenum can return to the feed water tank.

#### (4) Start of heating of water by pre-heater in feed water tank

Switch on the pre-heater in the feed water tank. Control the temperature of the feed water tank during the heating using the pre-heater. Because the tank is an open-air type, the temperature to be set for the feed water tank will be about [            ] or below so that boiling can not occur in the tank.

#### (5) Filling of liquid storage tank and gas-liquid separation tank with water

Fill the liquid storage tank and gas-liquid separation tank with water through the water filling line after the temperature in the feed water tank reaches the specified temperature. The water level should be detectable.

(6) Start of heating of water by heating device

Switch on the heater of the heating device in order to heat the reflooding water from about [ ] to about [ ], if the inlet water temperature is about [ ] as a test condition. At this time, set an appropriate specific thermal dose using a manual Silicon-Controlled Rectifier (SCR; Thyristor) for the heater of the heating device, and adjust the temperature using the set value of the feed water tank temperature for setting the reflooding water flowing-in temperature.

(7) Control of water temperature in cooler

Adjust the flow rate of the cooling water supplied to the cooler on the return line to prevent returning of the reflooding water with a temperature of more than about [ ], if the inlet water temperature is about [ ].

## 4.2 Preparation of Steam System

(1) Start of boiler

Start the boiler and begin to supply steam into the system.

(2) Setting of pressure

Control the pressure in the system with the pressure control valve mounted on the steam line to obtain the specified constant pressure.

(3) Start of heat trace

Start the heat traces for the liquid storage tank, gas-liquid separation tank and the piping from the outlet of the test section to the outlet of the steam flow meter.

### **4.3 Start of Heating of Test Section**

#### (1) Heating of test section

Start heating of the test section by switching on the heater of the test section. Perform heating at this time up to the specified temperature with the SCR, by monitoring the temperature distribution in the test section in the axial direction.

#### (2) Holding of temperature of test section

Manually adjust the temperature of test section when the specified temperature is reached, so that a constant temperature can be maintained for a while. Monitor the temperature distribution in the test section in the axial direction again.

### **4.4 Start of Reflooding**

#### (1) Start of reflooding

Close the solenoid-operated valve on the return line connected to the lower plenum in order to start reflooding the cooling hole, and simultaneously shut off the power to the heater of the test section.

#### (2) Monitoring of items

Monitor the pressures and temperatures for any anomalies during the reflooding.

### **4.5 End of Reflooding**

The reflooding and measurement are completed after the inner wall is quenched throughout the full length of the cooling hole. The time duration of the reflooding will be less than [ ] minutes. The time duration of a test from “start of feed water pump” described in Section 4.1 (2) until “end of reflooding” described in Section 4.5 is about 10 hours.

If there is any problem, stop the equipment immediately.

## 5.0 TEST CONDITIONS

The thermal-hydraulic behavior in the NR of US-APWR can be affected by the conditions of the reflooding rate, inlet water temperature, initial metal temperature and pressure. Therefore, seven test cases including a reproducibility test and a case [ ] were performed. The test conditions used in the reflooding tests are shown in Table 5-1. The number of test runs and test conditions were appropriately determined based on an evaluation of the LBLOCA analysis results with the US-APWR plant parameters by WCOBRA/TRAC (M1.0), which is shown in Appendix C. The values of the parameters were determined so as to include the results of the US-APWR plant analysis using WCOBRA/TRAC(M1.0). The ranges of the parameters are wide enough to confirm the code applicability under the US-APWR LBLOCA conditions.

The thermal-hydraulic behavior through the NR cooling hole in these tests is in transient state because high temperature of NR metal is decreased by the reflooding water. However, some test conditions such as reflooding rate, inlet water temperature and upper plenum pressure are maintained constant in these tests.

**Table 5-1 Test Conditions\***





**Figure 5-1 Inlet of Test Section**

## 6.0 TEST RESULTS

In order to investigate the sensitivity of the thermal-hydraulic behavior in the NR to the test conditions, such as reflooding water velocity, reflooding water temperature, initial metal temperature, and upper plenum pressure, the test data were obtained for the following items:

- Flow regime at the outlet of the test section,
- Steam outlet flow rate, which was converted into the integrated steam outlet flow,
- Water film and lump outlet flow rate, which was converted into the integrated water film and lump outlet flow,
- Water droplet outlet flow rate, which was converted into the integrated water droplet outlet flow,
- Metal temperature distribution at different axial locations along the test section,
- Fluid temperature at different axial locations along the test section,
- Liquid fraction (accordingly void fraction) at different axial locations along the test section,
- Water film existence at different axial locations along the test section.

### (1) Flow Regime at Outlet of Test Section (Figure 6-1 ~ Figure 6-7)

During the test, various steam-water two-phase flow regimes were observed at the outlet of the test section. A flow visualization study was performed with a video camera. Figure 6-1 through Figure 6-7 show the still images of the representative two-phase flow regimes at the outlet of the test section for each of the test runs specified in Table 5-1, respectively.

The characteristics of the flow regimes observed in each test run are described in the following.

#### Run 1-1 (Reference Case)

Initial stage [ \_\_\_\_\_ ]



( )

Intermediate stage [ \_\_\_\_\_ ]

( )

Final stage [ \_\_\_\_\_ ]

( )

### **Run 1-2 (Reproducibility Test)**

The flow regimes were similar to those observed in the reference case (Run 1-1). As described in the following section, the transient behaviors of the outlet flow rates of the steam and water, and the temperature distributions in the test section were also similar to those measured in the reference case. Therefore, it can be said that this reflooding test is reproducible.

### **Run 2-1 (Case with Decreased Reflooding Water Velocity, [ \_\_\_\_\_ ])**

Initial stage [ \_\_\_\_\_ ]

( )

Intermediate stage [ \_\_\_\_\_ ]

( )

---

**Runs 3-1, 4-1, 5-1, and 6-1**

**(2) Water Droplet Diameter at Outlet of Test Section** (Figure 6-8, Figure 6-9)

Figure 6-8 shows the transient behavior of the water droplet diameter. The Sauter Mean Diameter (SMD) was used in defining the diameter of the water droplet and was obtained from the water droplet diameter distribution, as shown in Figure 6-9, measured by a background-light Particle Image Analyzer (PIA). The SMD with a single peak distribution, such as the Gaussian distribution, is normally larger than the mode, and therefore, the SMDs in Figure 6-8 were larger than the modes.

**NOTE**

The water droplet diameters for Run 1-2 and Run 6-1 were not measured because the behaviors of the temperatures and the outlet flows were the same as those for the reference case.

---

**(3) Flow Rate at Outlet of Test Section** (Figure 6-10 ~ Figure 6-14)



More detailed test results are described in the following sections.

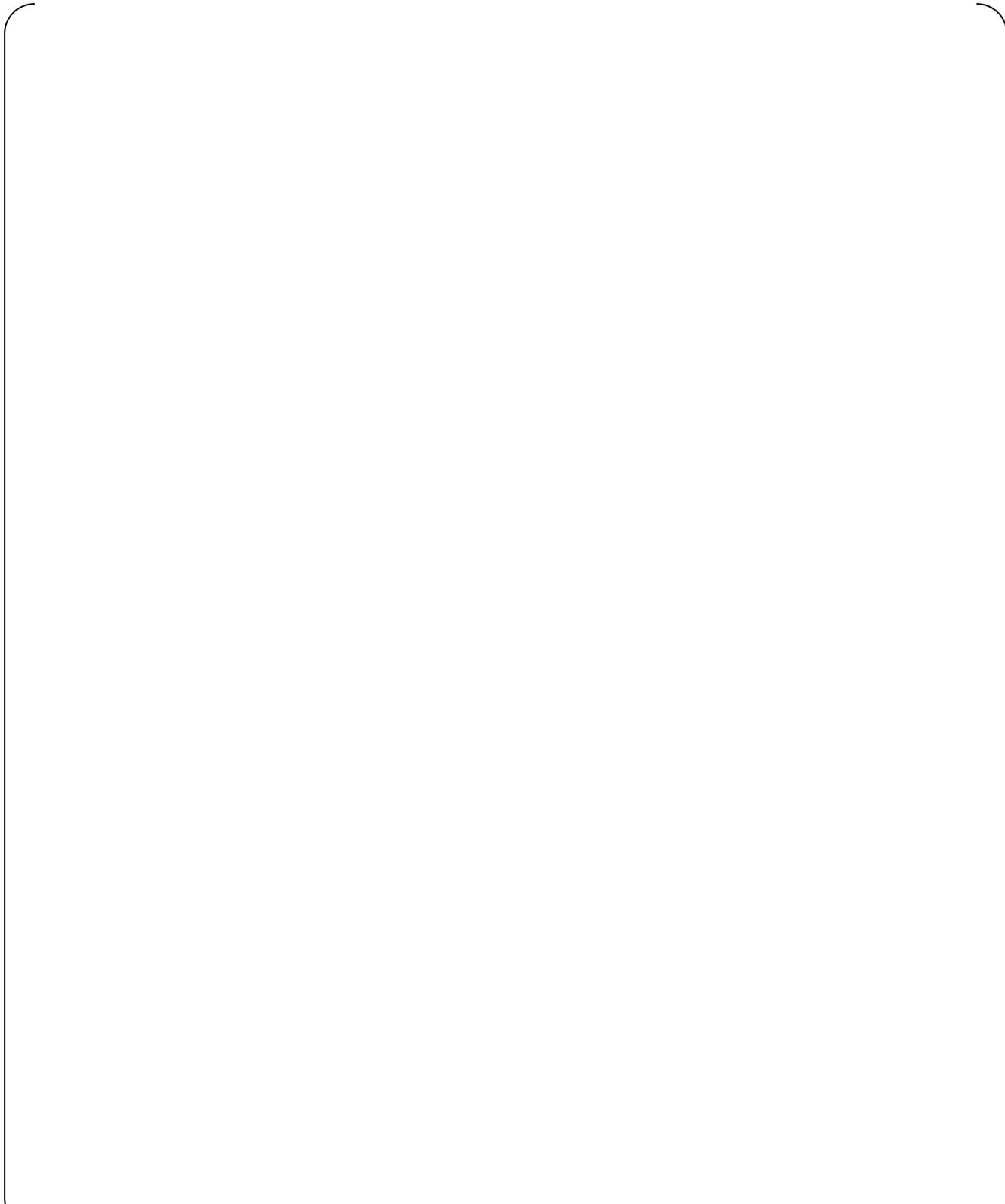


**Figure 6-1 Water Droplet and Lump Behaviors at Outlet of Test Section  
(Run 1-1: Reference Case)**

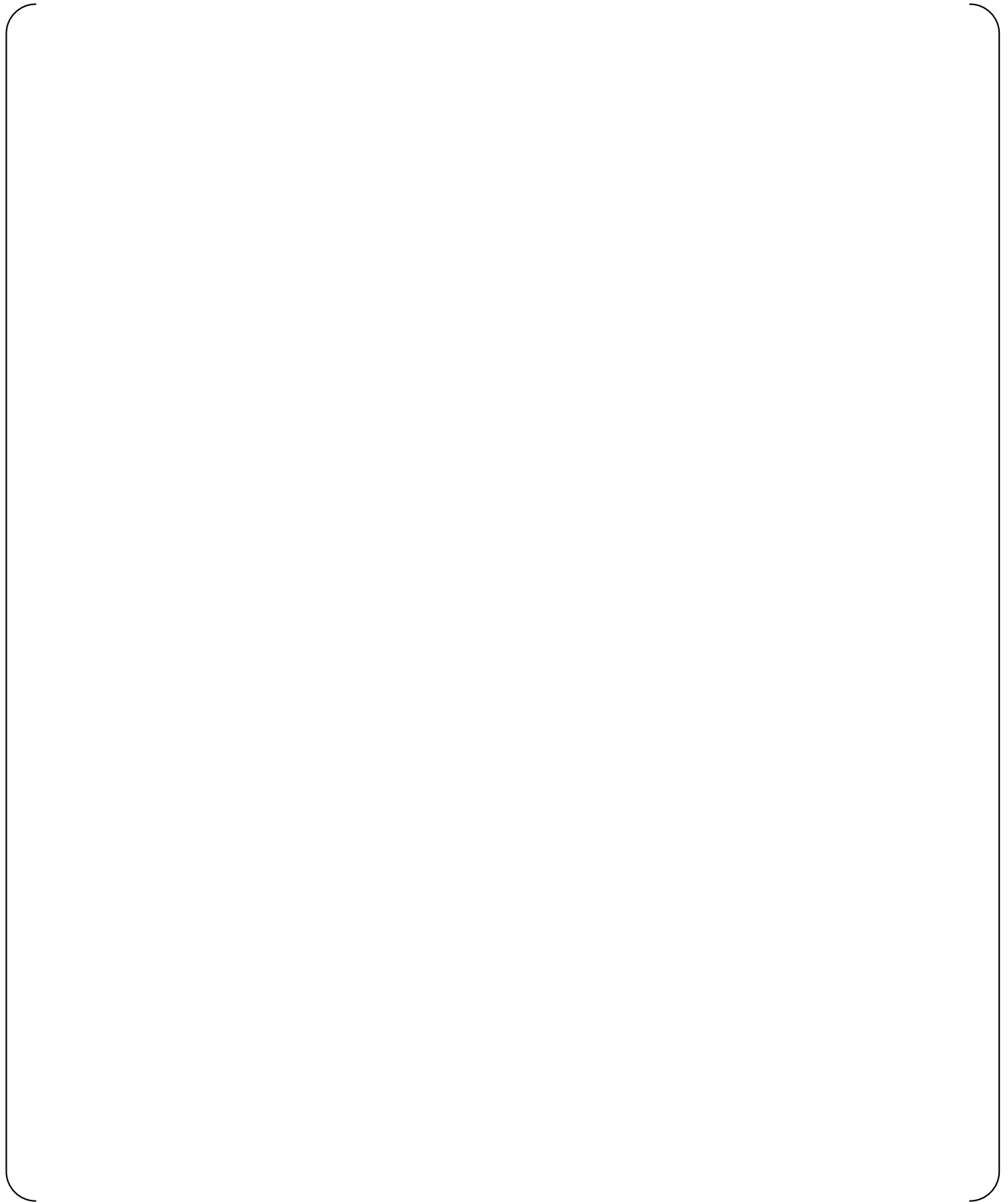


**Figure 6-2 Water Droplet and Lump Behaviors at Outlet of Test Section  
(Run 1-2: Reproducibility)**







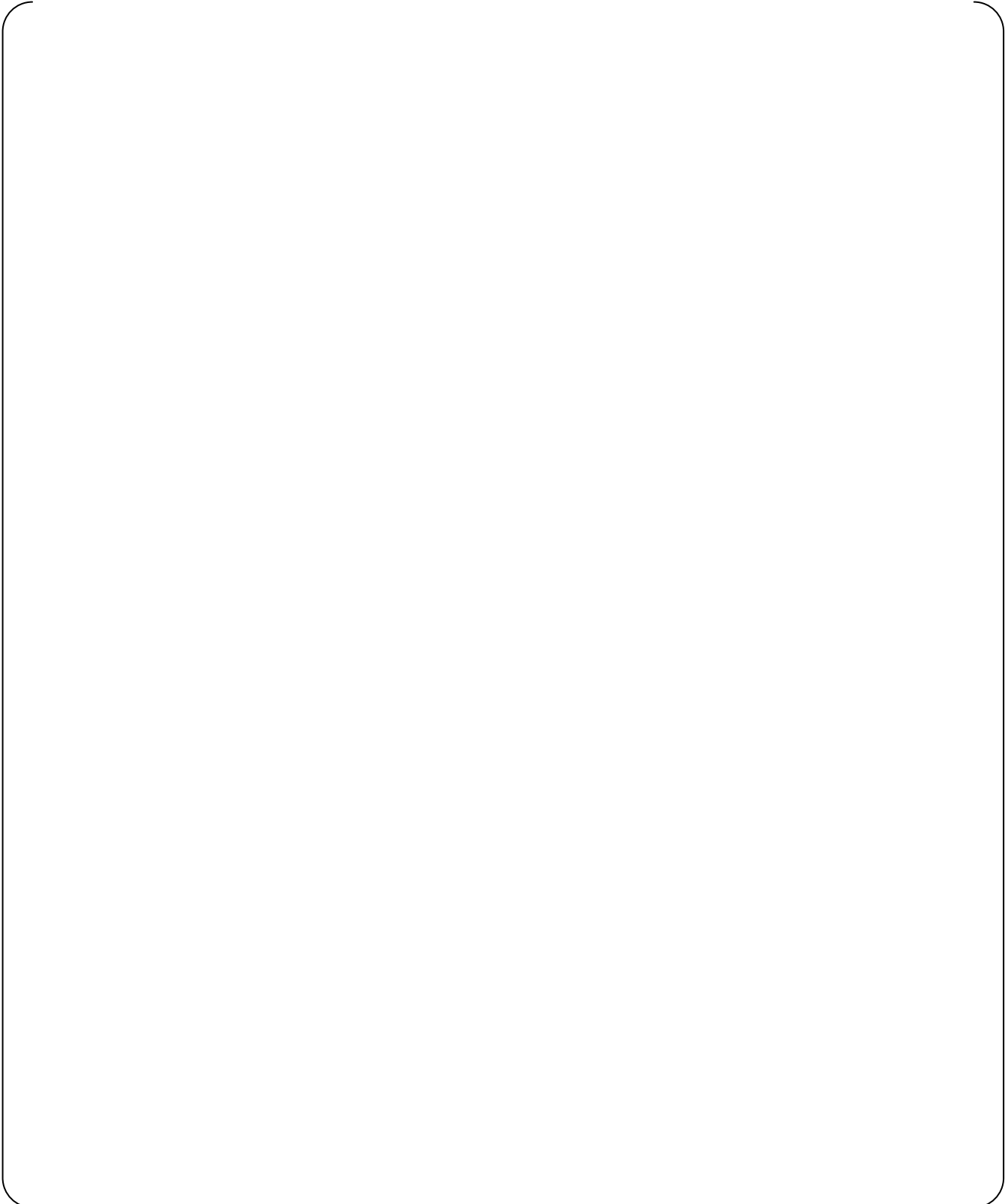


**Figure 6-6 Water Droplet and Lump Behaviors at Outlet of Test Section  
(Run 5-1: Upper Plenum Pressure = [ ])**

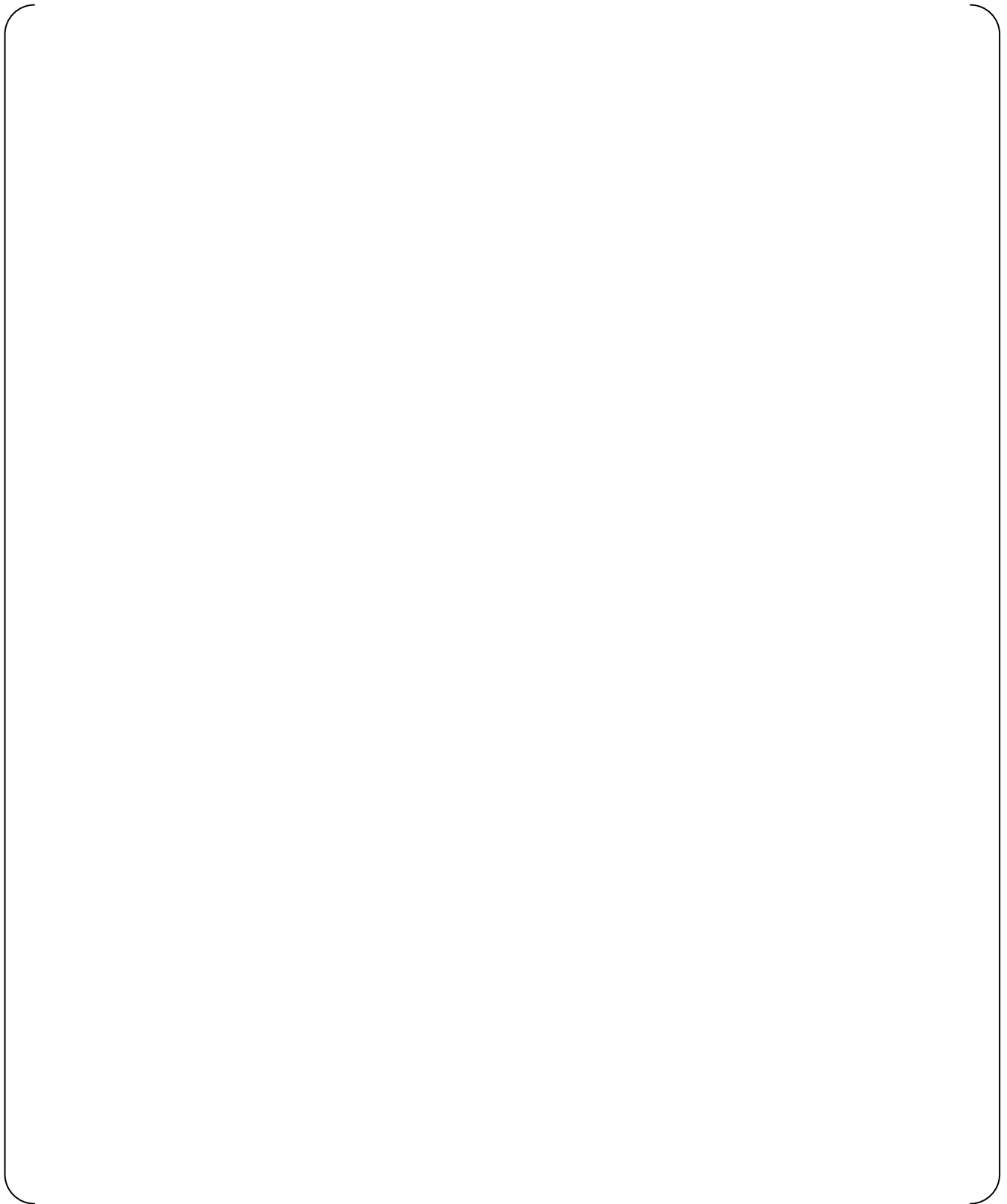


**Figure 6-7 Water Droplet and Lump Behaviors at Outlet of Test Section**  
(Run 6-1: [ ])



**Figure 6-8 Water Droplet Diameter Measured at Outlet of Test Section**



**Figure 6-9 Water Droplet Diameter Distribution  
(Run 1-1: Reference Case, 10-20 sec (approx.))**

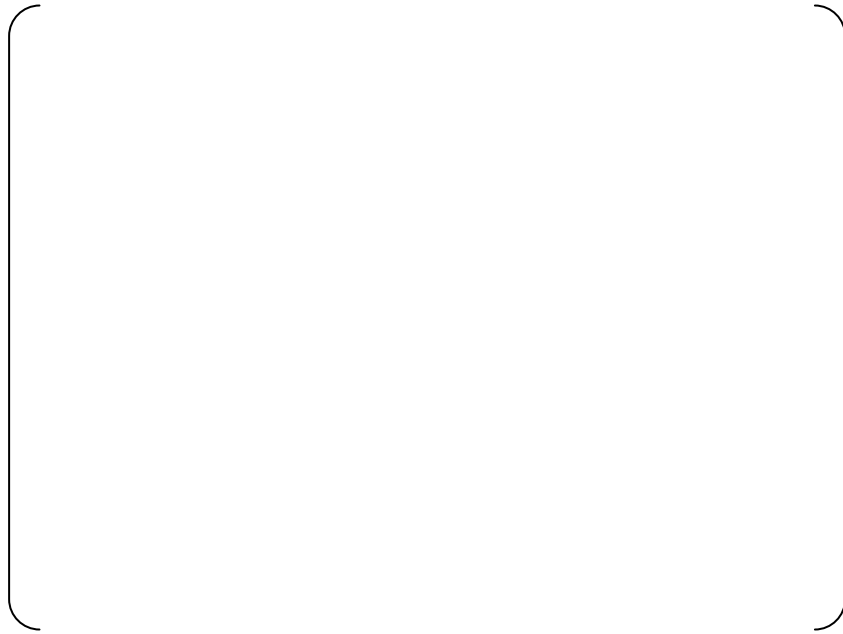


**Figure 6-10 Integrated Total Inlet Flow from Measured Data**



**Figure 6-11 Integrated Total Outlet Flow from Measured Data**



**Figure 6-12 Total Outflow-to-Inflow Ratio from Measured Data**



**Figure 6-13 Integrated Water Outlet Flow from Measured Data**

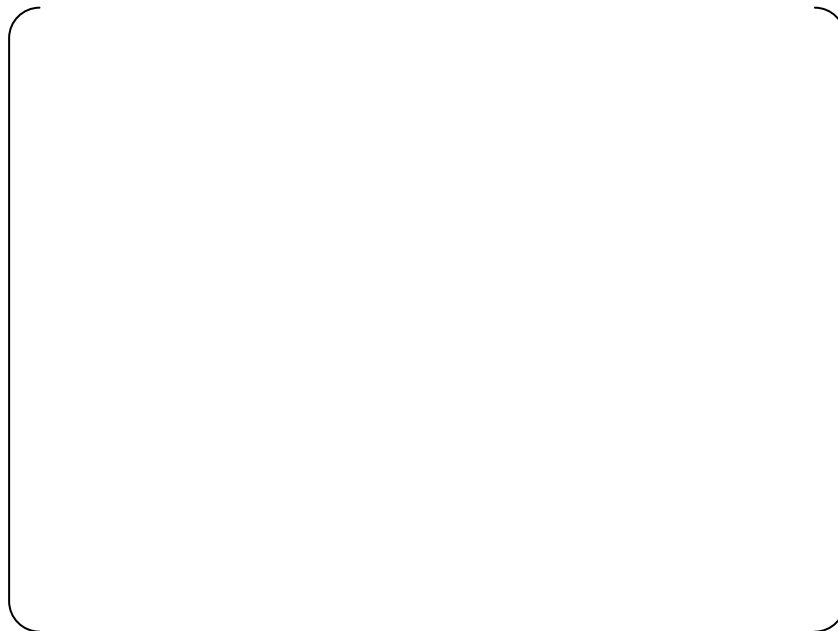
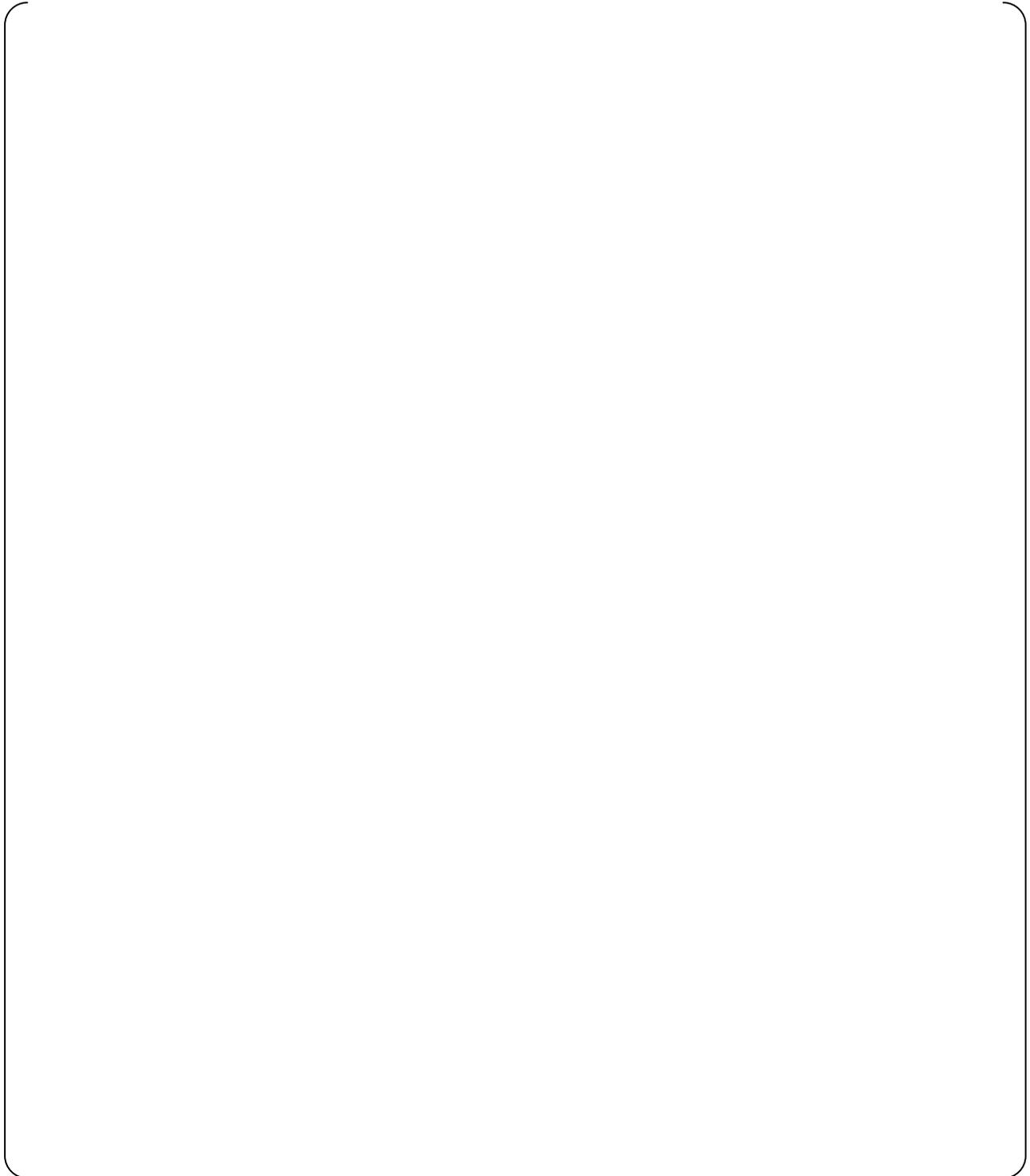


**Figure 6-14 Integrated Steam Outlet Flow from Measured Data**

**6.1 Run 1-1 (Reference Case)**

**(1) Temperature and Quench Front Propagation (Figure 6-15, Figure 6-16)**



---

**6.2 Run 1-2 (Reproducibility Test)**

**(1) Flow Rate at Outlet of Test Section (Figure 6-17)**

In Figure 6-17, the integrated total outlet flow, outflow-to-inflow ratio, water outlet flow, and steam outlet flow measured in Run 1-2 are compared with those measured in Run 1-1 (reference case). As can be seen in each graph of Figure 6-17, the two test results agreed very well with each other. Therefore, the reproducibility of the test has been confirmed.

**(2) Temperature and Quench Front Propagation (Figure 6-18, Figure 6-19)**

Figure 6-18 shows the transient metal temperature distributions measured in Run 1-2. There existed little differences between Run 1-1 and Run 1-2. As shown in Figure 6-19, the propagation of the quench front to the downstream with respect to time that can be seen from the metal temperature transients can also be confirmed from the non-dimensional detected voltage measured by the liquid film sensor.

**6.3 Run 2-1 (Case with Decreased Reflooding Water Velocity, [ ])**

**(1) Flow Rate at Outlet of Test Section (Figure 6-20)**

[ ]

**(2) Temperature and Quench Front Propagation** (Figure 6-21, Figure 6-22)



**6.4 Run 3-1 (Case with Decreased Reflooding Water Temperature, [ ])**

**(1) Flow Rate at Outlet of Test Section** (Figure 6-23)



**(2) Temperature and Quench Front Propagation** (Figure 6-24, Figure 6-25)



**6.5 Run 4-1 (Case with Decreased Initial Metal Temperature, [ ])**

**(1) Flow Rate at Outlet of Test Section** (Figure 6-26)



**(2) Temperature and Quench Front Propagation** (Figure 6-27, Figure 6-28)





**6.6 Run 5-1 (Case with Increased Upper Plenum Pressure, [ ])**

**(1) Flow Rate at Outlet of Test Section (Figure 6-29)**



**(2) Temperature and Quench Front Propagation (Figure 6-30, Figure 6-31)**







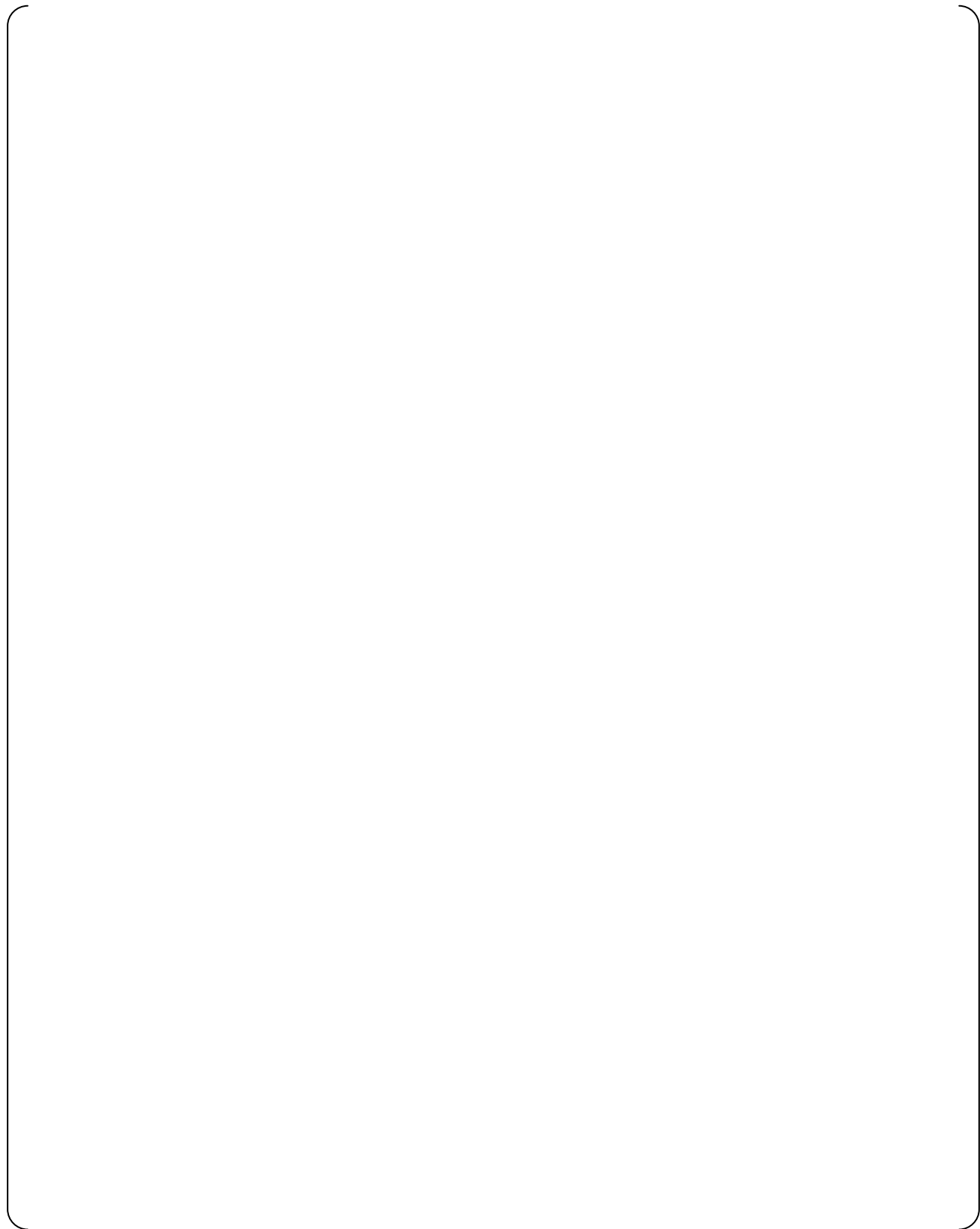


**Figure 6-15 Measured Metal Temperature Distribution  
(Run 1-1: Reference Case)**

**Figure 6-16 Measured Metal Temperature, Liquid Fraction, and Liquid Film  
(Run 1-1: Reference Case)**



**Figure 6-17 Measured Integrated Steam and Water Outlet Flows  
(Run 1-2: Reproducibility)**

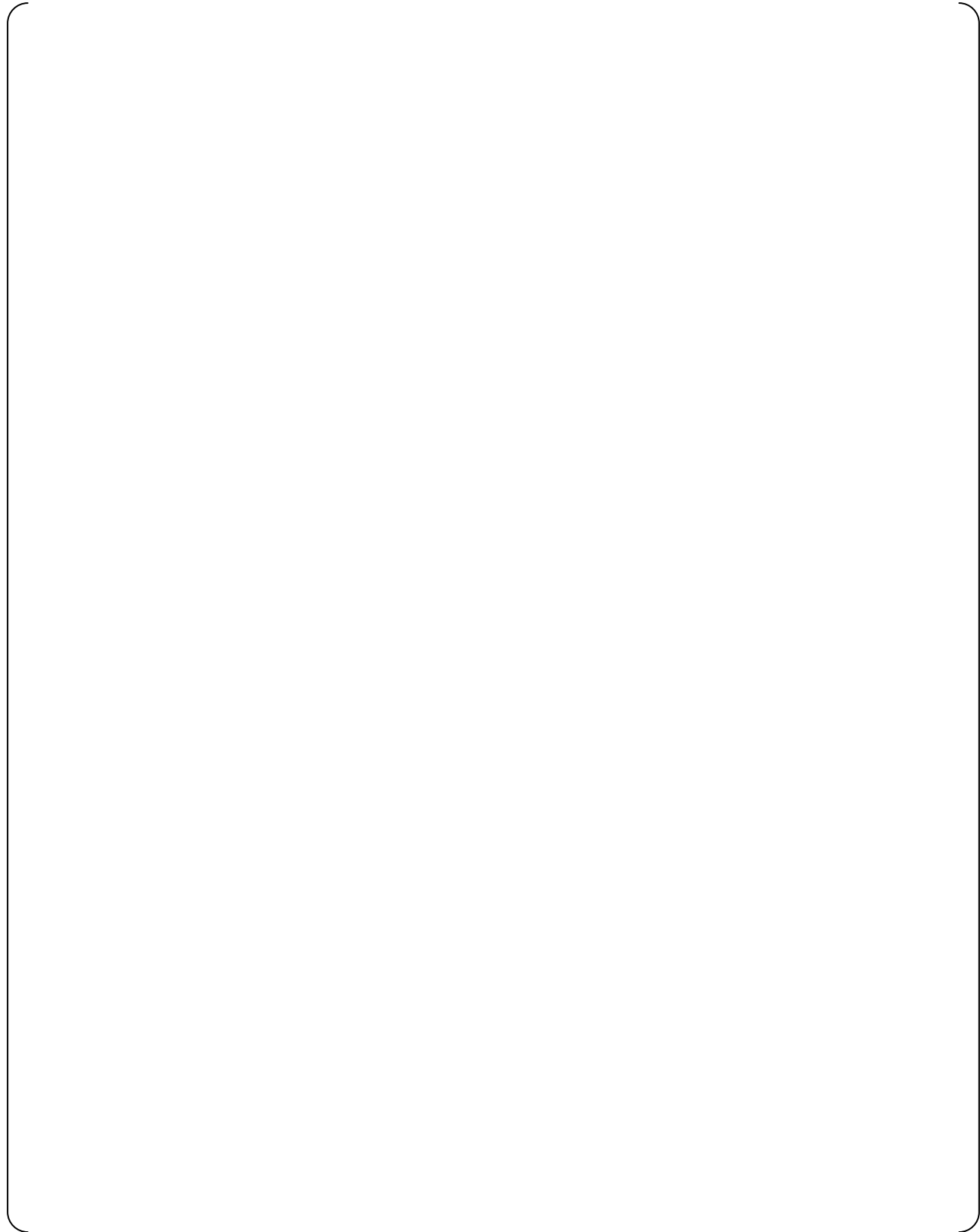


**Figure 6-18 Measured Metal Temperature Distribution  
(Run 1-2: Reproducibility)**

**Figure 6-19 Measured Metal Temperature, Liquid Fraction, and Liquid Film  
(Run 1-2: Reproducibility)**



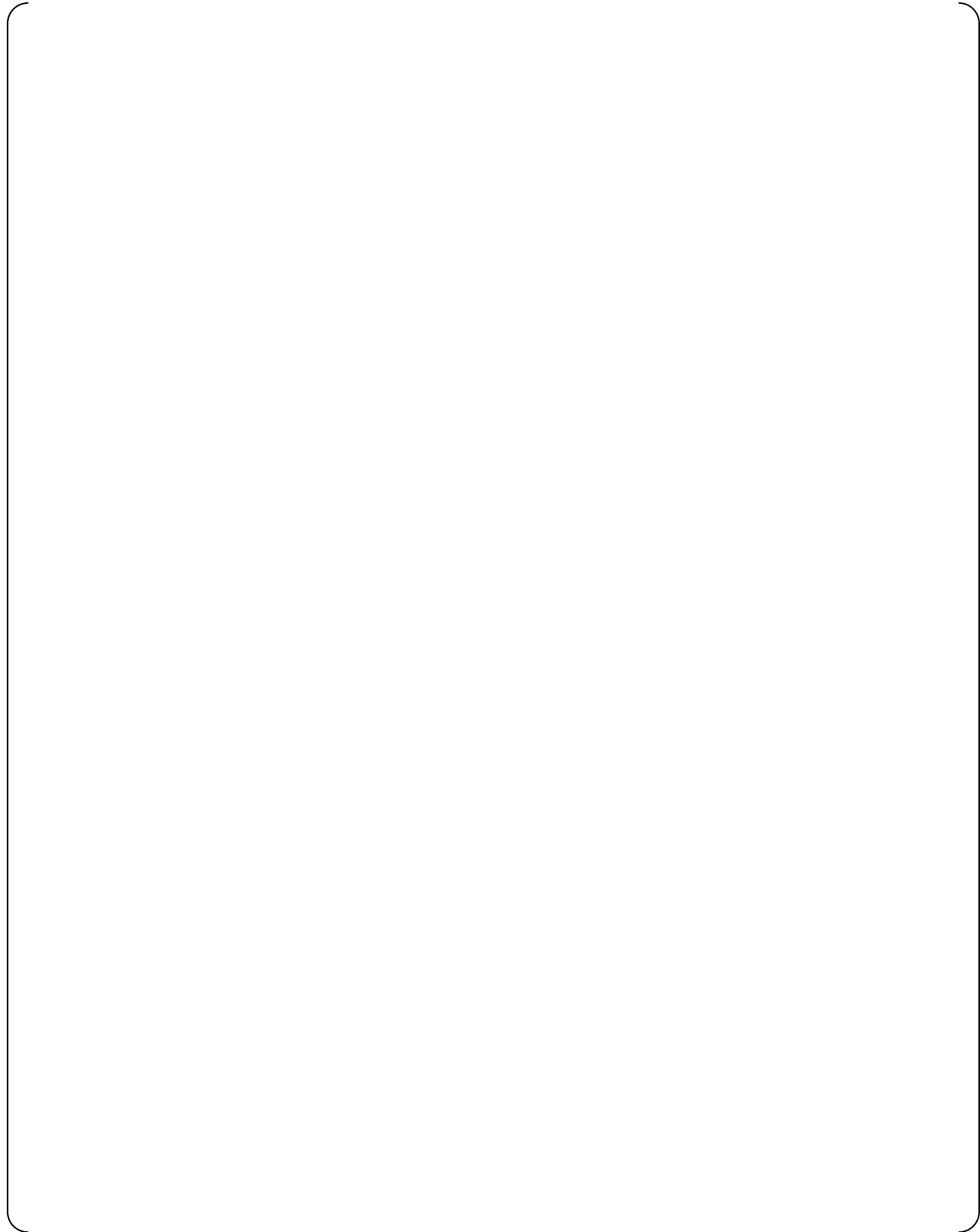


**Figure 6-21 Measured Metal Temperature Distribution  
(Run 2-1: Reflooding Water Velocity = [ ])**

**Figure 6-22 Measured Metal Temperature, Liquid Fraction, and Liquid Film  
(Run 2-1: Reflooding Water Velocity = [ ])**





**Figure 6-25 Measured Metal Temperature, Liquid Fraction, and Liquid Film  
(Run 3-1: Reflooding Water Temperature = [ ])**



**Figure 6-26 Measured Integrated Steam and Water Outlet Flows  
(Run 4-1: Initial Metal Temperature = [                      ])**



**Figure 6-28 Measured Metal Temperature, Liquid Fraction, and Liquid Film  
(Run 4-1: Initial Metal Temperature = [ ])**



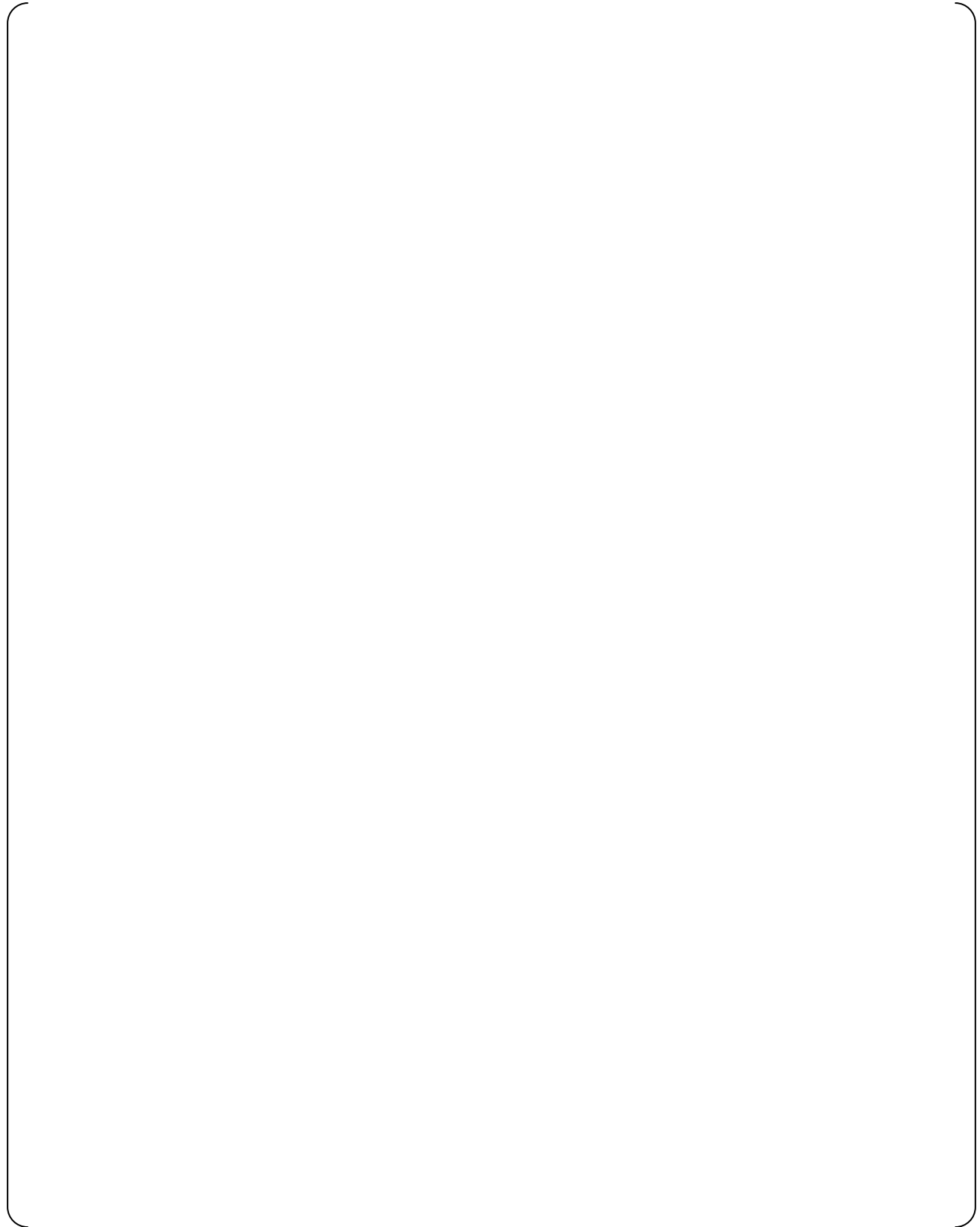


**Figure 6-30 Measured Metal Temperature Distribution  
(Run 5-1: Upper Plenum Pressure = [ ])**

**Figure 6-31 Measured Metal Temperature, Liquid Fraction, and Liquid Film  
(Run 5-1: Upper Plenum Pressure = [ ])**



**Figure 6-32 Measured Integrated Steam and Water Outlet Flows  
(Run 6-1: [ ])**



**Figure 6-34 Measured Metal Temperature, Liquid Fraction, and Liquid Film  
(Run 6-1: [ ])**



**Figure 6-35 Flow Pattern in Inlet of Test Section**



### 7.3 Analysis Results

For the five cases as shown in Table 7-1, the thermal-hydraulic analyses were performed by using the WCOBRA/TRAC(M1.0) code. Some of the code calculation results are compared with the measured data in Figures 7-13 through 7-27, and are described for each of the five cases in the following.

#### 7.3.1 Run 1-1 (Reference Case)

Figure 7-13 (a) compares the integrated total outlet flow predicted by WCOBRA/TRAC(M1.0) with that measured in Run 1-1. To provide some measure of the relative amount of the total outlet flow, the integrated total inlet flow is also shown in the same figure. [

]

Figures 7-13 (c) and 7-13 (d) show the integrated water film & lump and water droplet outlet flows, respectively, predicted by the code with those measured in the test. [

]

**7.3.2 Run 2-1 (Case with Decreased Reflooding Water Velocity, [**  
**])**

Figures 7-16 (a) and 7-16 (b) compare the integrated total outlet flow and total outflow-to-inflow ratio, respectively, predicted by WCOBRA/TRAC(M1.0) with those measured in Run 2-1.

Figures 7-16 (c) and 7-16 (d) show the integrated water film & lump and water droplet outlet flows, respectively, predicted by the code with those measured in the test. [

]

The inside metal temperatures predicted by the code are compared with the measured data in Figure 7-17. Likewise, the outside metal temperatures predicted by the code are compared with the measured data in Figure 7-18. [

]

### 7.3.3 Run 3-1 (Case with Decreased Reflooding Water Temperature, [ ])

Figures 7-19 (a) and 7-19 (b) compare the integrated total outlet flow and total outflow-to-inflow ratio, respectively, predicted by WCOBRA/TRAC(M1.0) with those measured in Run 3-1.

Figures 7-19 (c) and 7-19 (d) show the integrated water film & lump and water droplet outlet flows, respectively, predicted by the code with those measured in the test. [

]

[ ]

#### 7.3.4 Run 4-1 (Case with Decreased Initial Metal Temperature, [ ])

Figures 7-22 (a) and 7-22 (b) compare the integrated total outlet flow and total outflow-to-inflow ratio, respectively, predicted by WCOBRA/TRAC(M1.0) with those measured in Run 4-1.

[ ]

Figures 7-22 (c) and 7-22 (d) show the integrated water film & lump and water droplet outlet flows, respectively, predicted by the code with those measured in the test. [ ]

] ]

[ ]

#### 7.3.5 Run 5-1 (Case with Increased Upper Plenum Pressure, [ ])

Figures 7-25 (a) and 7-25 (b) compare the integrated total outlet flow and total outflow-to-inflow ratio, respectively, predicted by WCOBRA/TRAC(M1.0) with those measured in Run 5-1.

[ ]

Figures 7-25 (c) and 7-25 (d) show the integrated water film & lump and water droplet outlet flows, respectively, predicted by the code with those measured in the test. [ ]

]

[

### **7.3.6 Summary of Analysis Results**

Based on the analysis results for each of the five cases described in Subsections 7.3.1 through 7.3.5, the results of the confirmatory analyses using WCOBRA/TRAC(M1.0) can be summarized as follows:

[

---

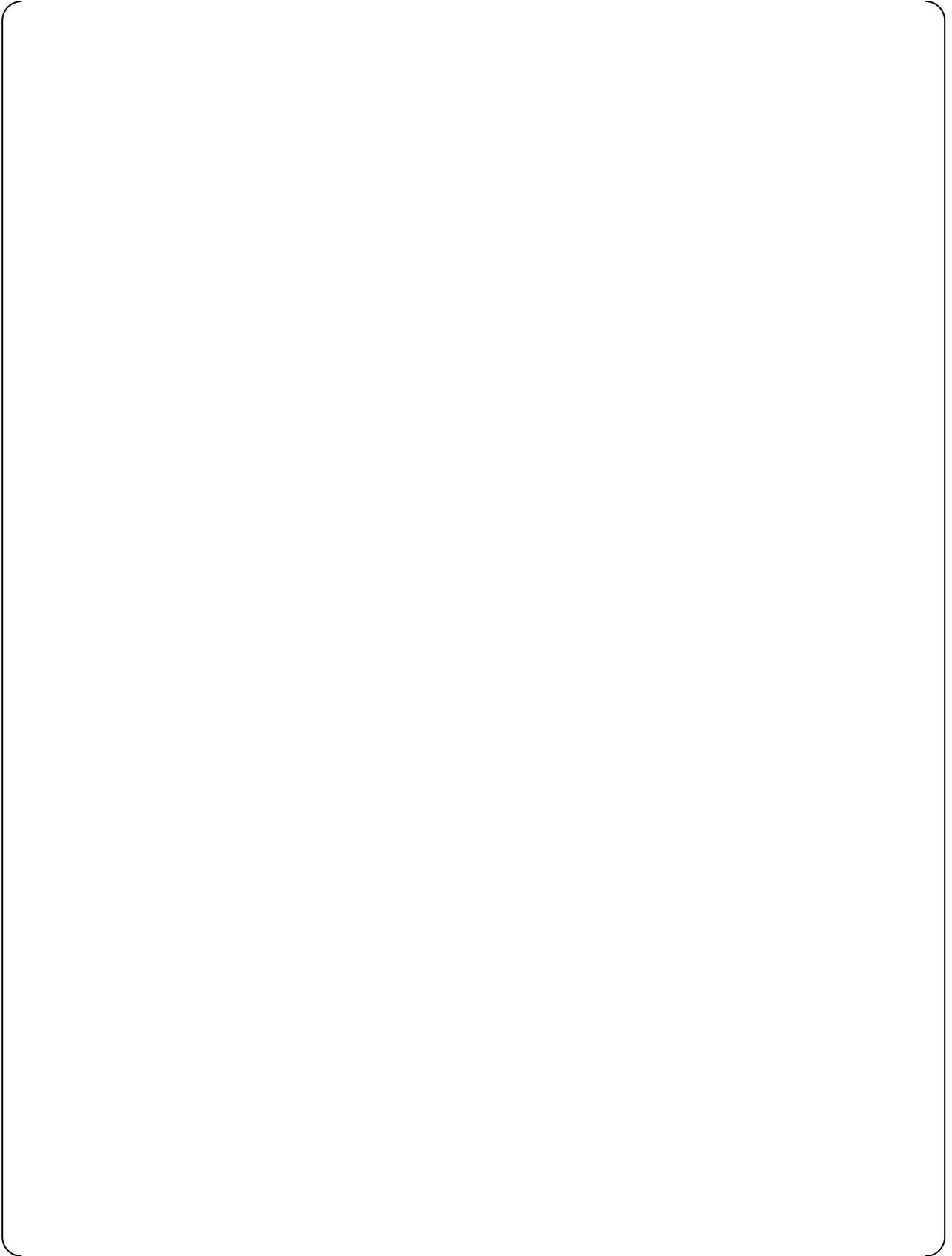
The quantification of the code prediction uncertainty is described in the following sections.

**7.4 Sensitivity of PCT for US-APWR to Energy Released from NR Metal**



**7.5 Estimation of Uncertainty in PCT for US-APWR Predicted by WCOBRA/TRAC(M1.0)**





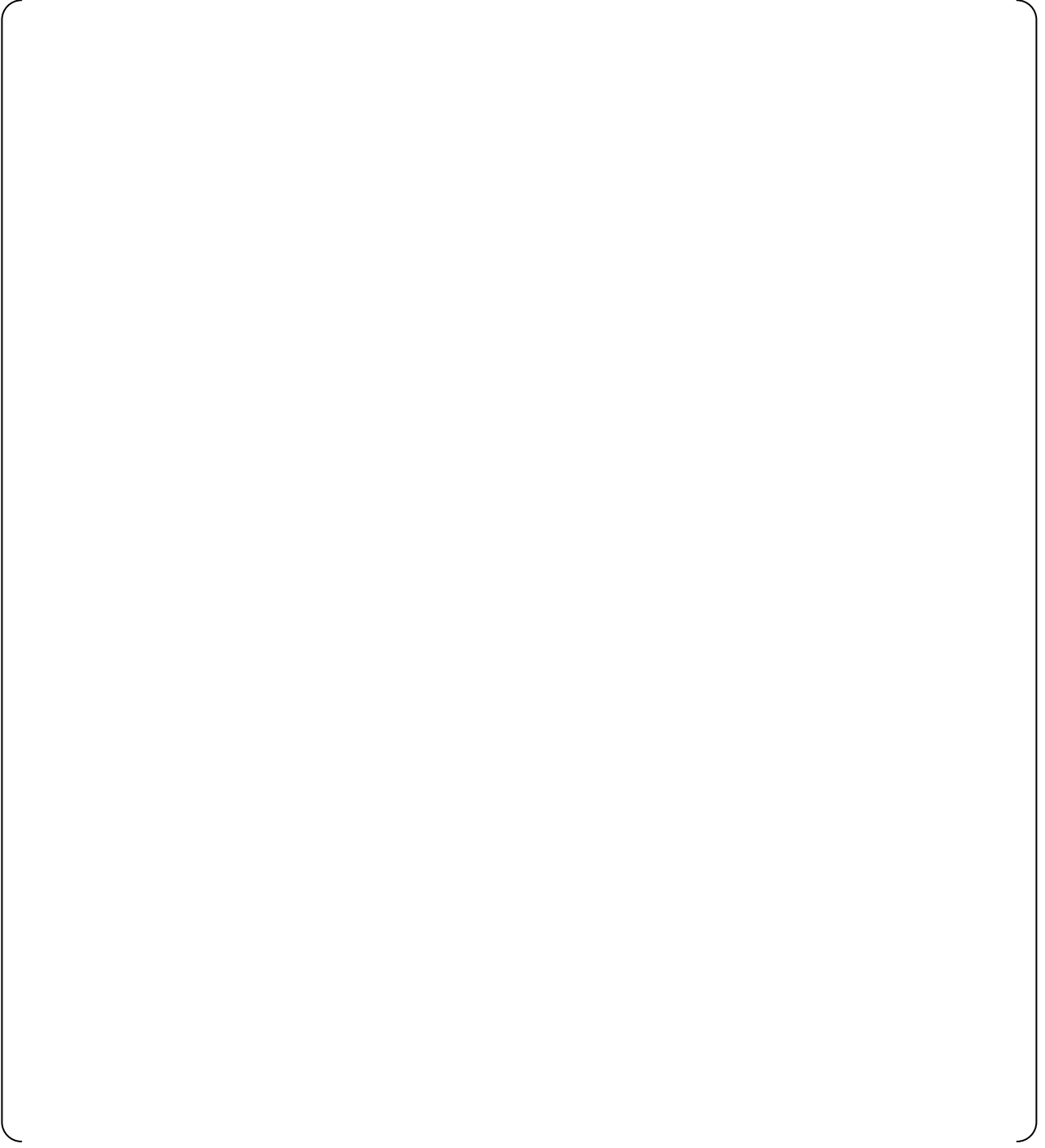


**Table 7-1    Conditions Used in Confirmatory Analyses Using WCOBRA/TRAC(M1.0)**

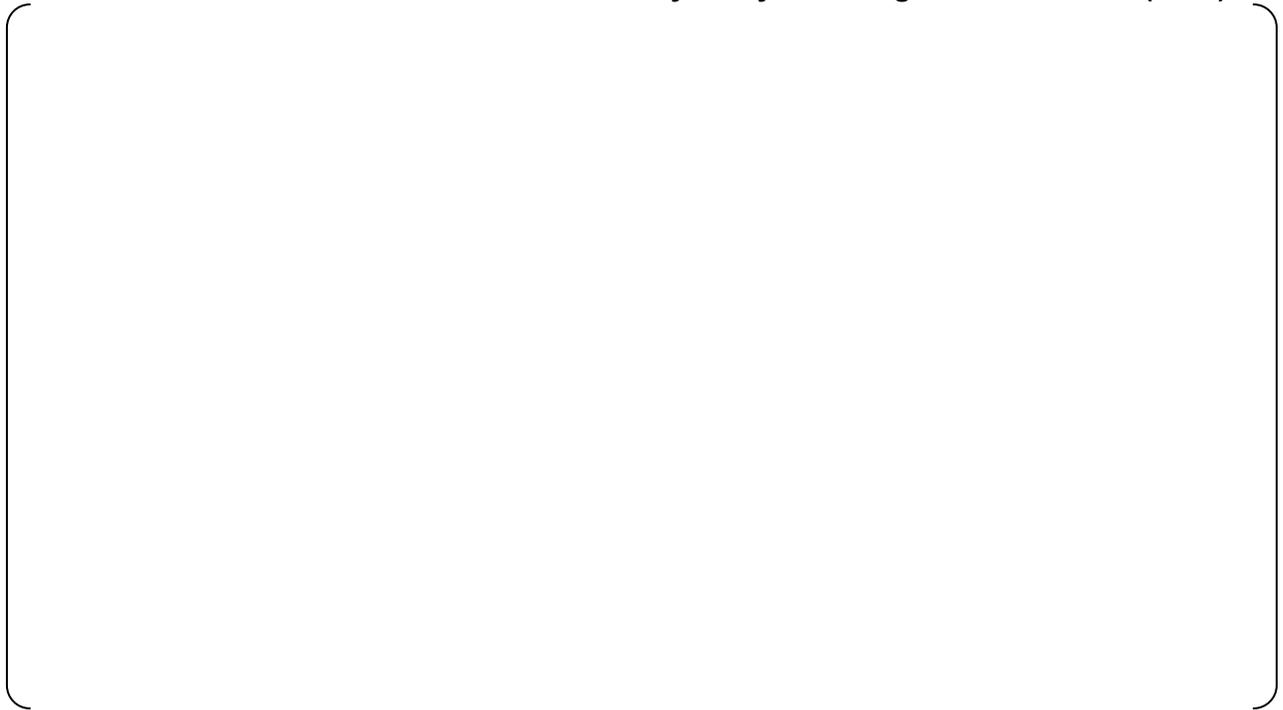


**Table 7-2    Uncertainty in Released Metal Energy Predicted by WCOBRA/TRAC(M1.0)**



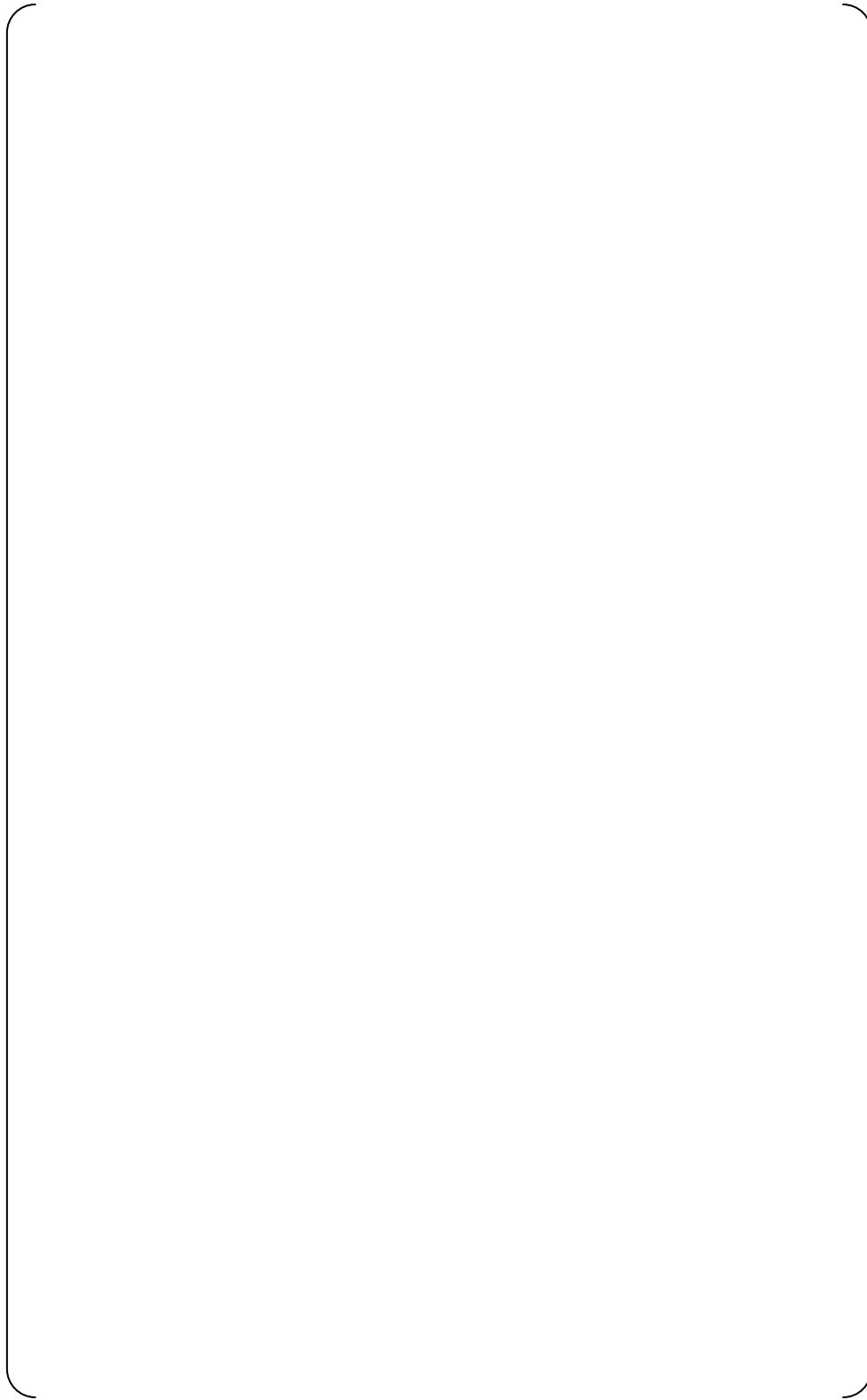


**Figure 7-1 Nodalization of Test Section for WCOBRA/TRAC(M1.0) Calculation**

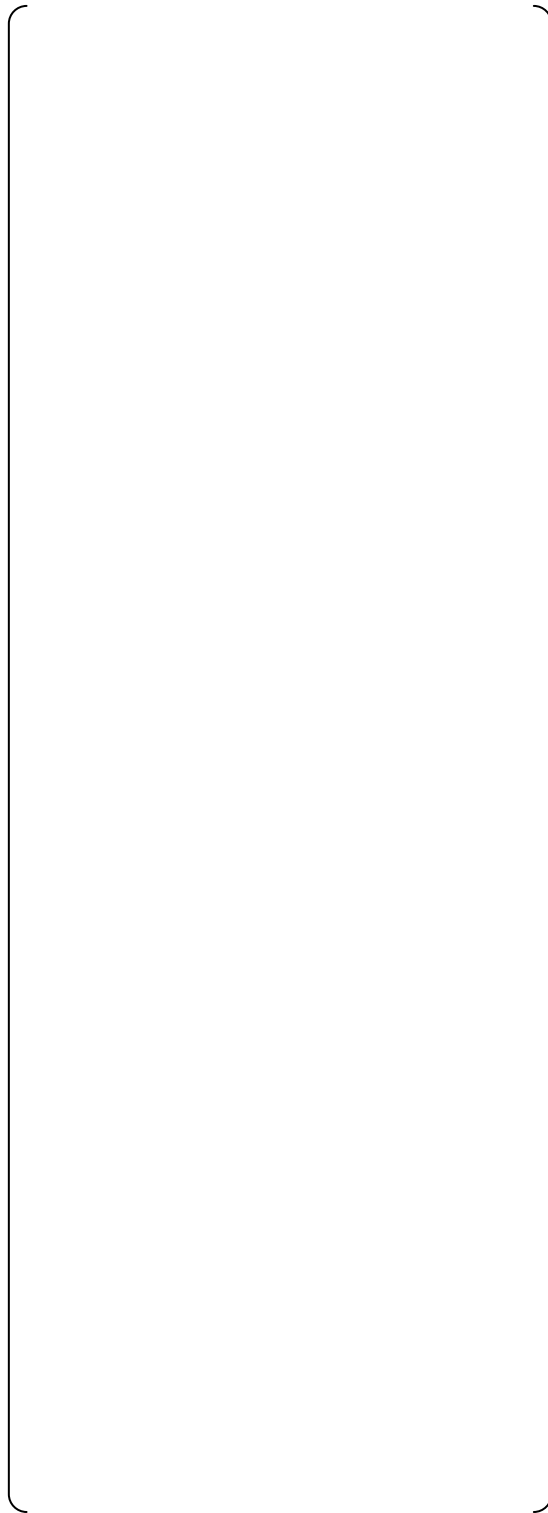


**Figure 7-2 Comparison of Axial Locations for Data Measurements and Axial Nodes for WCOBRA/TRAC(M1.0) Calculation**



**Figure 7-3** Transient Inlet Flow Boundary Condition for WCOBRA/TRAC(M1.0) Calculation (Run 1-1: Reference Case)



**Figure 7-4** Transient Outlet Pressure Boundary Condition for WCOBRA/TRAC(M1.0) Calculation (Run 1-1: Reference Case)



**Figure 7-5** Transient Inlet Flow Boundary Condition for WCOBRA/TRAC(M1.0) Calculation (Run 2-1: Reflooding Water Velocity = [ ])



**Figure 7-6** Transient Outlet Pressure Boundary Condition for WCOBRA/TRAC(M1.0) Calculation (Run 2-1: Reflooding Water Velocity = [ ])



**Figure 7-7** Transient Inlet Flow Boundary Condition for WCOBRA/TRAC(M1.0) Calculation (Run 3-1: Reflooding Water Temperature = [ ])



**Figure 7-8** Transient Outlet Pressure Boundary Condition for WCOBRA/TRAC(M1.0) Calculation (Run 3-1: Reflooding Water Temperature = [ ])



**Figure 7-9** Transient Inlet Flow Boundary Condition for WCOBRA/TRAC(M1.0) Calculation (Run 4-1: Initial Metal Temperature = [ ] )



**Figure 7-10** Transient Outlet Pressure Boundary Condition for WCOBRA/TRAC(M1.0) Calculation (Run 4-1: Initial Metal Temperature = [ ] )



**Figure 7-11 Transient Inlet Flow Boundary Condition for WCOBRA/TRAC(M1.0) Calculation (Run 5-1: Upper Plenum Pressure = [ ])**



**Figure 7-12 Transient Outlet Pressure Boundary Condition for WCOBRA/TRAC(M1.0) Calculation (Run 5-1: Upper Plenum Pressure = [ ])**

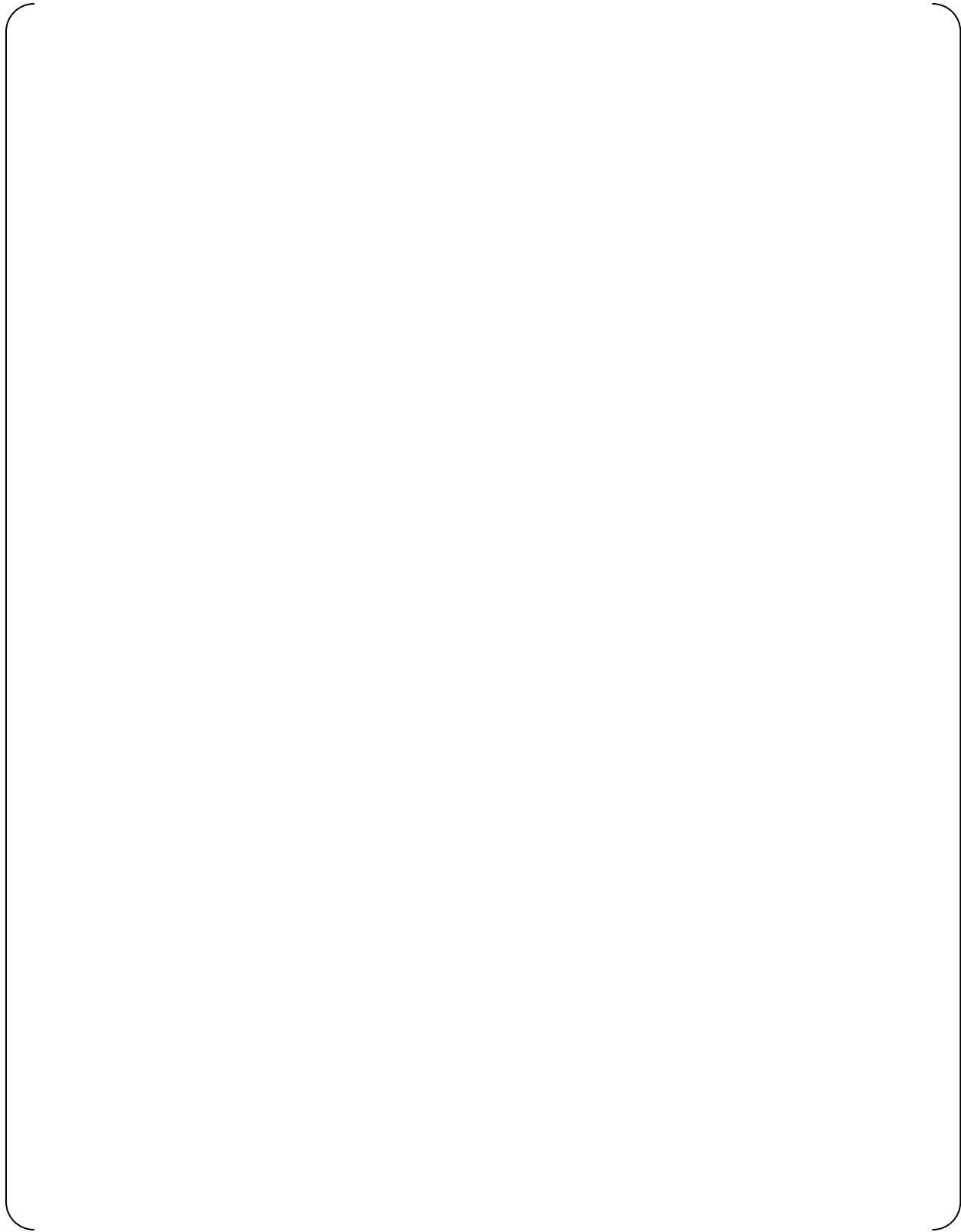


**Figure 7-13 Comparison of Integrated Outlet Flows Predicted by WCOBRA/TRAC(M1.0) with Measured Data (Run 1-1: Reference Case)**

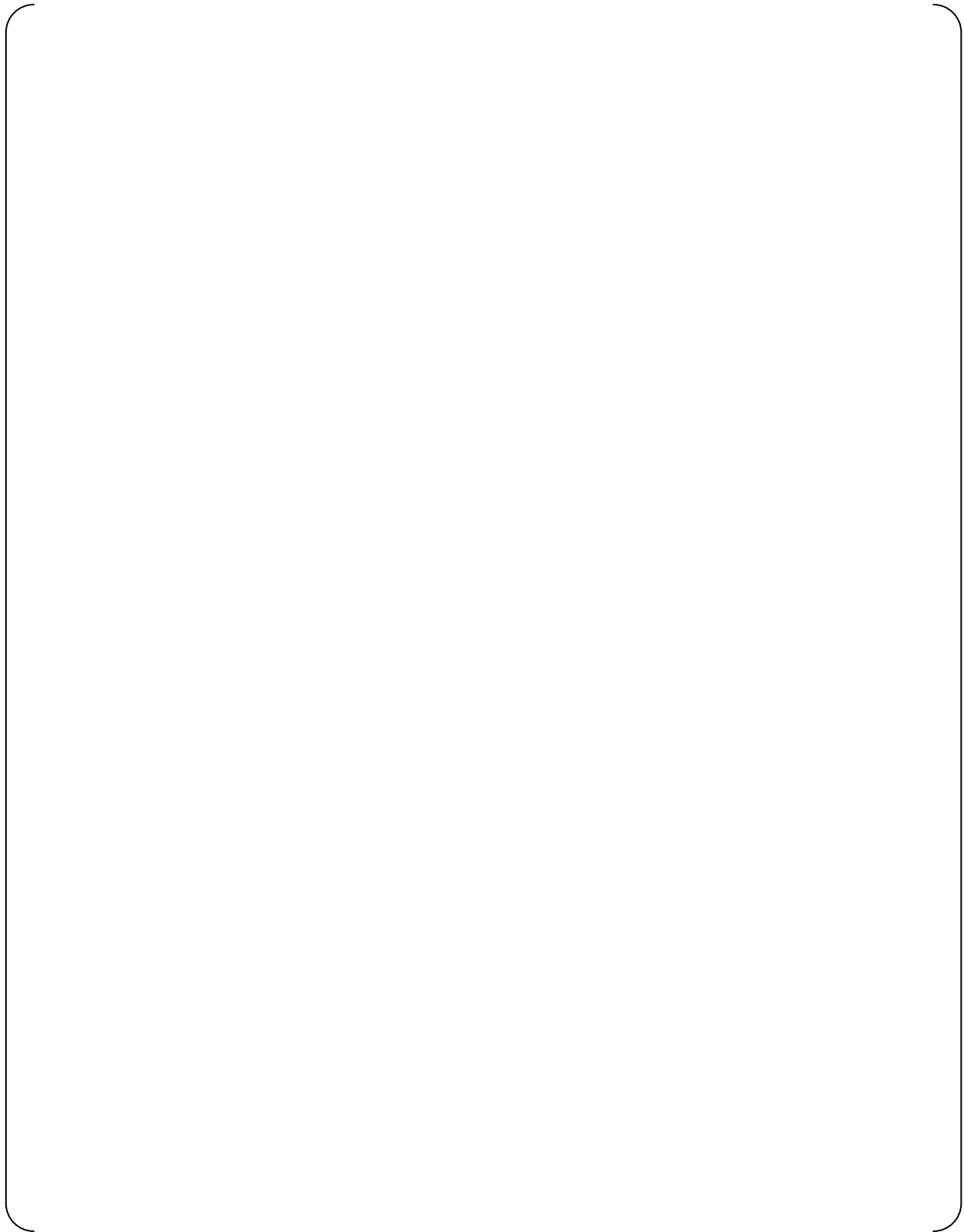


**Figure 7-14 Comparison of Inside Metal Temperature Distribution Predicted by WCOBRA/TRAC(M1.0) with Measured Data (Run 1-1: Reference Case)**

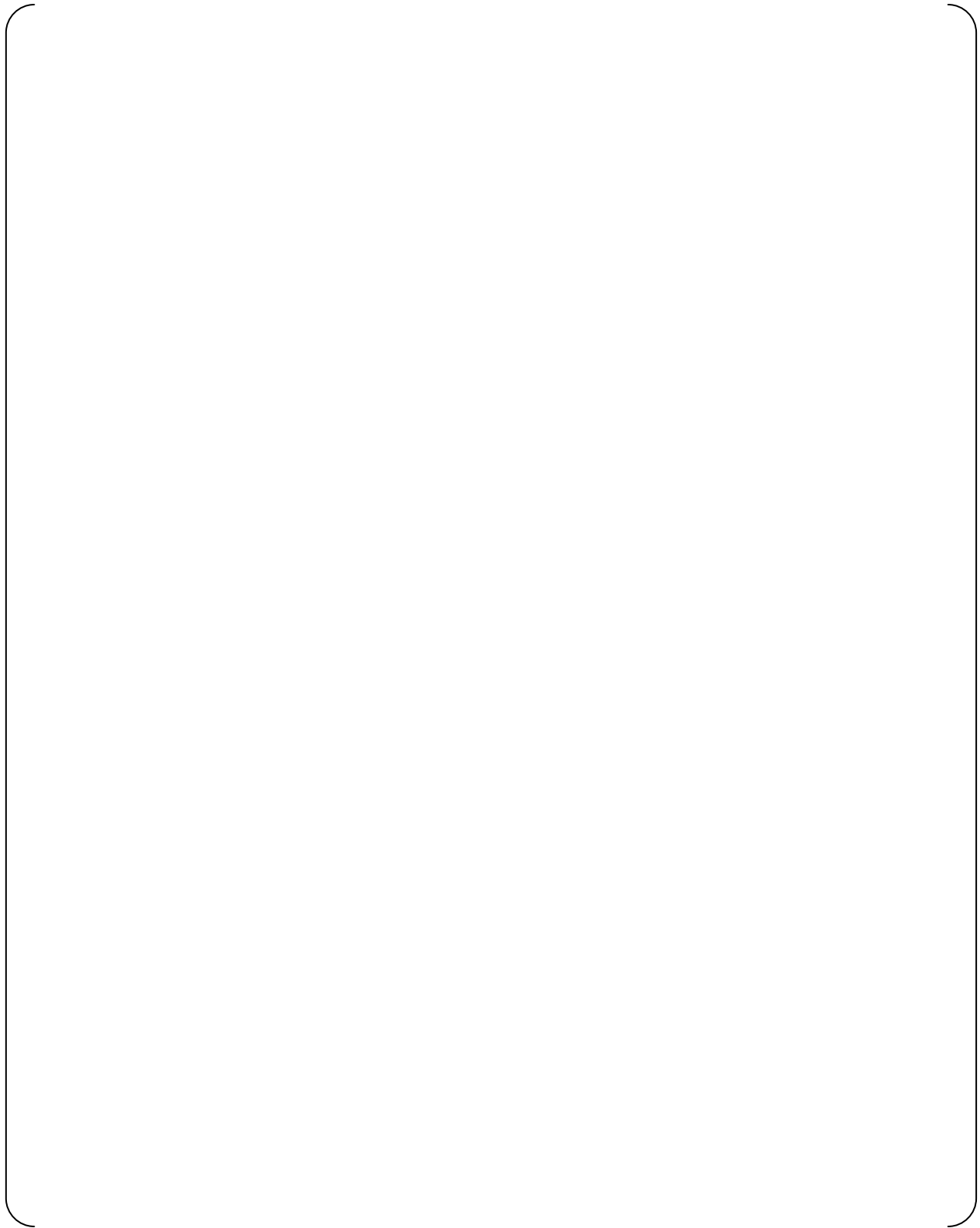


**Figure 7-15 Comparison of Outside Metal Temperature Distribution Predicted by WCOBRA/TRAC(M1.0) with Measured Data (Run 1-1: Reference Case)**

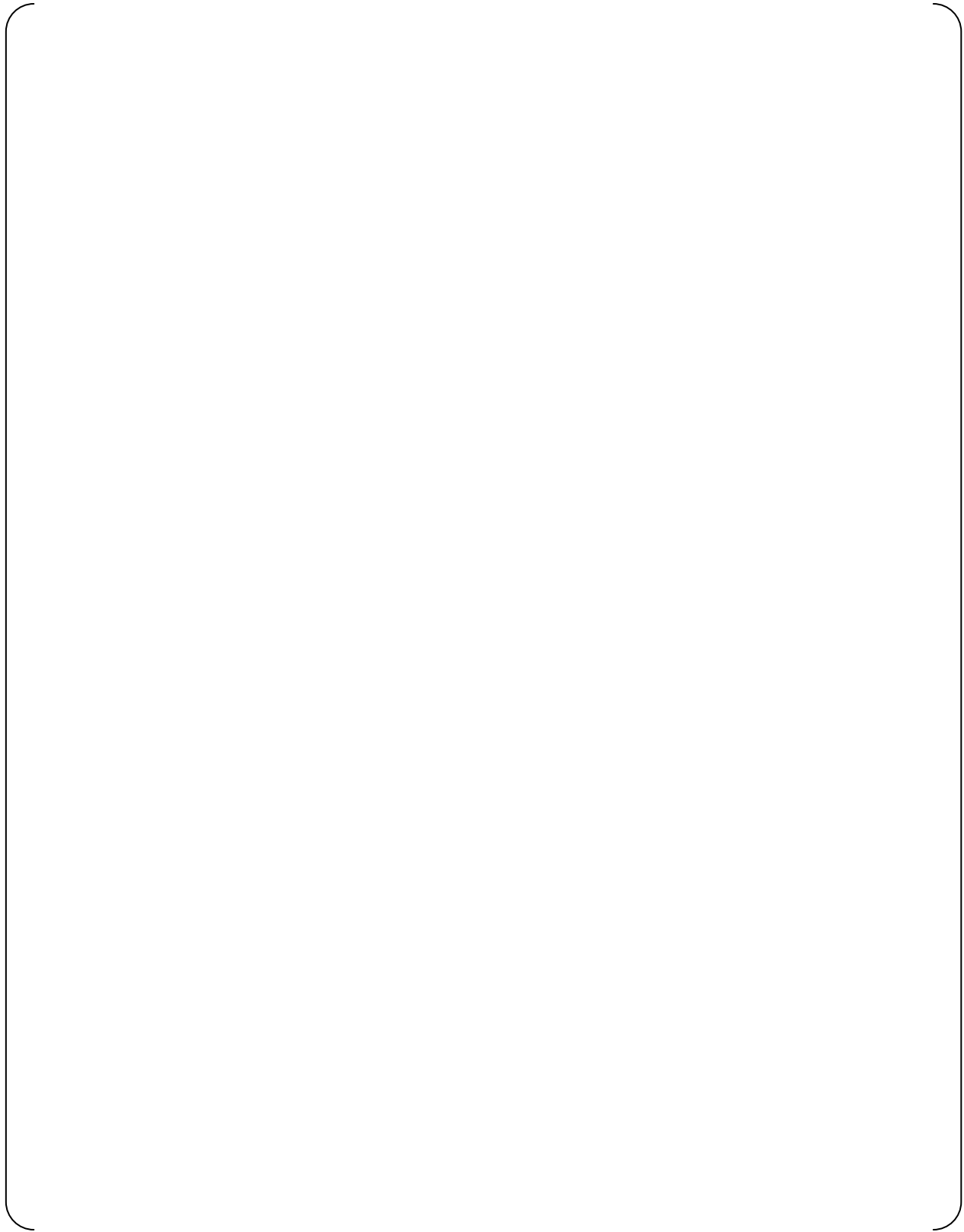


**Figure 7-16 Comparison of Integrated Outlet Flows Predicted by WCOBRA/TRAC(M1.0) with Measured Data (Run 2-1: Reflooding Water Velocity = [ ])**

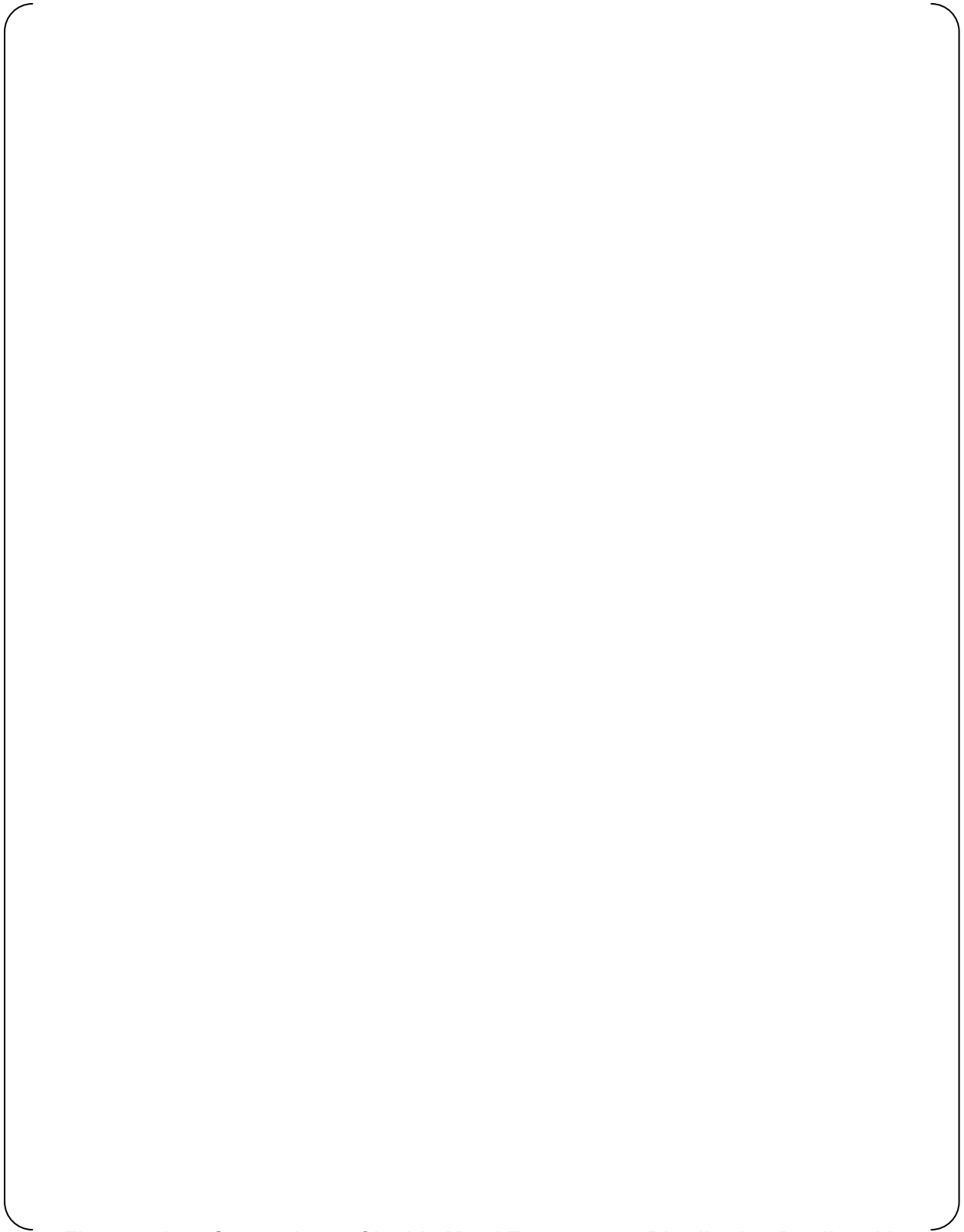


**Figure 7-17 Comparison of Inside Metal Temperature Distribution Predicted by WCOBRA/TRAC(M1.0) with Measured Data (Run 2-1: Reflooding Water Velocity = [ ])**

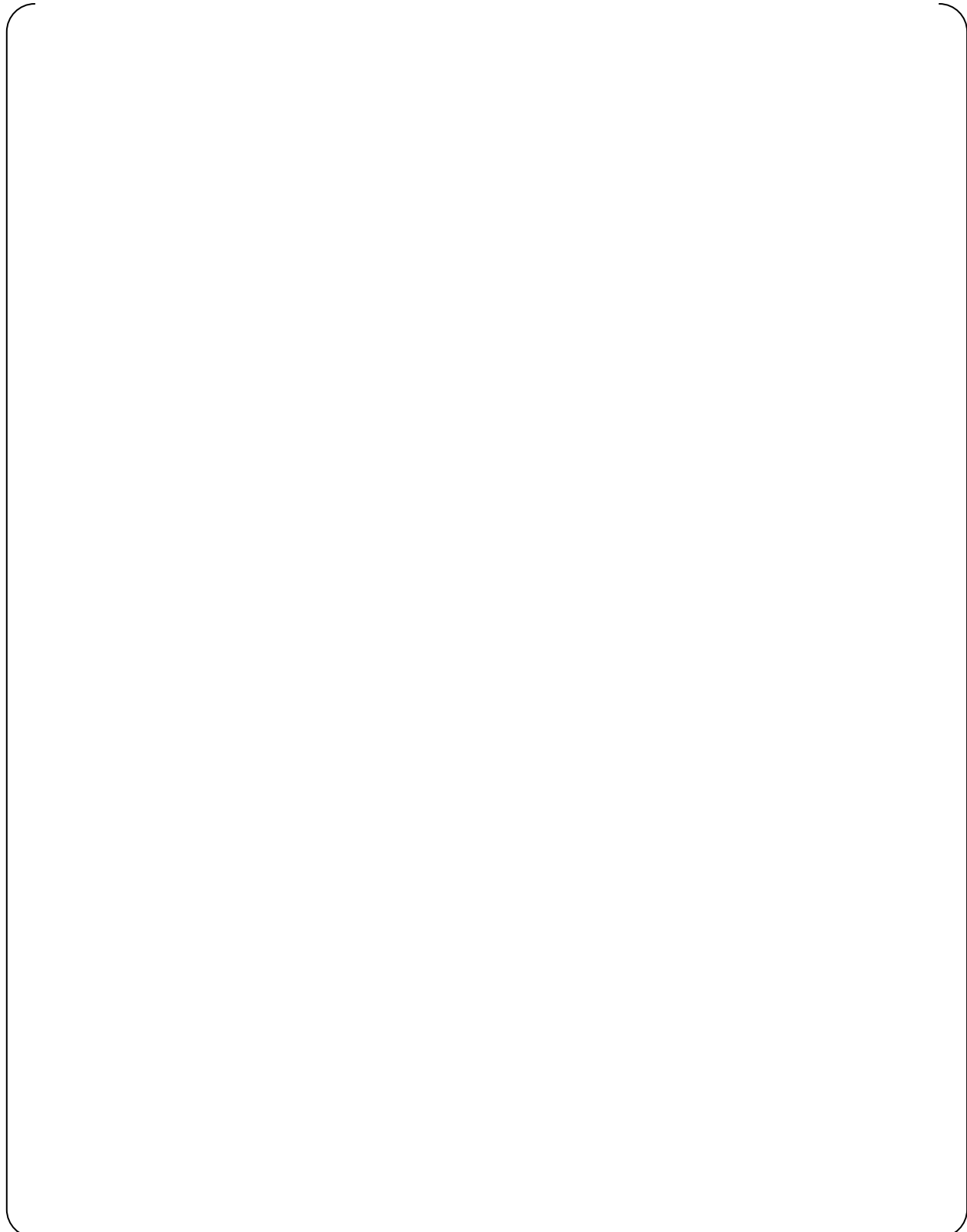


**Figure 7-18 Comparison of Outside Metal Temperature Distribution Predicted by WCOBRA/TRAC(M1.0) with Measured Data (Run 2-1: Reflooding Water Velocity = [ ])**

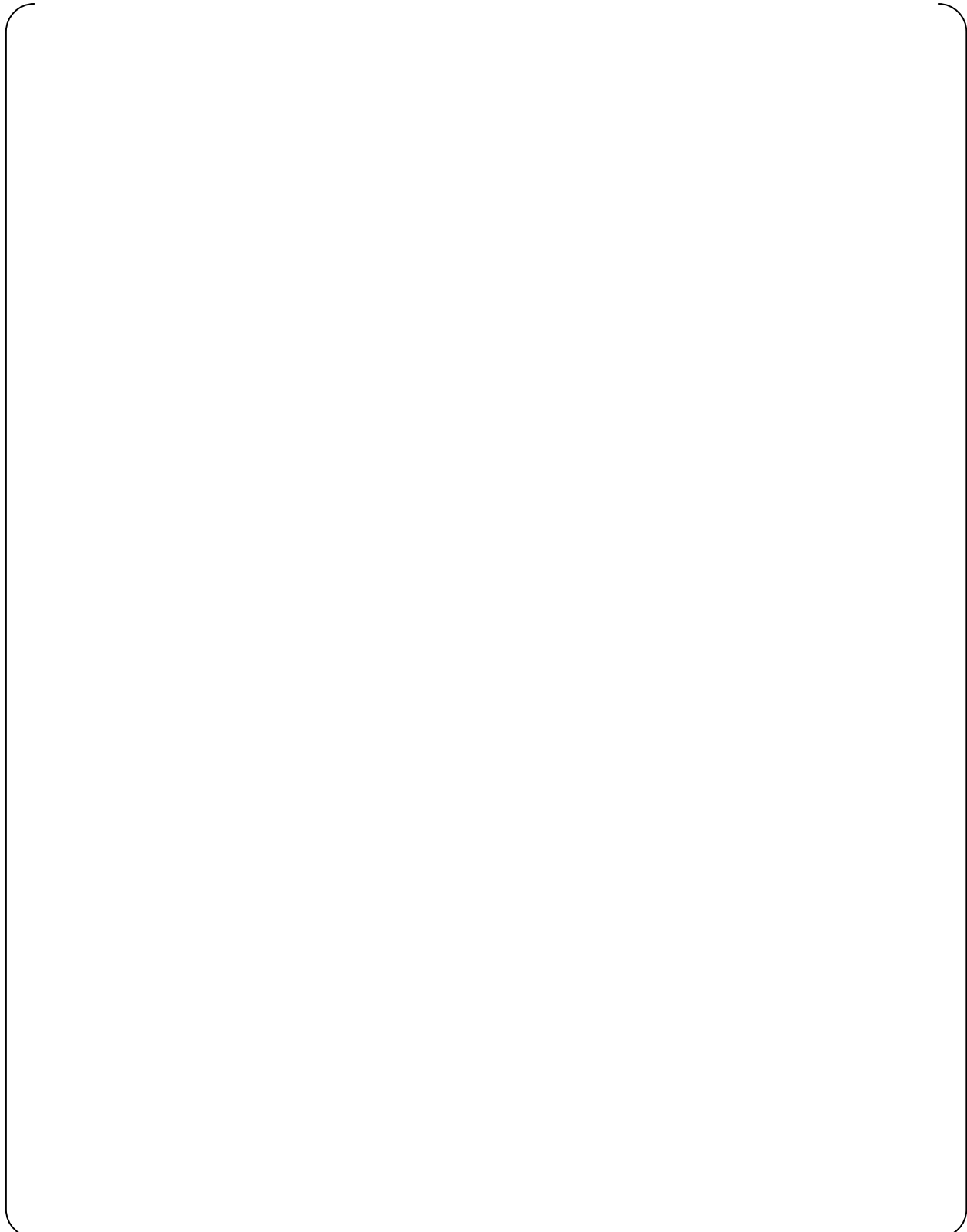


**Figure 7-19 Comparison of Integrated Outlet Flows Predicted by WCOBRA/TRAC(M1.0) with Measured Data (Run 3-1: Reflooding Water Temperature = [ ])**

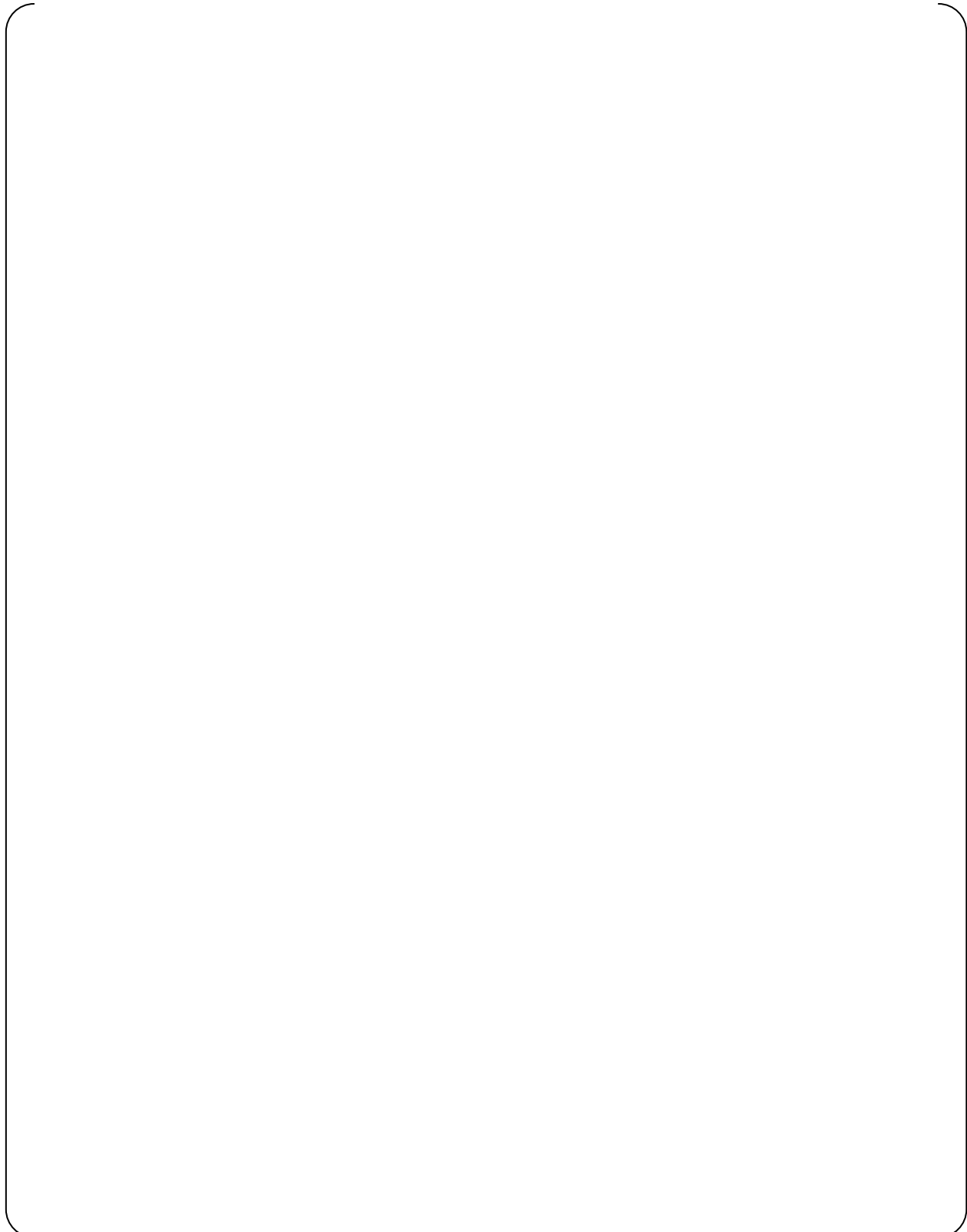


**Figure 7-20 Comparison of Inside Metal Temperature Distribution Predicted by WCOBRA/TRAC(M1.0) with Measured Data (Run 3-1: Reflooding Water Temperature = [ ])**

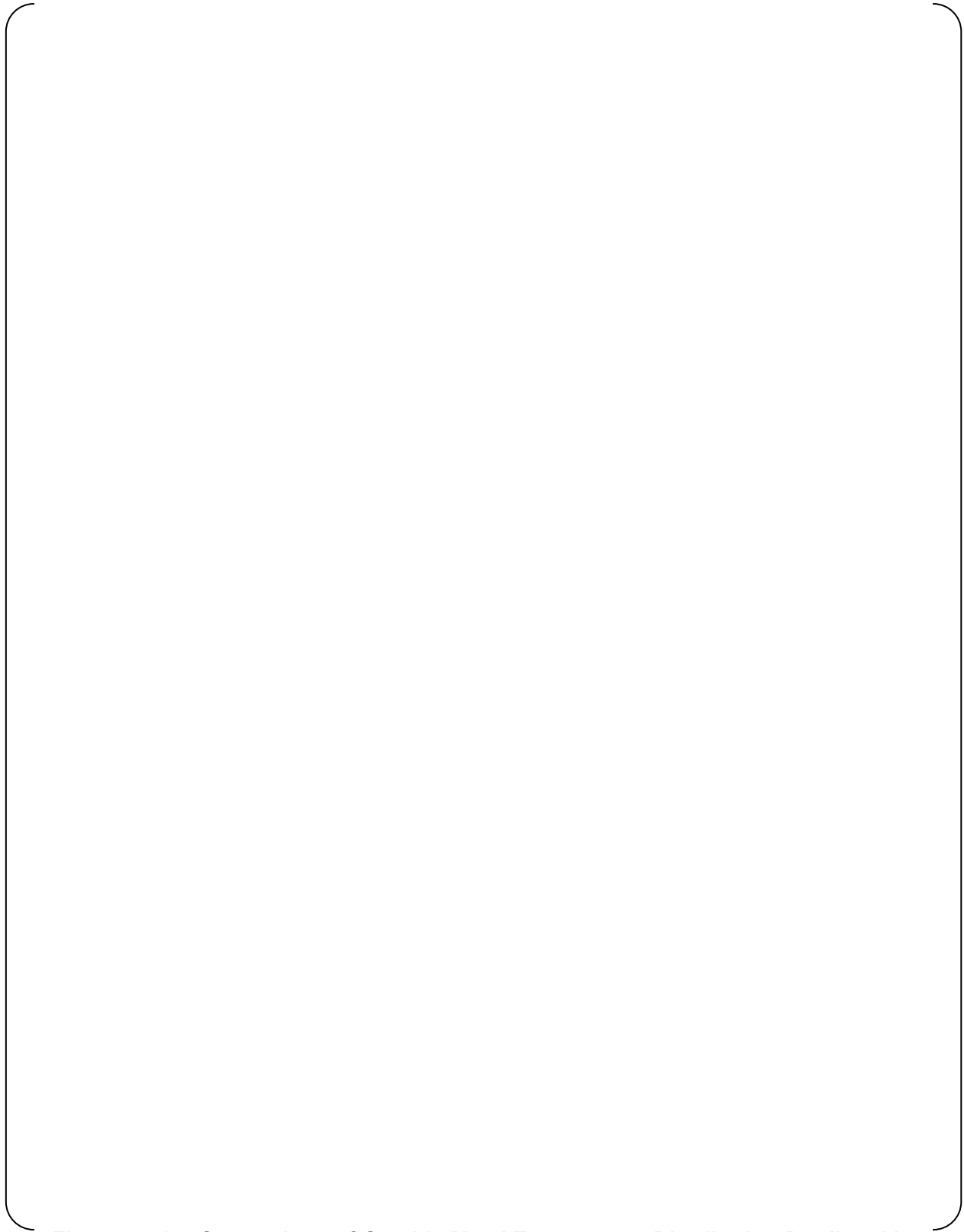


**Figure 7-21 Comparison of Outside Metal Temperature Distribution Predicted by WCOBRA/TRAC(M1.0) with Measured Data (Run 3-1: Reflooding Water Temperature = [ ])**

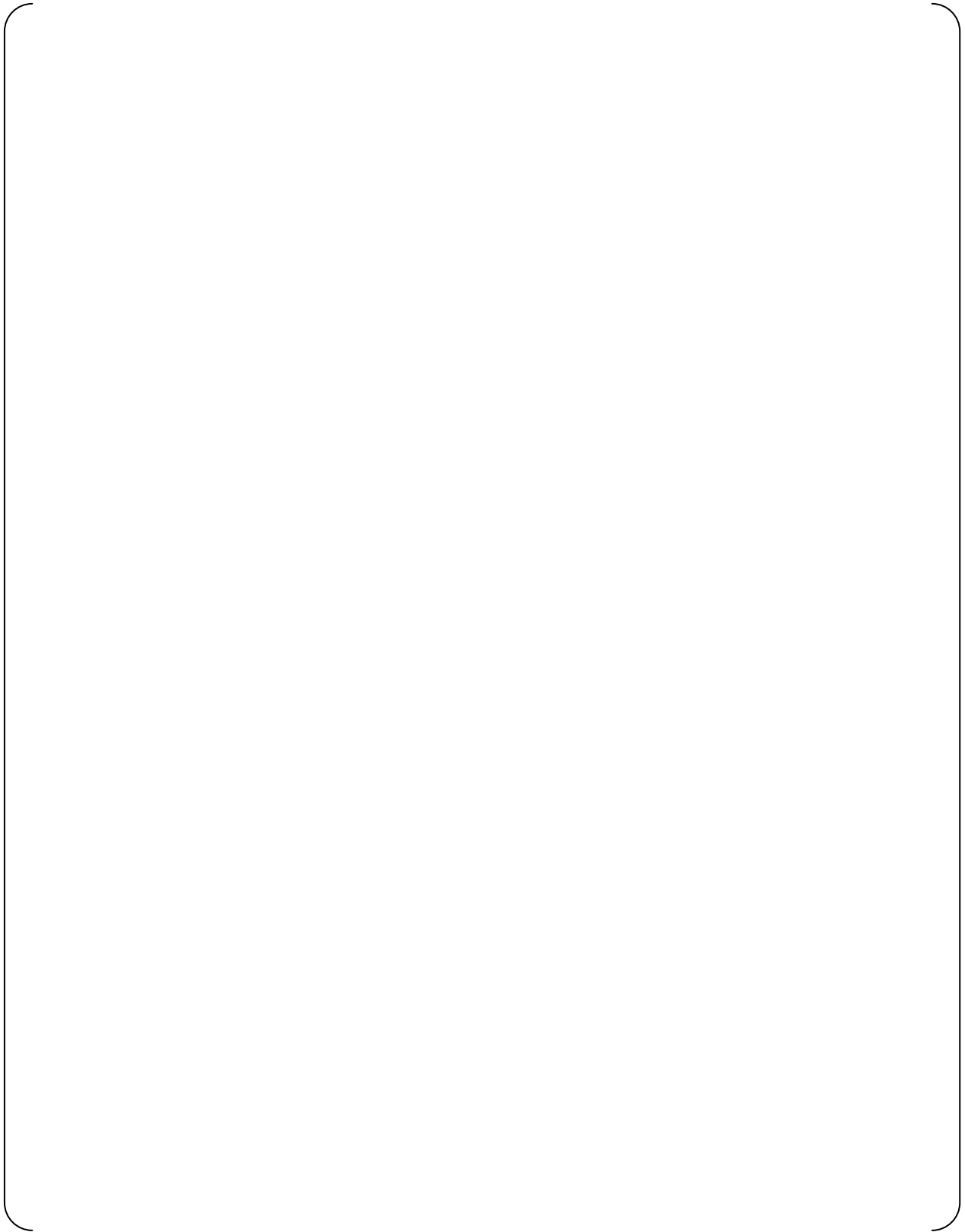


**Figure 7-22 Comparison of Integrated Outlet Flows Predicted by  
WCOBRA/TRAC(M1.0) with Measured Data  
(Run 4-1: Initial Metal Temperature = [ ])**

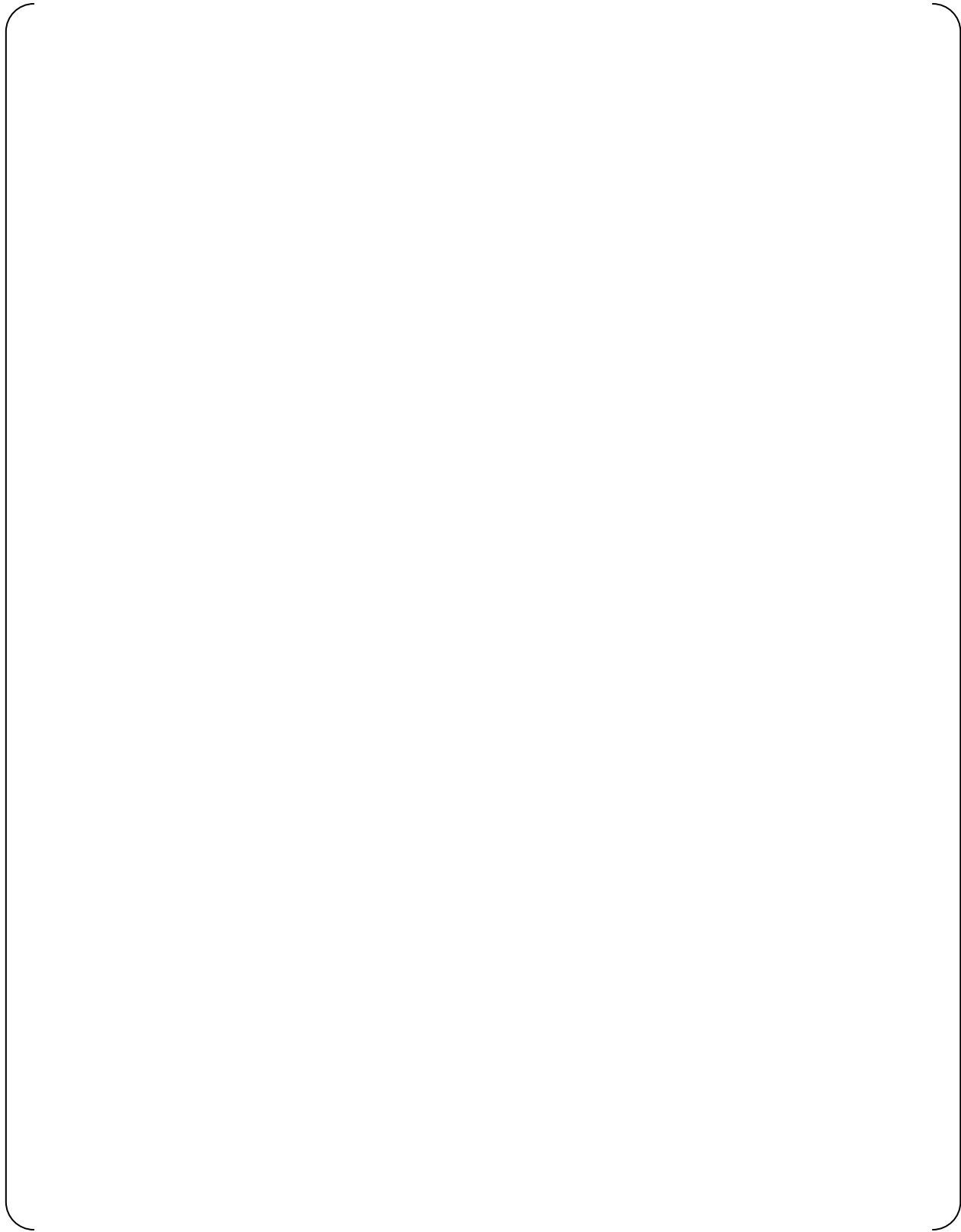


**Figure 7-23 Comparison of Inside Metal Temperature Distribution Predicted by WCOBRA/TRAC(M1.0) with Measured Data (Run 4-1: Initial Metal Temperature = [ ])**

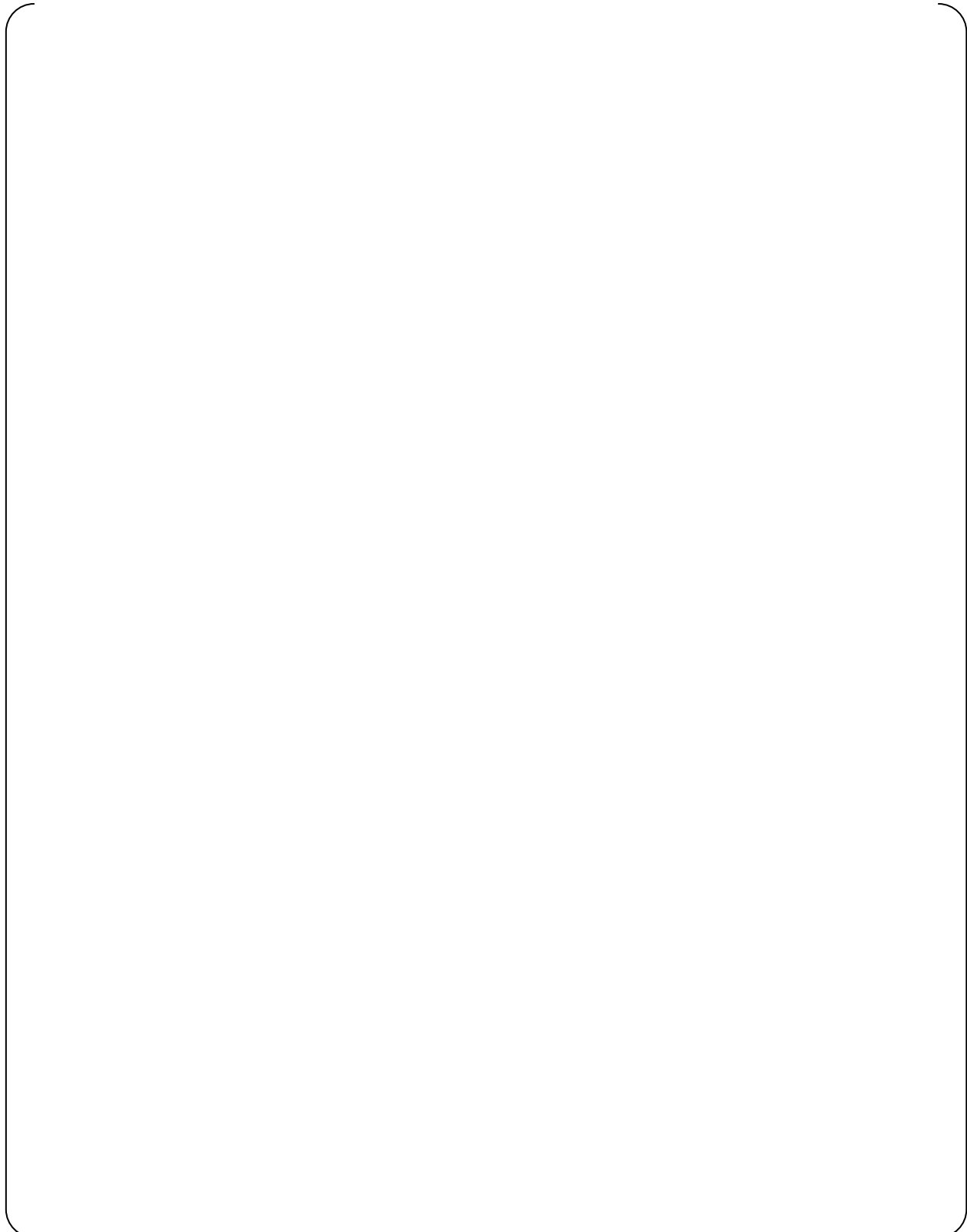


**Figure 7-24 Comparison of Outside Metal Temperature Distribution Predicted by WCOBRA/TRAC(M1.0) with Measured Data (Run 4-1: Initial Metal Temperature = [ ])**

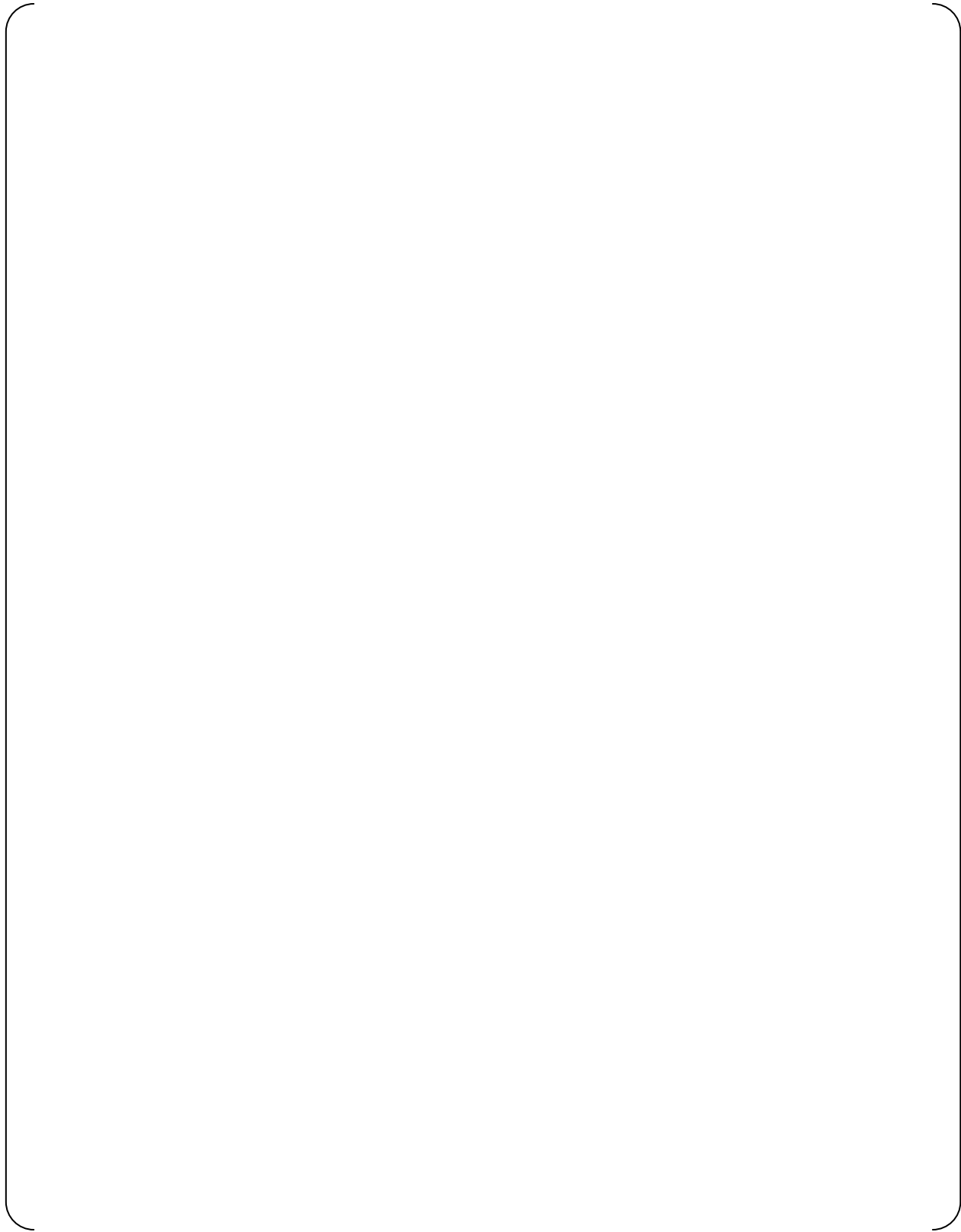


**Figure 7-25 Comparison of Integrated Outlet Flows Predicted by  
WCOBRA/TRAC(M1.0) with Measured Data  
(Run 5-1: Upper Plenum Pressure = [ ])**

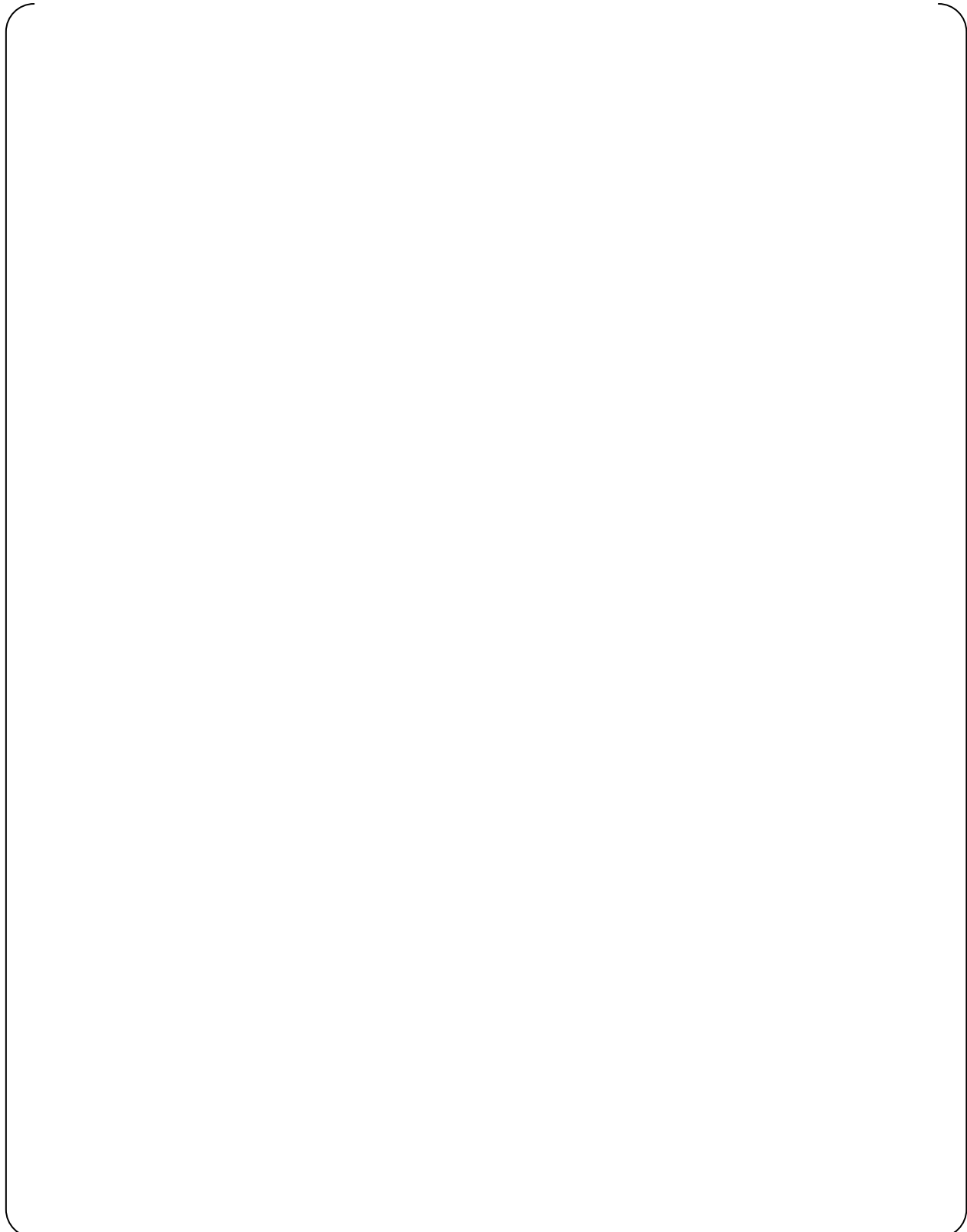


**Figure 7-26 Comparison of Inside Metal Temperature Distribution Predicted by WCOBRA/TRAC(M1.0) with Measured Data (Run 5-1: Upper Plenum Pressure = [ ])**

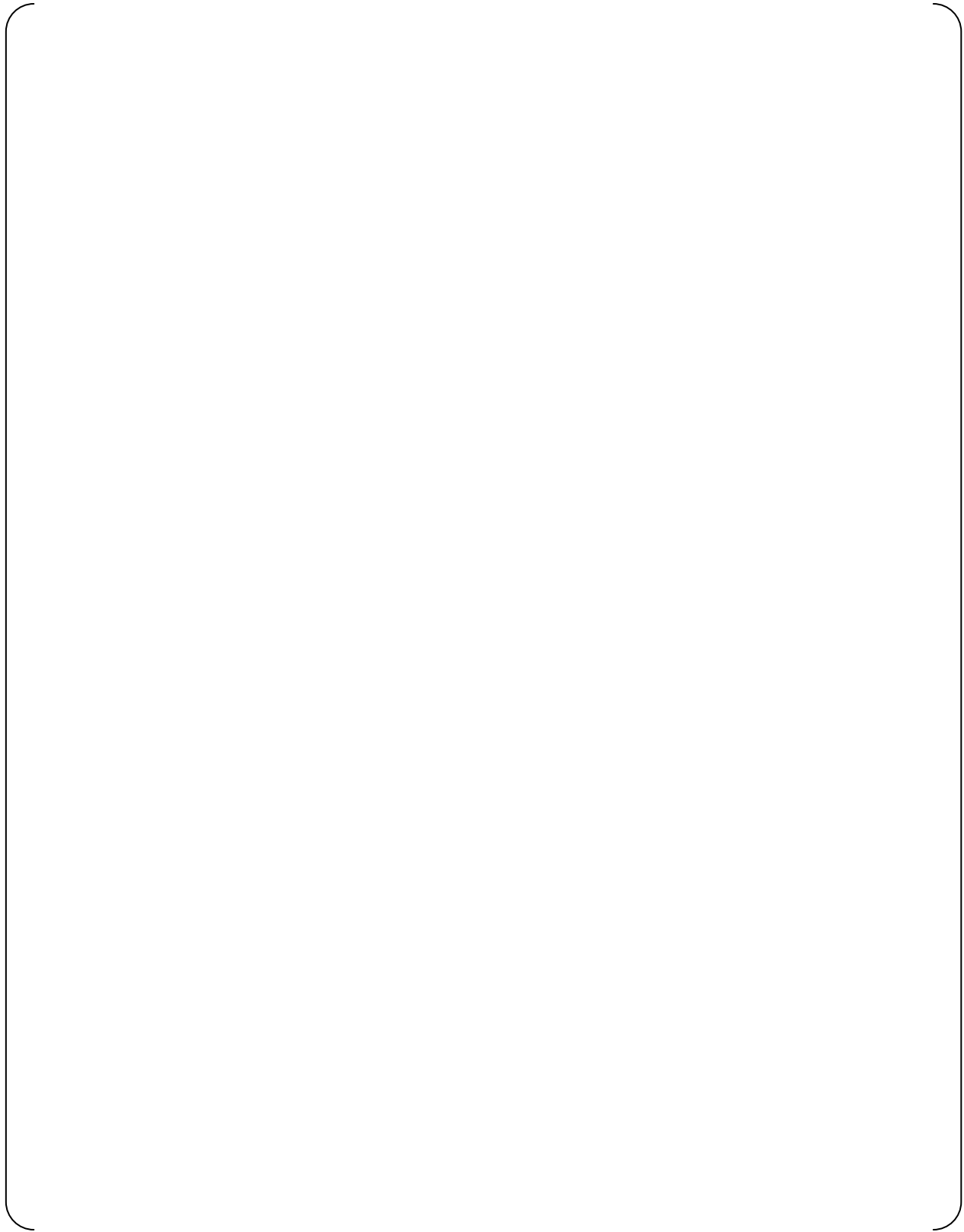


**Figure 7-27 Comparison of Outside Metal Temperature Distribution Predicted by WCOBRA/TRAC(M1.0) with Measured Data (Run 5-1: Upper Plenum Pressure = [ ])**



**Figure 7-28 Effect of Neutron Reflector on Peak Cladding Temperature in US-APWR during LBLOCA Reflooding Phase**



**Figure 7-29 Comparison of Energy Released from NR Metal Predicted by WCOBRA/TRAC(M1.0) with Measured Data (Run 3-1: Reflooding Water Temperature = [ ])**



**Figure 7-30 Uncertainty in Prediction of Energy Released from NR Metal by WCOBRA/TRAC(M1.0) (Run 3-1: Reflooding Water Temperature = [ ])**

## 8.0 CONCLUSIONS

In order to confirm the applicability of the WCOBRA/TRAC(M1.0) code to the thermal-hydraulic analysis of the NR in the US-APWR during the LBLOCA reflooding phase, a series of reflooding tests and thermal-hydraulic analyses using WCOBRA/TRAC(M1.0) were performed. The NR reflooding confirmatory tests were performed using the test section of the same length, hydraulic diameter, heat capacity, and material as those of the NR in the US-APWR. The confirmatory analyses were performed using WCOBRA/TRAC(M1.0) and the key parameters predicted by the code were compared with the measured test data. [

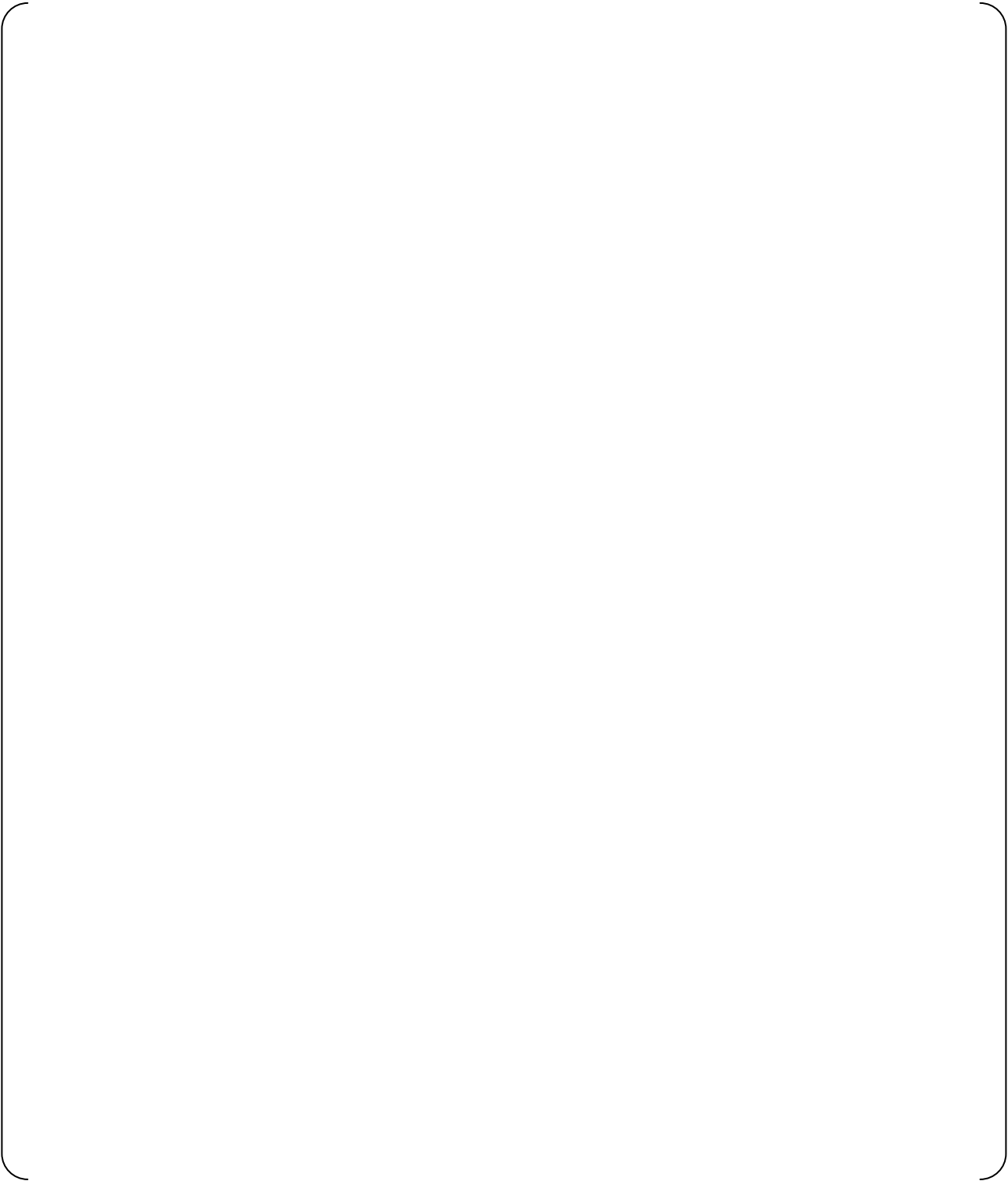
] Therefore, it has been confirmed that the WCOBRA/TRAC(M1.0) code can be applied to the thermal-hydraulic analysis of the NR in the US-APWR during the LBLOCA reflooding phase.

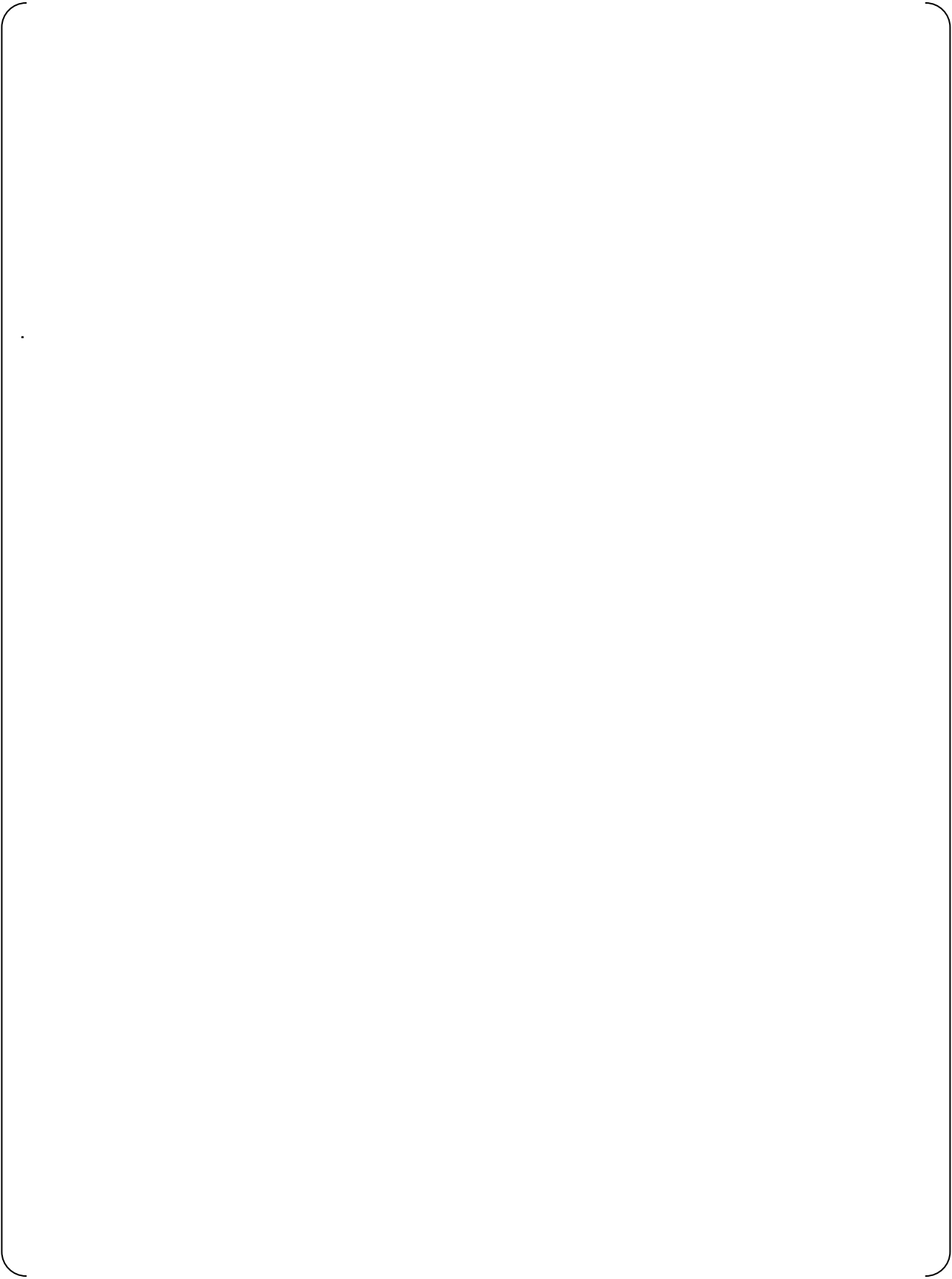
**9.0 REFERENCES**

1. Suzuta, T. and Teramae, T., "Large Break LOCA Code Applicability Report for US-APWR," MUAP-07011-P(R0), Mitsubishi Heavy Industries, Ltd., July 2007.
2. Babelli, I., Revankar, S. T., and Ishii, M., "Flow Visualization Study of Post-Critical Heat Flux in Inverted Flow," Nuclear Engineering and Design, Vol. 146, pp. 15-24, 1994.

**APPENDIX A Calibration of Measurement Systems**

**A.1 Calibration of Measurement System in Test Period**





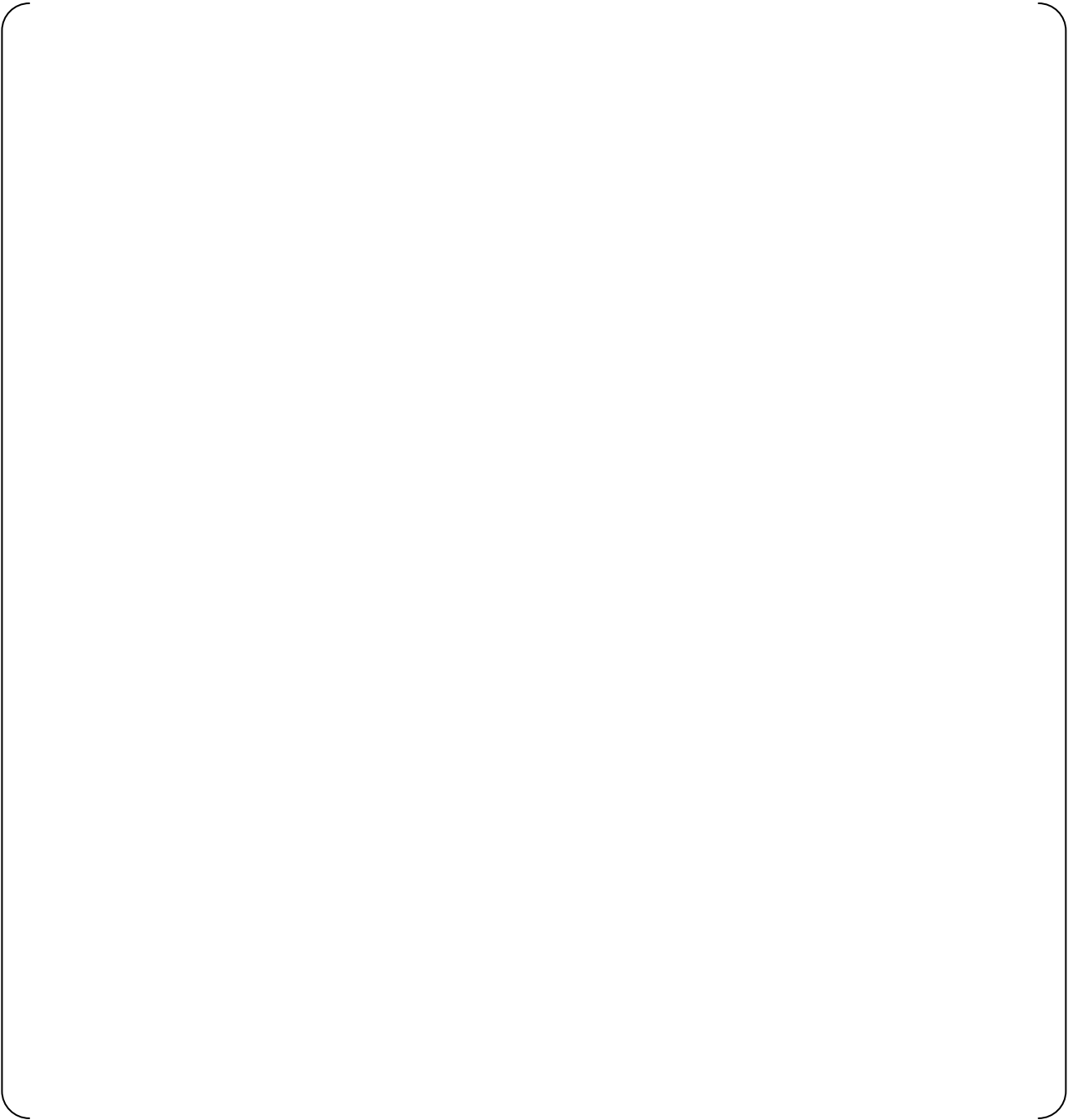


**Table A-1 Calibration and Confirmation of Soundness of Measurement System throughout Test Period**

**A.2 Calibration and Soundness Confirmation Results**



**Table A-2 Calibration Results**

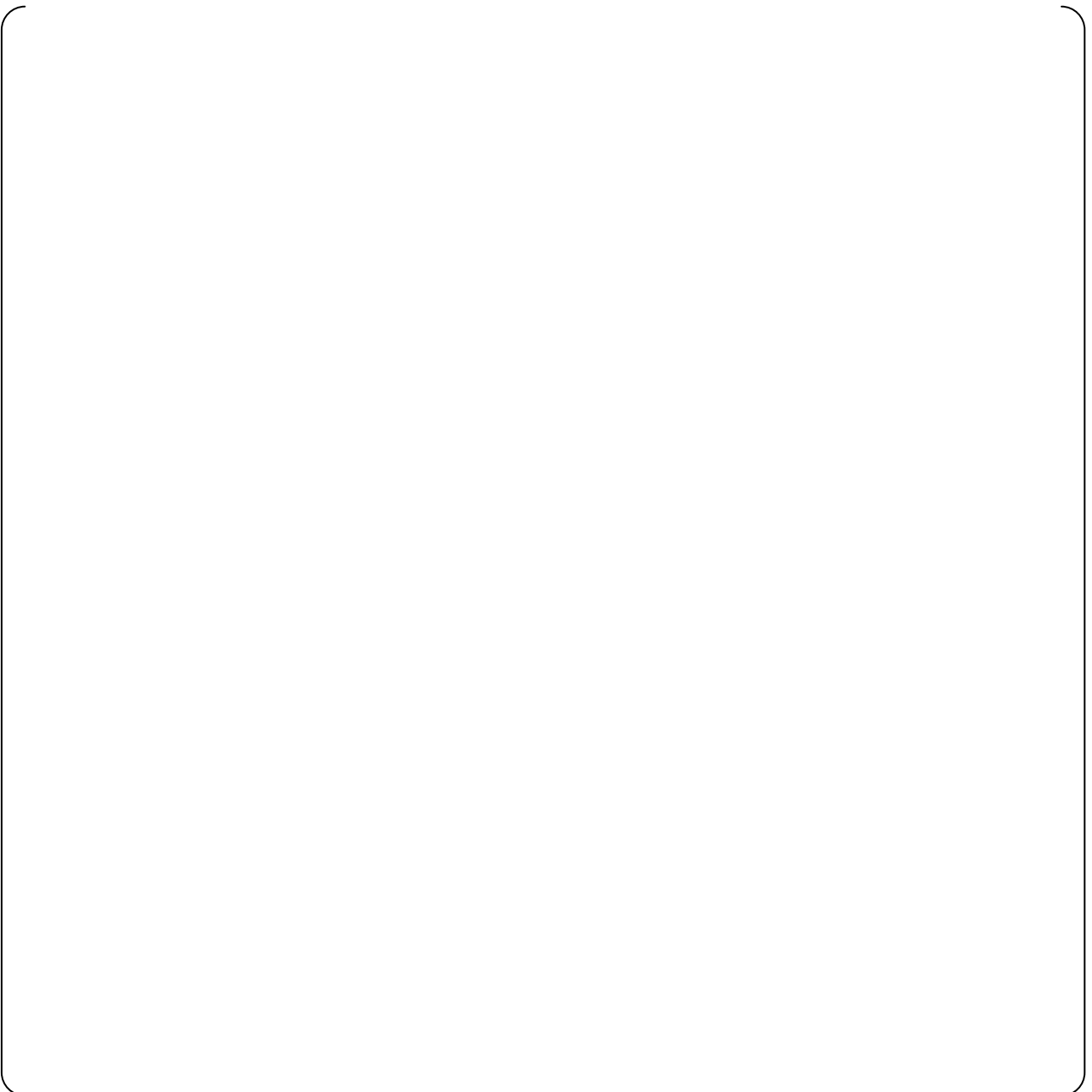


## **APPENDIX B Measurement System Uncertainty**

### **B.1 Abstract**

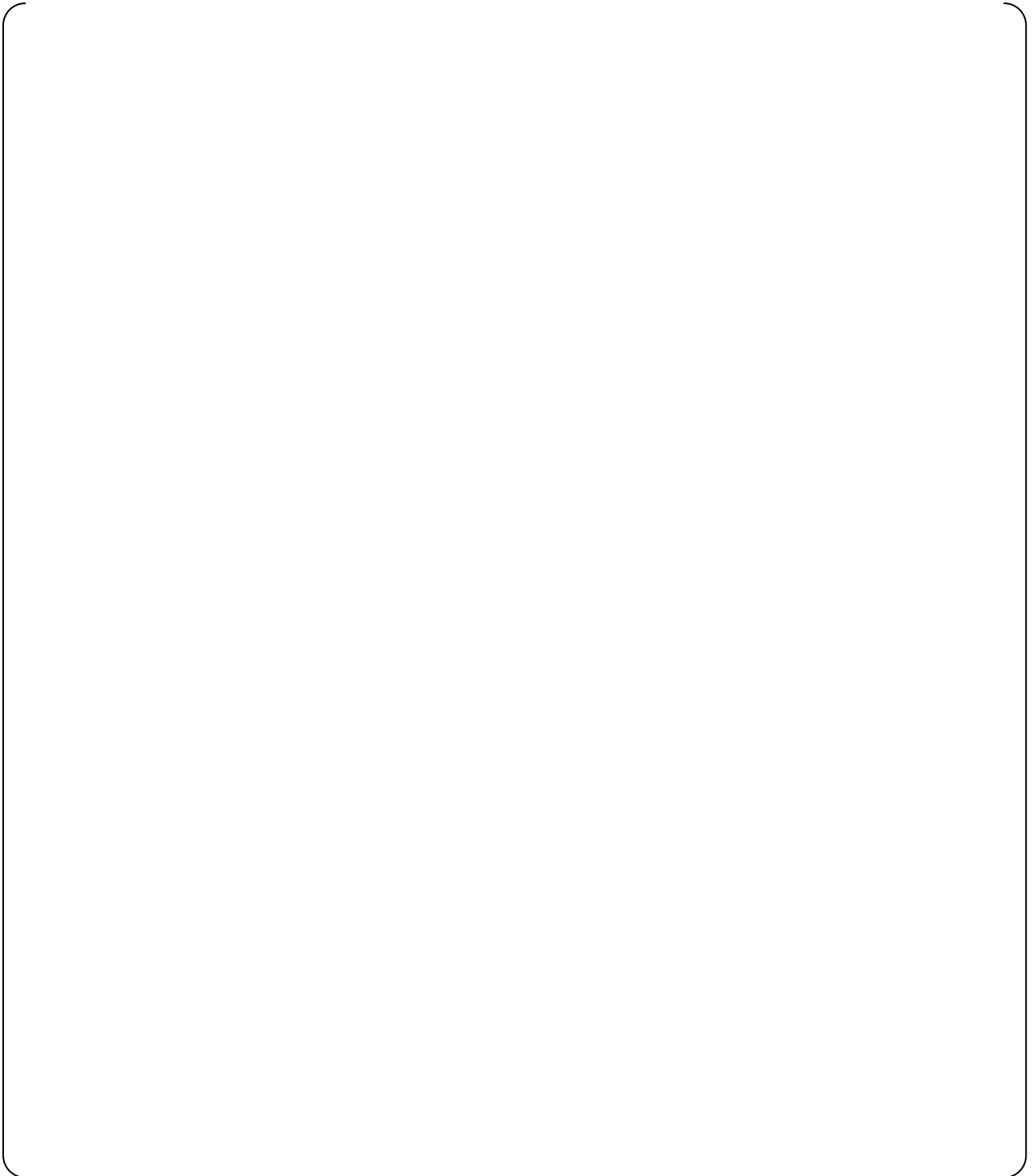
This document describes the measurement uncertainties in the test data measured by instruments.

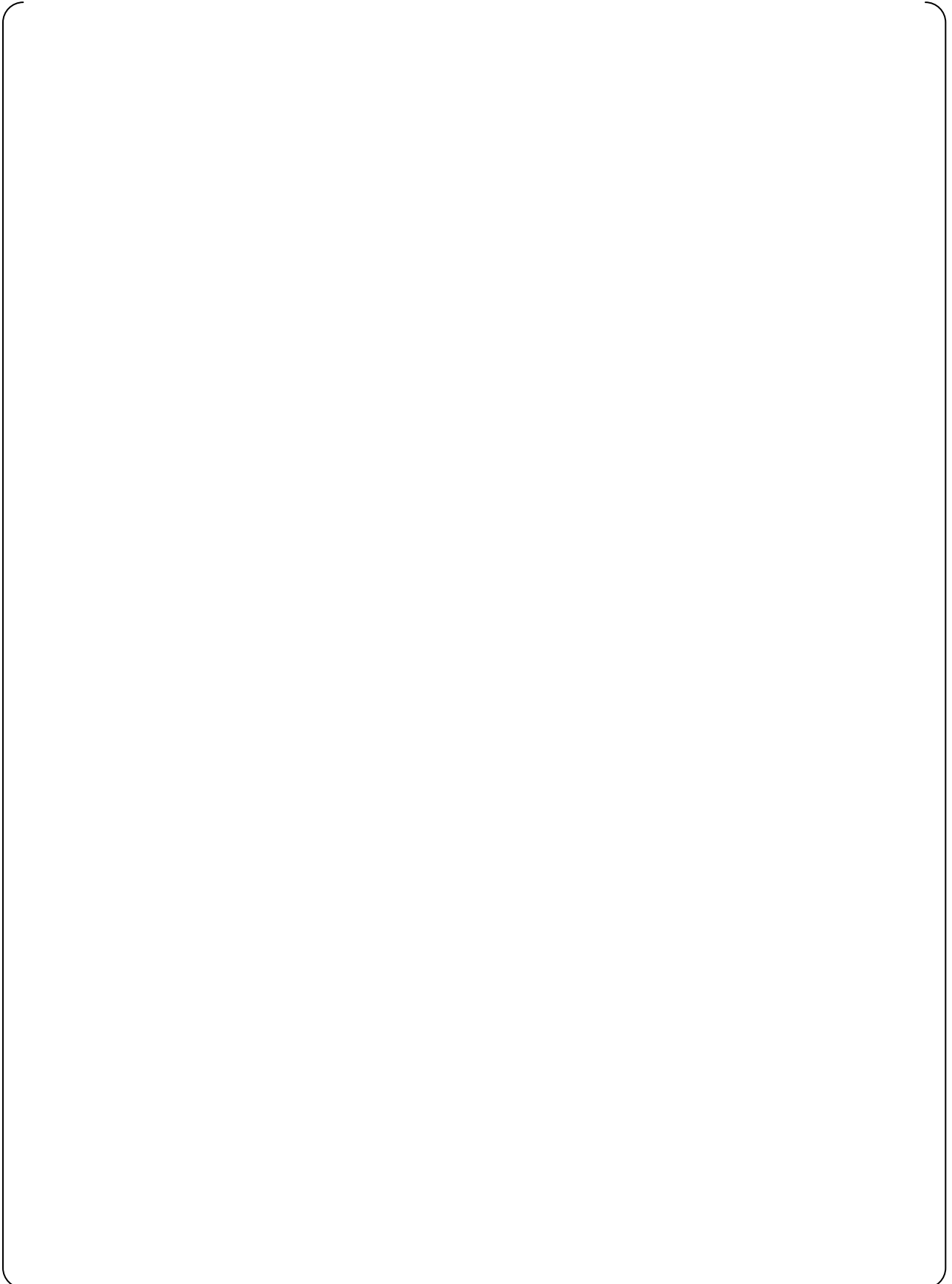
### **B.2 Concept of Uncertainty**

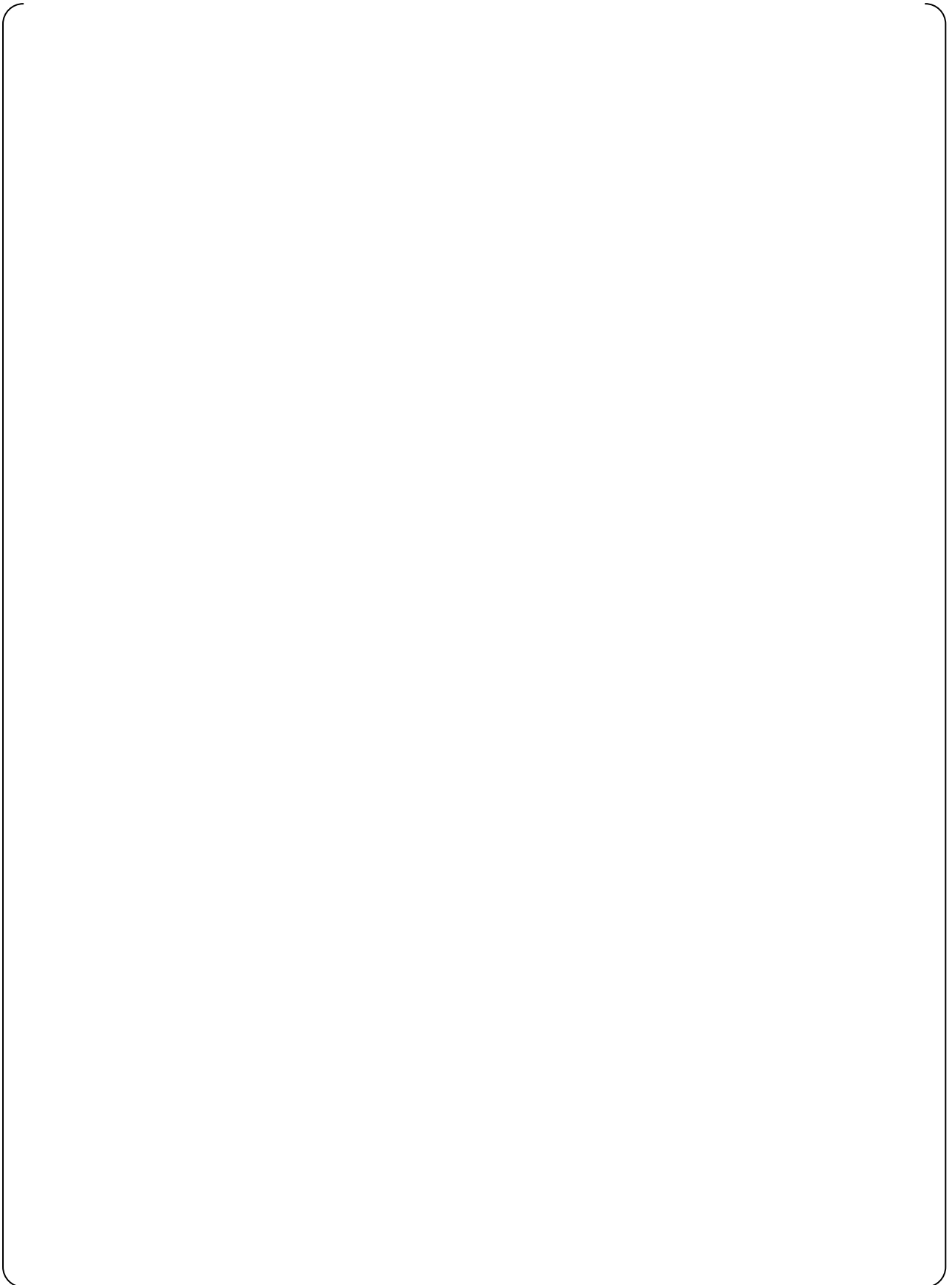


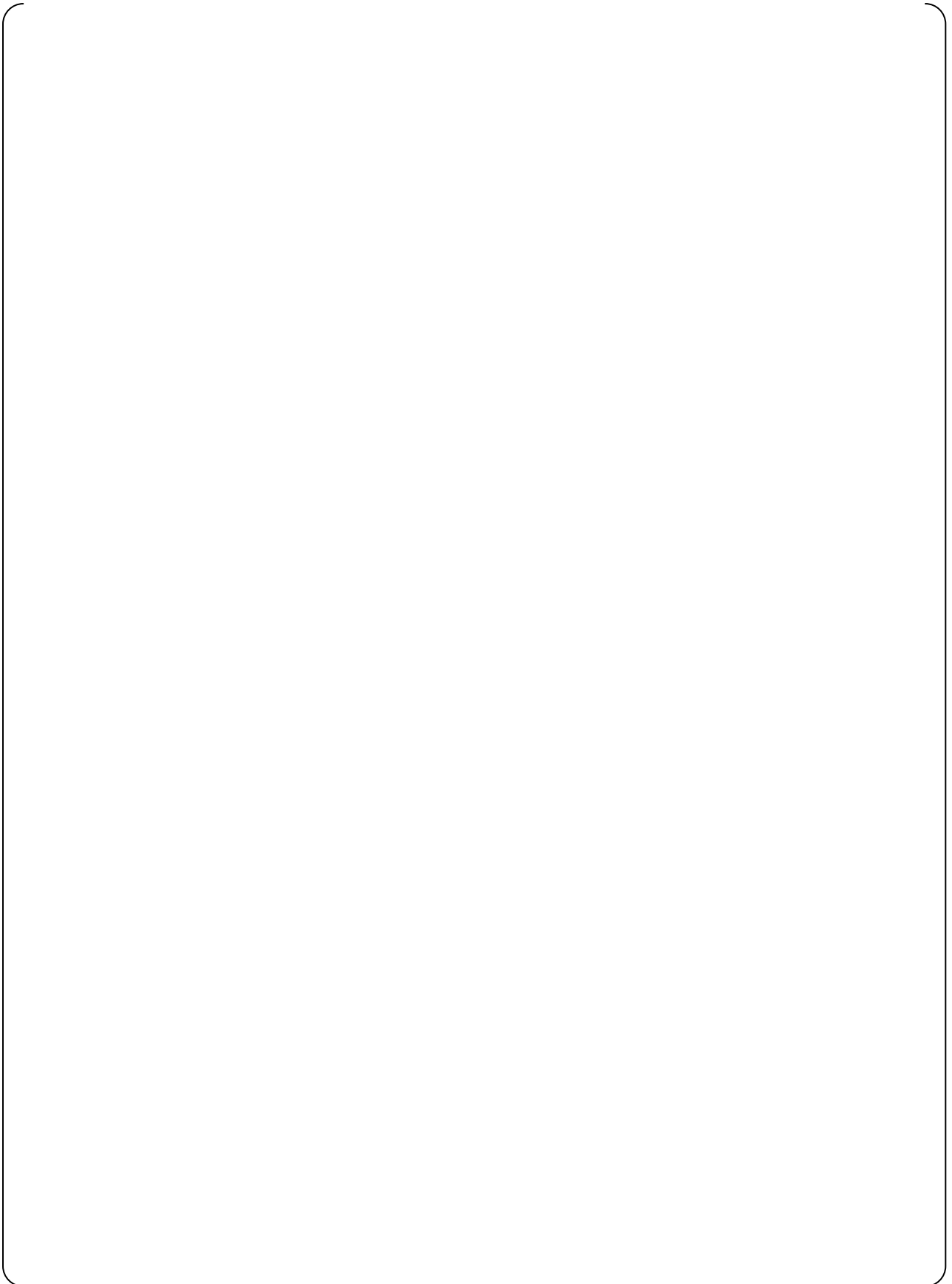


**B.3 Uncertainties of Measurement Systems**







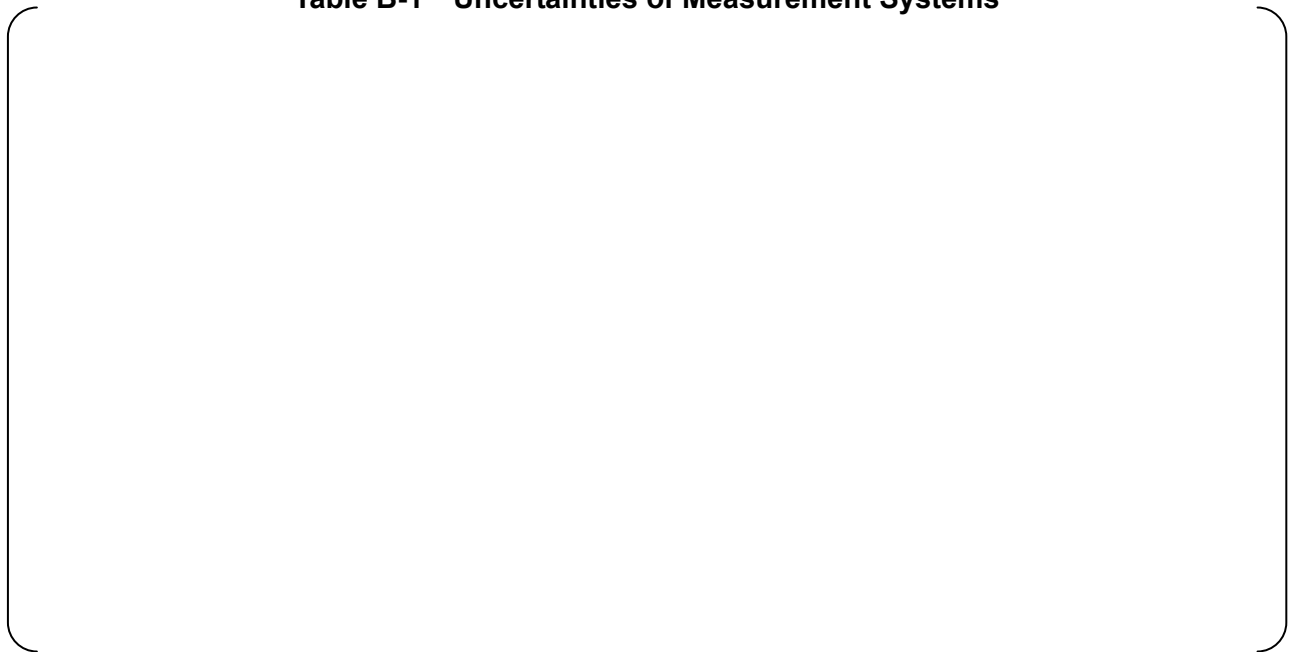




**B.4 Summary of Uncertainties**

The uncertainties of the measurement systems described in Section B.3 are summarized in Table B-1.

**Table B-1 Uncertainties of Measurement Systems**



## **APPENDIX C Sensitivity Analysis of US-APWR for NR Reflooding Test**

### **C.1 OBJECTIVE**

The thermal-hydraulic behavior in the NR of US-APWR can be affected by the conditions of the reflooding rate, inlet water temperature, initial metal temperature and pressure, whose ranges to be covered in the test should be confirmed through the sensitivity analysis using WCOBRA/TRAC(M1.0). The objective of this sensitivity analysis is to confirm the ranges of the reflooding rate, inlet water temperature, initial metal temperature and pressure in the NR of US-APWR during the reflooding phase in the LBLOCA scenario. The number of test runs and test conditions were appropriately determined based on an evaluation of the LBLOCA analysis results with the US-APWR plant parameters by WCOBRA/TRAC(M1.0).

### **C.2 MODEL DESCRIPTION AND ASSUMPTIONS**

#### **C.2.1 Nodalization**

The nodalization of US-APWR for the sensitivity analysis using WCOBRA/TRAC(M1.0) is the same as that described in Ref. C-1 and is briefly described as follows.

##### **(1) Vessel Model**



(2) **Core Model**

(3) **Loop Model**

### **C.2.2 Models of Plant Analysis for Sensitivity Analysis**

As described in Ref. C-1, the “Hot Wall” flow regime is more appropriate than the “Normal Wall” flow regime for the NR. A model to select either of the two flow regimes (Hot Wall and Normal Wall) depending on the wall temperature is implemented in the WCOBRA/TRAC(M1.0) code. The same model as the one described in Ref. C-1 is used about homologous pump curves for the US-APWR RCP and containment pressure calculation in the sensitivity analysis.

### **C.3 ANALYSIS CONDITIONS**

As discussed in Ref. C-1, the hot wall phenomena during the reflood phase in the NR is ranked “Medium” in the LBLOCA PIRT for US-APWR. The design of US-APWR is based on that of the conventional PWRs. Therefore, the thermal-hydraulic behavior during the LOCA for US-APWR is the same as that for a conventional 4-loop PWR. And during the reflood

---

phase, the NR will reflood in a similar manner as the core.

The thermal-hydraulic behavior during the reflood is influenced by the conditions at the time of Bottom of Core Recovery (BOCREC), which is influenced by the break size. Therefore, a sensitivity study on the break sizes was performed and the thermal-hydraulic conditions at which the reflood PCT becomes conservative were confirmed. The thermal-hydraulic behavior in the NR cooling hole is affected by the conditions of the reflooding rate, inlet water temperature, initial metal temperature and pressure. The thermal-hydraulic condition that core cooling becomes conservative was confirmed.

The conditions and assumptions for the major LOCA parameters used in the sensitivity analysis using WCOBRA/TRAC(M1.0) are listed in Table C-3.

#### **C.4 ANALYSIS RESULTS**

The cold leg break spectrum analysis for the double-ended guillotine break and split break cases were performed and the analysis results are summarized in Tables C-4 and C-5, respectively. Figure C-10 shows the variations of the reflood PCT with the equivalent break size for the two break types. The equivalent break size is defined as the product of the Coefficient of Discharge ( $C_d$ ) and the break area ( $A_{break}$ ) divided by the cold leg cross-sectional area ( $ACL$ ). Figures C-11 and C-12 show the transient behaviors of the PCT for the double-ended guillotine break and split break cases, respectively.

As shown in Figure C-10, the case of  $C_d=2.0$  produced the limiting reflood PCT for the double-ended guillotine break, whereas the case of  $C_d=2.8$  produced the limiting reflood PCT for the split break, and the limiting reflood PCT for the split break is lower than that for the double-ended guillotine break.

As an example of the representative, Figures C-13 shows the collapsed liquid levels in the Hot Assembly (HA) and NR channels with  $C_d=1.2$  for the Double-Ended Cold-Leg Guillotine (DECLG) break. [

]

Figure C-15 shows the integral of vapor mass flow rate at outlet of core and the NR. As seen in the figure, [

] Figure C-16 shows the sum of integral of liquid and entrainment mass flow rate at outlet of core and the NR. As seen in Figure C-15 and Figure C-16, [

].

The thermal-hydraulic behavior in the NR during the reflood phase has the potential to influence the PCT. Therefore, it is necessary to confirm the ranges of the parameters that may have influences on the thermal-hydraulic behavior in the NR based on cases of higher PCT during the reflood phase. Then, the range of the parameter was estimated by the case of break size larger than  $Cd \cdot A_{break} / ACL = 2.0$ .

#### C.4.1 NR Reflooding Rate

The NR reflooding velocity was confirmed by approximating the slopes of the time integrals of the velocity at the NR inlet for all cases. As described in paragraph C4, the significant vapor and entrainment generation occurs in the NR during the first 120 seconds after BOCREC. Therefore, the integration of the velocity was divided into two sections of before PCT and around PCT. Figures C-17 shows the time integrals of the velocity at the NR inlet and their approximate slopes with all cases. As seen in Figure C-17, the NR reflooding velocity was larger than about [ ] around the time of the PCT occurrence. The range of the NR reflooding velocity was confirmed to be [ ]. Therefore, the test condition of NR reflooding rate was set to [

] which covers sufficiently the range of NR reflooding velocity shown in Figure C-17. Then the NR reflooding velocity for the reference test case was set to [ ] as bounding condition because larger velocity leads metal heat release to be large.

#### C.4.2 Initial Temperature of NR

In the sensitivity analysis, the maximum temperature of the NR ([ ]) assumed as a design value was used as the initial temperature of the NR. As shown in Figures C-18, the NR temperature at BOCREC was [ ]. The NR temperature decreased by only about [ ] during the blowdown phase, and the axial distribution of the initial NR temperature was maintained. Therefore, the NR will be cooled mainly during the reflood phase.

The range of the NR temperature for the test condition was set [ ], which covers the analysis results during the blowdown phase and at the beginning of the reflooding phase. The initial NR temperature for the reference test case was set to [ ] as higher-side temperature that includes some margin for the design value of [ ]. The lower-side temperature of the test condition was set to [ ] to obtain the range of sensitivity, which includes some margin for Tcold of [ ].

### C.4.3 Reflooding Water Temperature

Figures C-19 and C-20 show the temperature of the water in a lower plenum cell that is the nearest to the reactor core for cases with DECLG and split break, respectively. The range of the reflooding water temperature was [ ] after BOCREC as shown in Figures C-19 and C-20. The representative reflooding water temperature as the higher-side temperature of the test condition was set to [ ] as round value of the average reflooding water temperature. The higher-side temperature of [ ] has sub-cooling of [ ] under reference pressure condition of [ ] shown in Table C-6. The lower-side temperature of the test condition was set to [ ] to obtain the range of sensitivity, which has sub-cooling of [ ], i.e., three times the sub-cooling of [ ].

### C.4.4 Pressure

Figures C-21 and C-22 show the pressures at the outlet of the NR for cases with DECLG and split break, respectively. The pressure of the reference test case was set to [ ] because the lower-side pressure lasted longer than the higher-side pressure as shown in Figures C-21 and C-22. The higher-side pressure was set to [ ] psia that range of the result of Figure C-21 and C-22 were able to be covered all the cases except  $Cd \cdot A_{break} / ACL = 2.0$ .

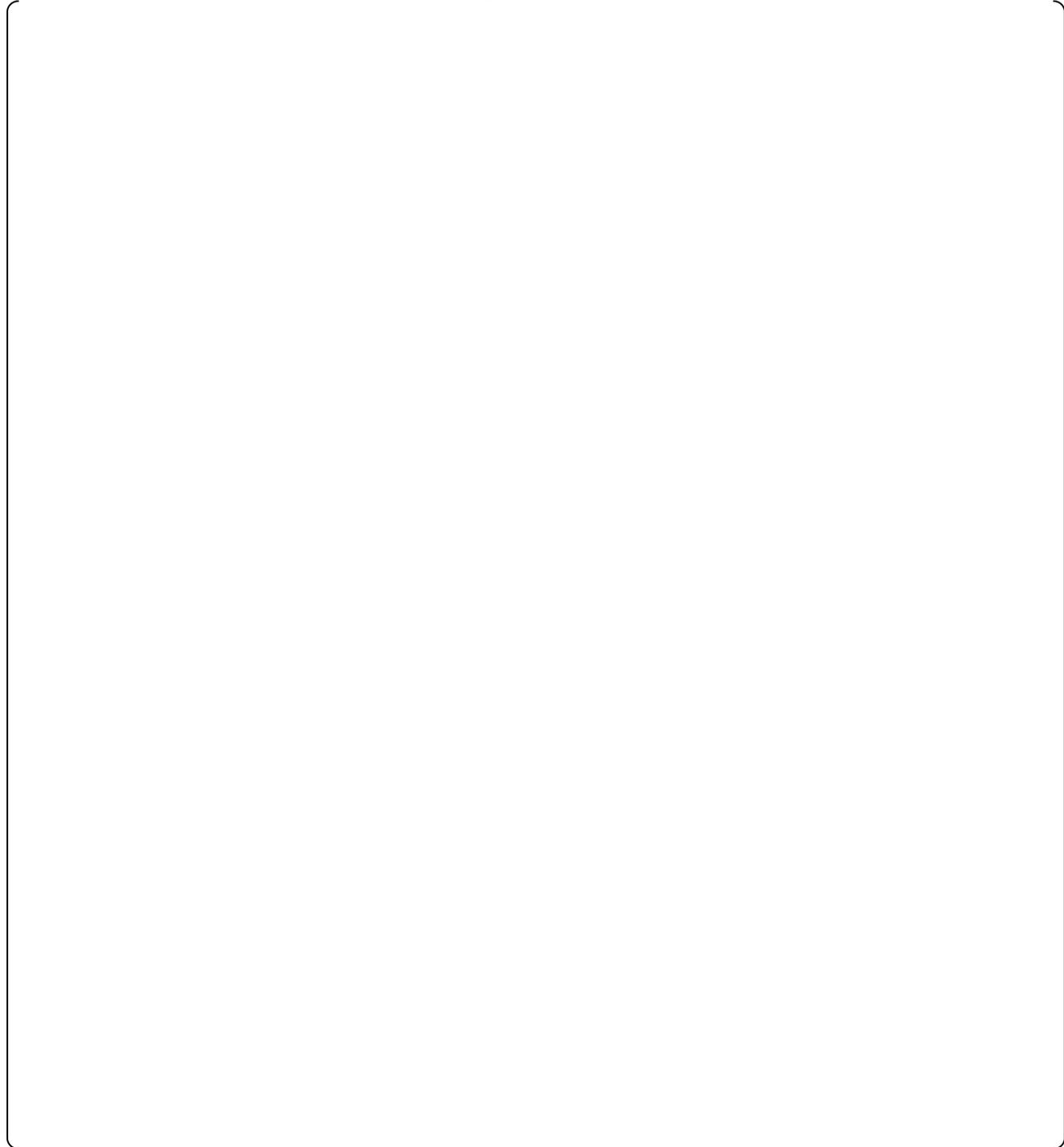
## C.5 SUMMARY

The sensitivity analyses using WCOBRA/TRAC(M1.0) were performed. The ranges of the key parameters that may have influences on the thermal-hydraulic behavior in the NR were confirmed by the sensitivity analysis results. The ranges of the key parameters used as the test conditions are summarized in Table C-6.

**C.6 REFERENCES**

- C-1. Suzuta, T. and Teramae, T., "Large Break LOCA Code Applicability Report for US-APWR," MUAP-07011-P(R0), Mitsubishi Heavy Industries, Ltd., July 2007.

**Table C-1 Channel Descriptions for US-APWR Vessel Model (1/3)**

A large, empty rectangular frame with rounded corners, intended for the table content. The frame is currently blank.

**Table C-1 Channel Descriptions for US-APWR Vessel Model (2/3)**

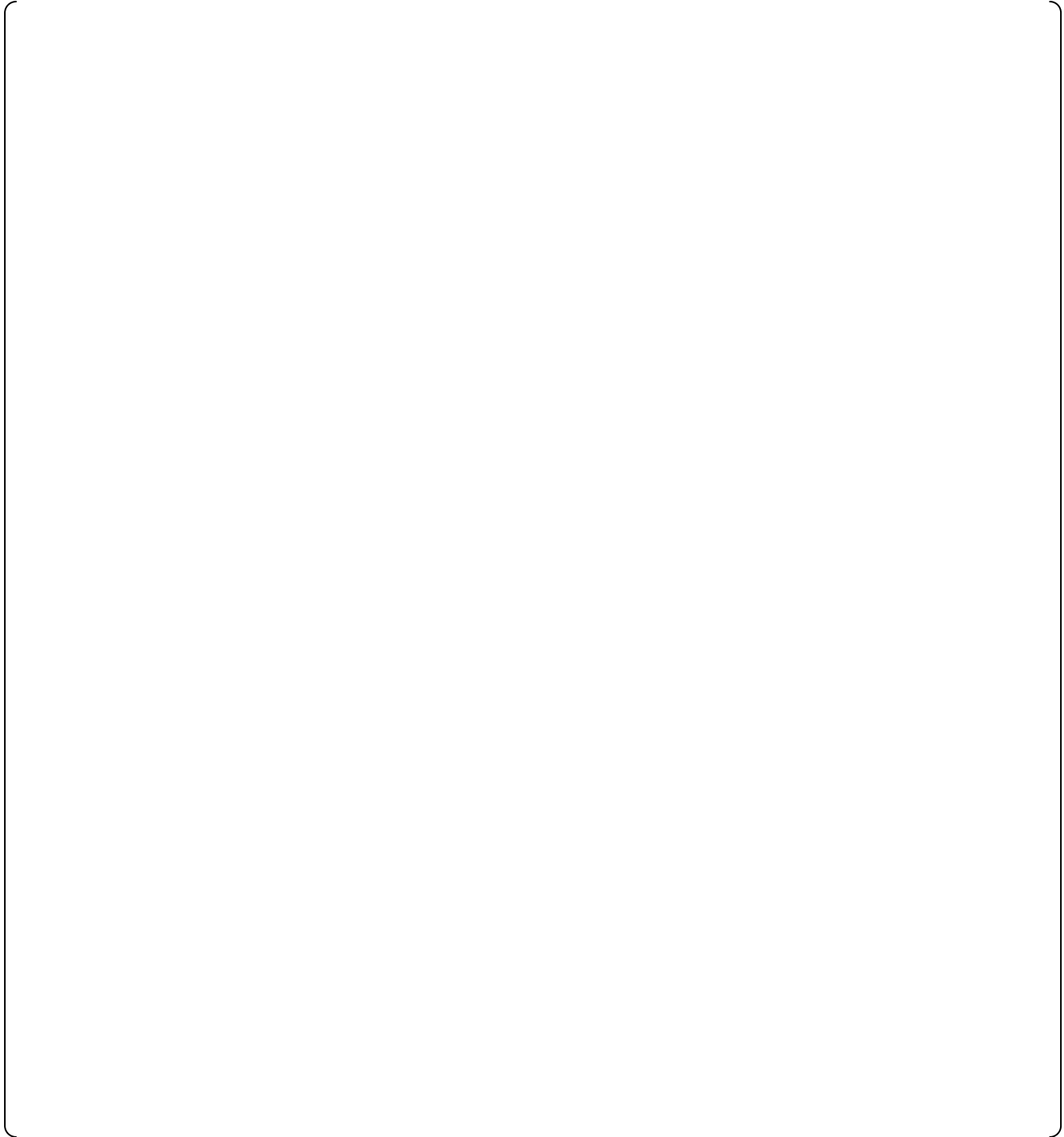


**Table C-1 Channel Descriptions for US-APWR Vessel Model (3/3)**



**Table C-2 Gap Connections for US-APWR Vessel Model (1/2)**

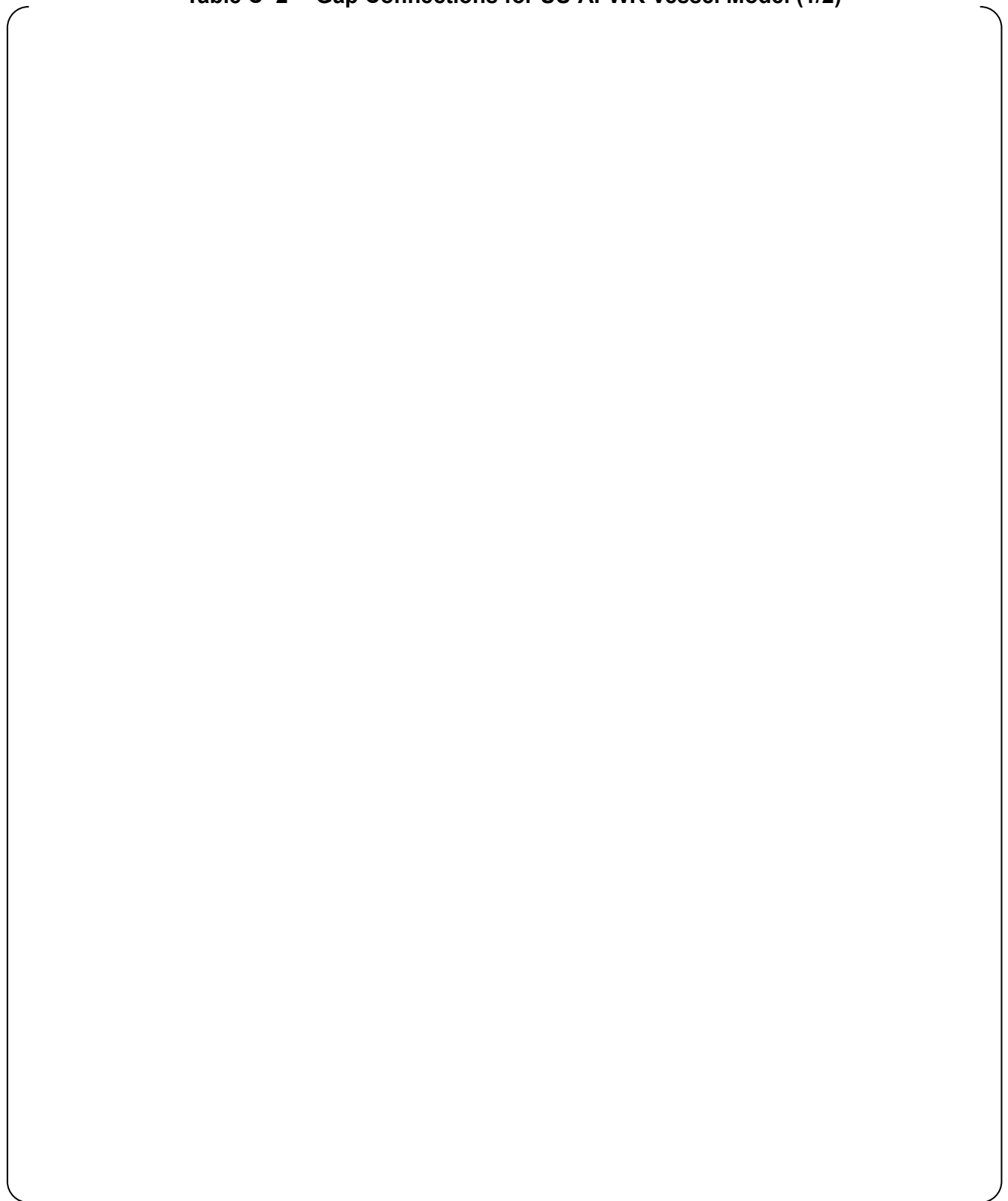


**Table C-2 Gap Connections for US-APWR Vessel Model (2/2)**



**Table C-3 Conditions for Sensitivity Analysis**

<b>Parameter</b>	<b>Values</b>
<b>Plant physical configuration</b>	
Fraction of SG tube plugged	10% (maximum)
Hot assembly location	Under the open hole
<b>Power-related Parameters</b>	
Core power	4451MWt (100%)
Peaking factor ( $F_Q$ )	2.6
Axial power distribution	Top skewed (Figure C-9)
Peripheral assembly power	0.2 (lower bound)
Hot assembly burnup	Beginning of life (BOL)
Fuel assembly type	17 X 17 ZIRLO™ cladding
<b>Initial RCS Fluid Condition</b>	
RCS average temperature	583.8°F
Pressurizer pressure	2250 psia
Primary coolant flow	112,000 gpm/loop (thermal design flow)
Accumulator temperature	95°F
Accumulator pressure	655 psia
Accumulator water volume	2152 ft <sup>3</sup>
<b>Accident Boundary Condition</b>	
Break location	Cold leg (in the loop with pressurizer)
Break type	Double-ended guillotine break Split break
Discharge coefficient	Cd=0.8,1.0,1.2,1.4 for Guillotine Cd=~1.4 for Split
Offsite Power	Not available
Number of SI pumps available	2
Safety Injection flow rate	Minimum
Safety Injection temperature	76°F
Safety Injection delay	118 sec
Containment pressure	Bounded (minimum)

**Table C-4 PCTs Calculated by WCOBRA/TRAC(M1.0) for Sensitivity Analysis (DECLG)**

	Cd*Abreak/ACL			
Reflood PCT (°F)				
Reflood PCT Occurrence Time (sec)				
Reflood PCT Position (ft)				
BOCREC Time (sec)				

**Table C-5 PCTs Calculated by WCOBRA/TRAC(M1.0) for Sensitivity Analysis (SPLIT)**

	Cd*Abreak/ACL			
Reflood PCT (°F)				
Reflood PCT Occurrence Time (sec)				
Reflood PCT Position (ft)				
BOCREC Time (sec)				

**Table C-6 Summary of Conditions for NR Reflooding Test**

Parameter	Range
Reflooding Rate	
Initial Metal Temperature	
Reflooding Water Temperature	
Pressure	

\*: Reference case test condition

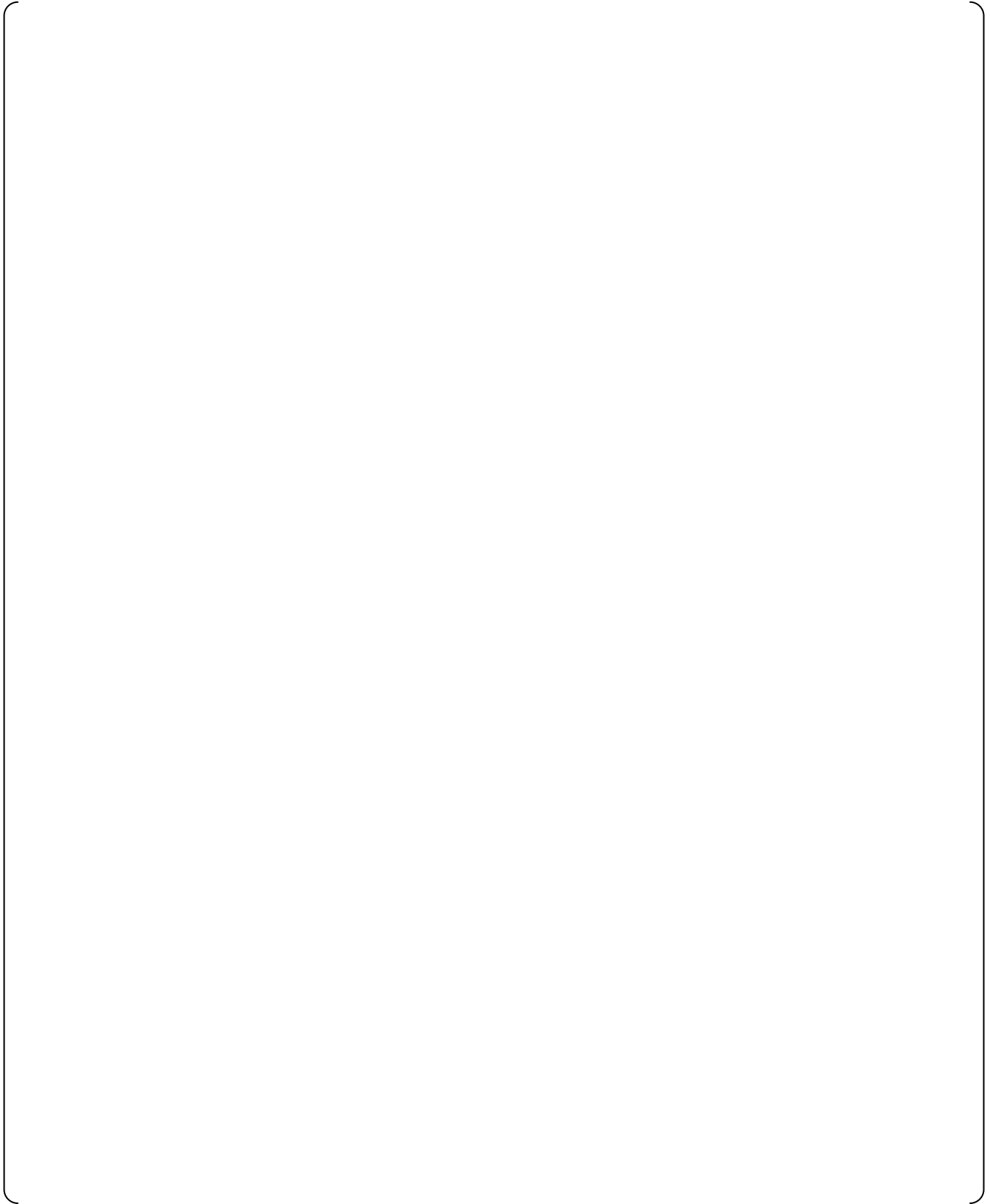


**Figure C-1 US-APWR Vessel (Vertical View)**

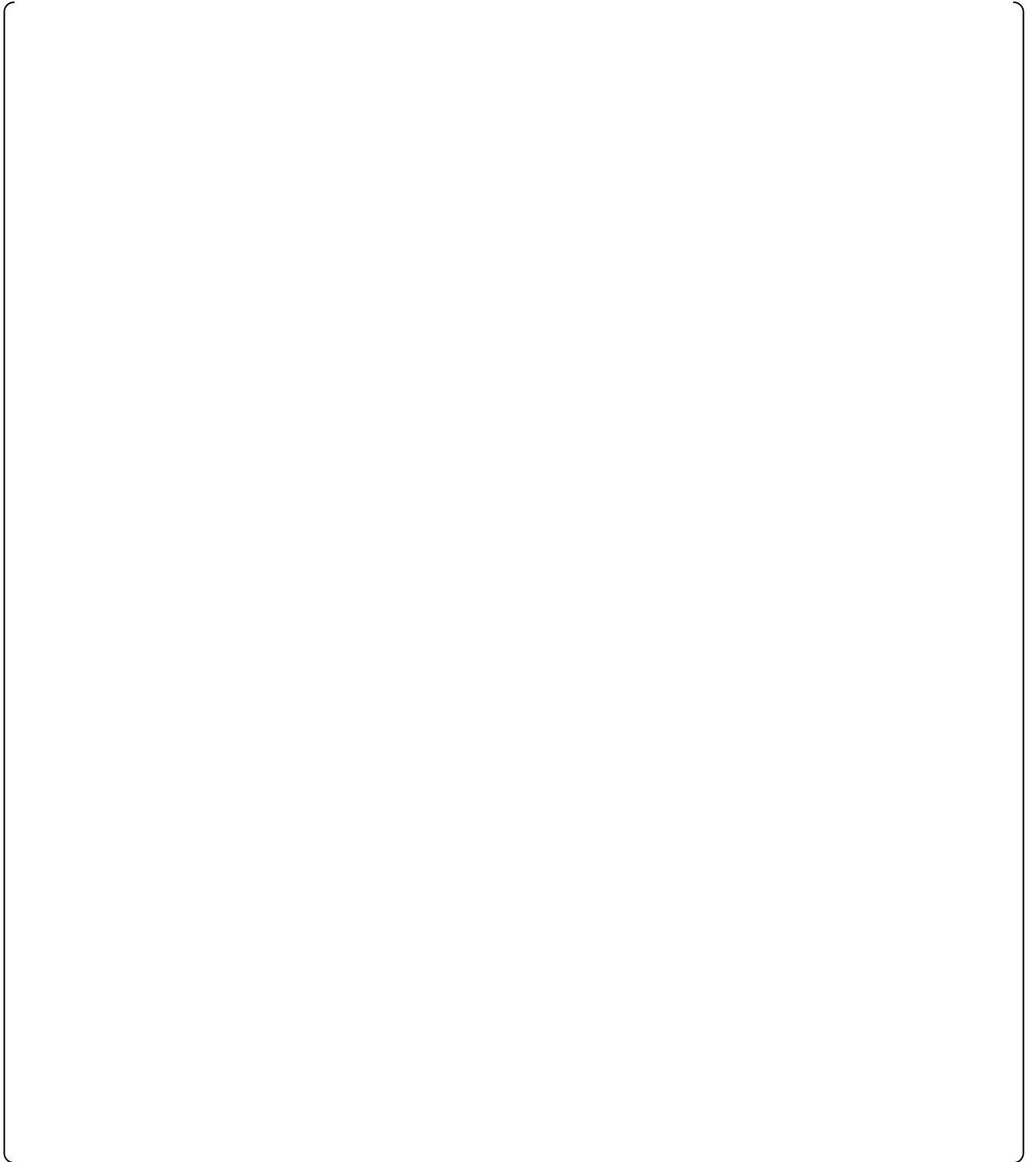


**Figure C-2 US-APWR Vessel Noding for Hot Assembly Under Open Hole  
(Vertical View)**

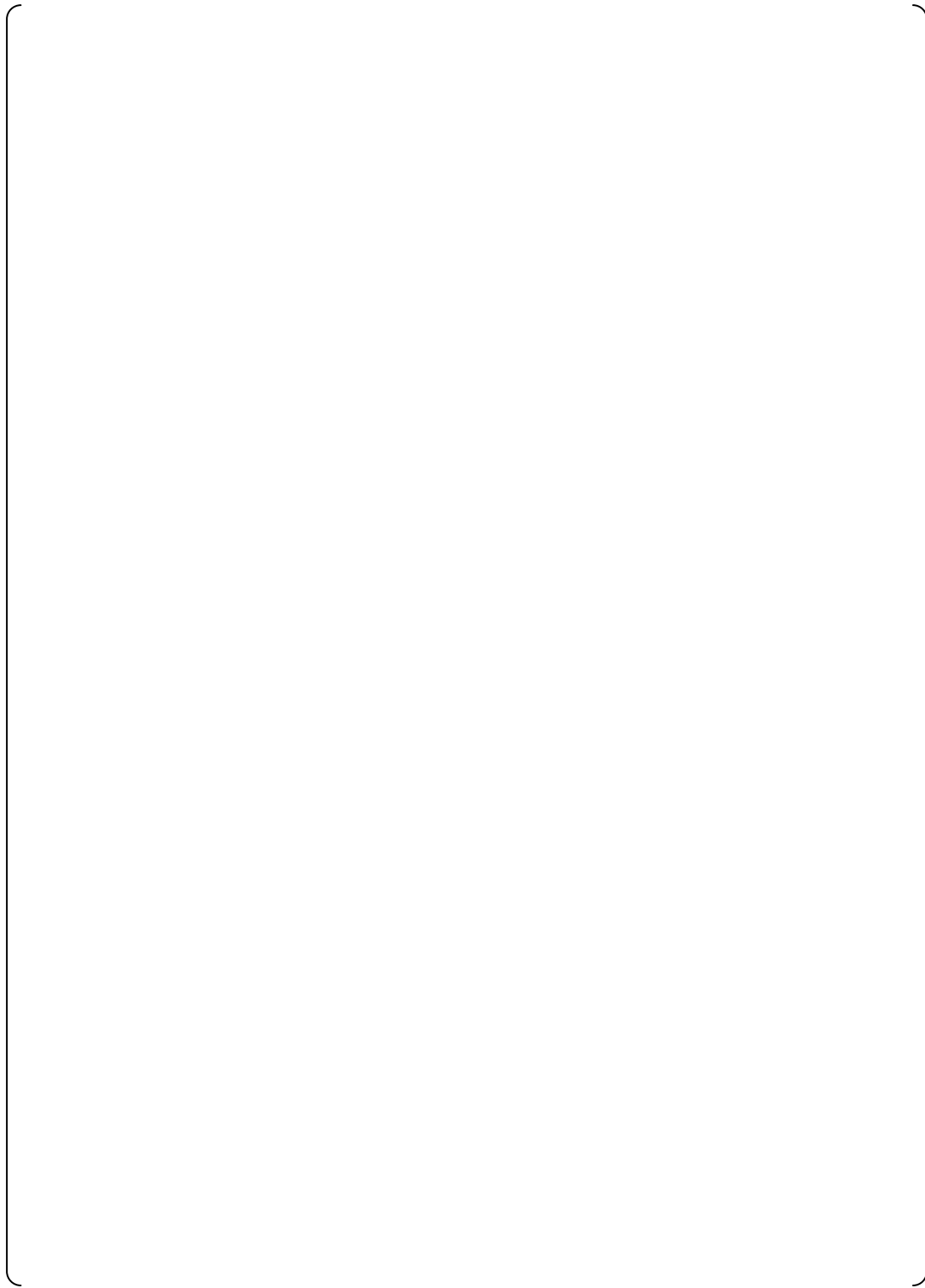


**Figure C-3 US-APWR Vessel Sections 1 to 2 (Horizontal View)**

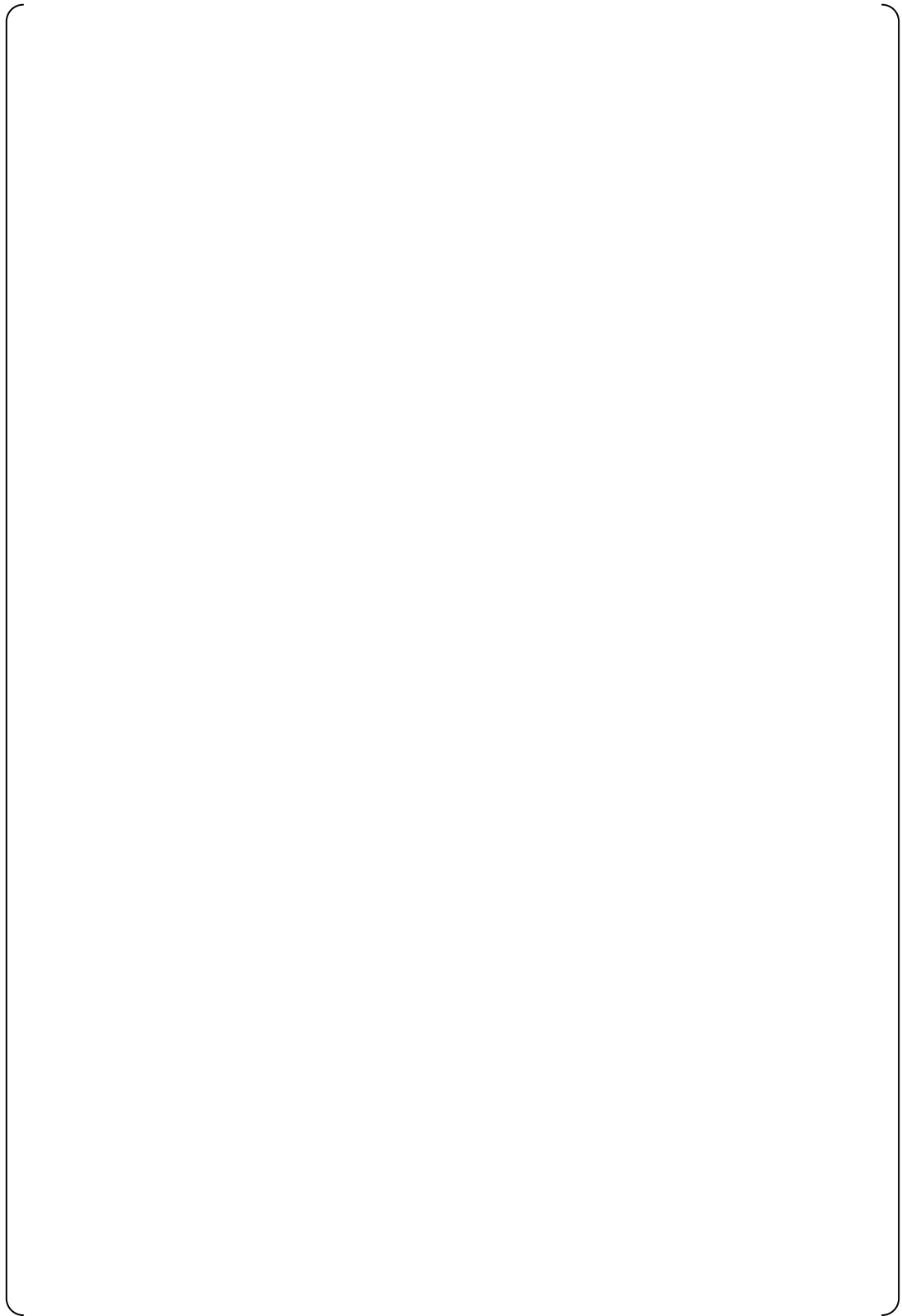


**Figure C-4 US-APWR Vessel Sections 3 to 4 (Horizontal View)**

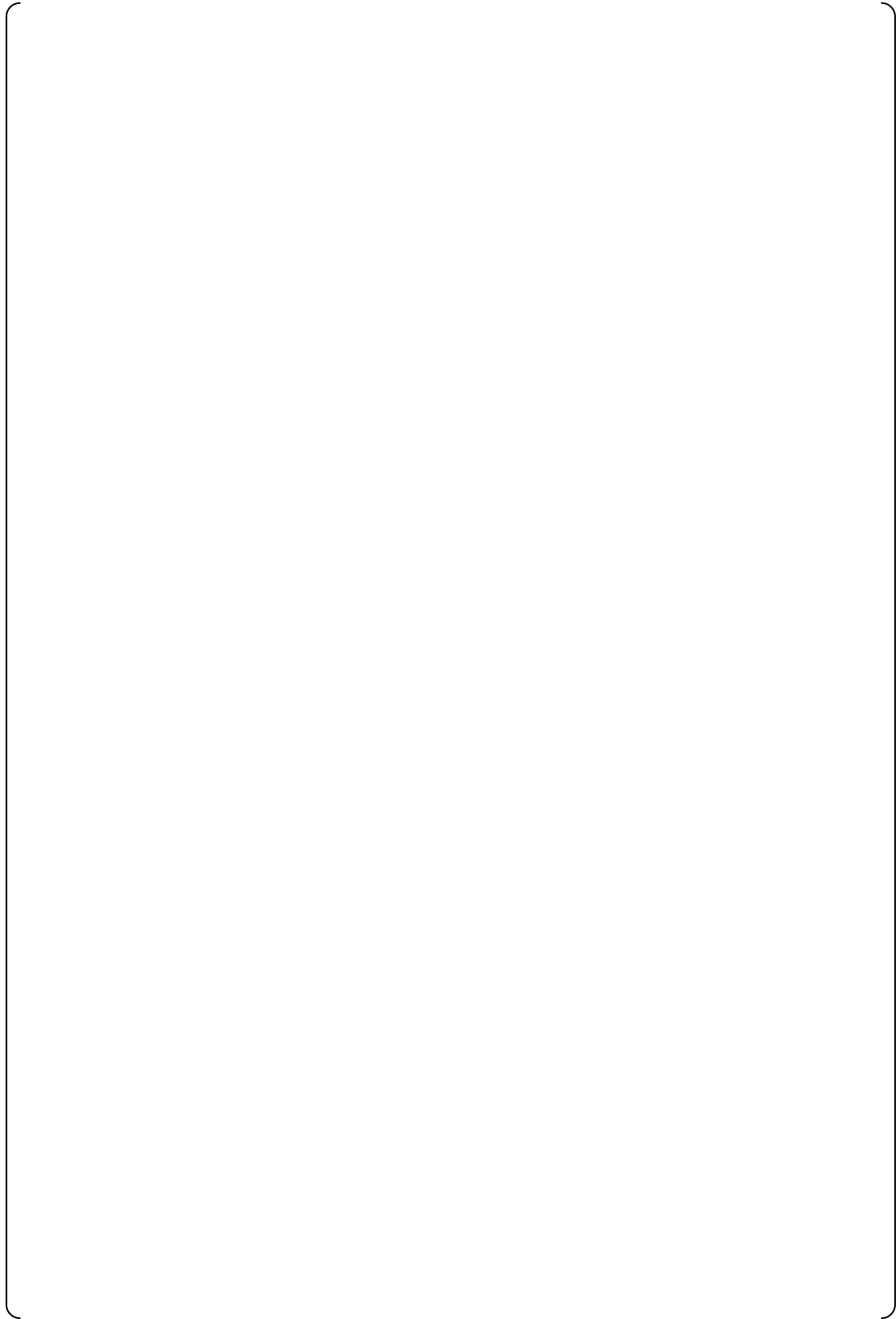


**Figure C-5 US-APWR Vessel Sections 5 to 6 (Horizontal View)**

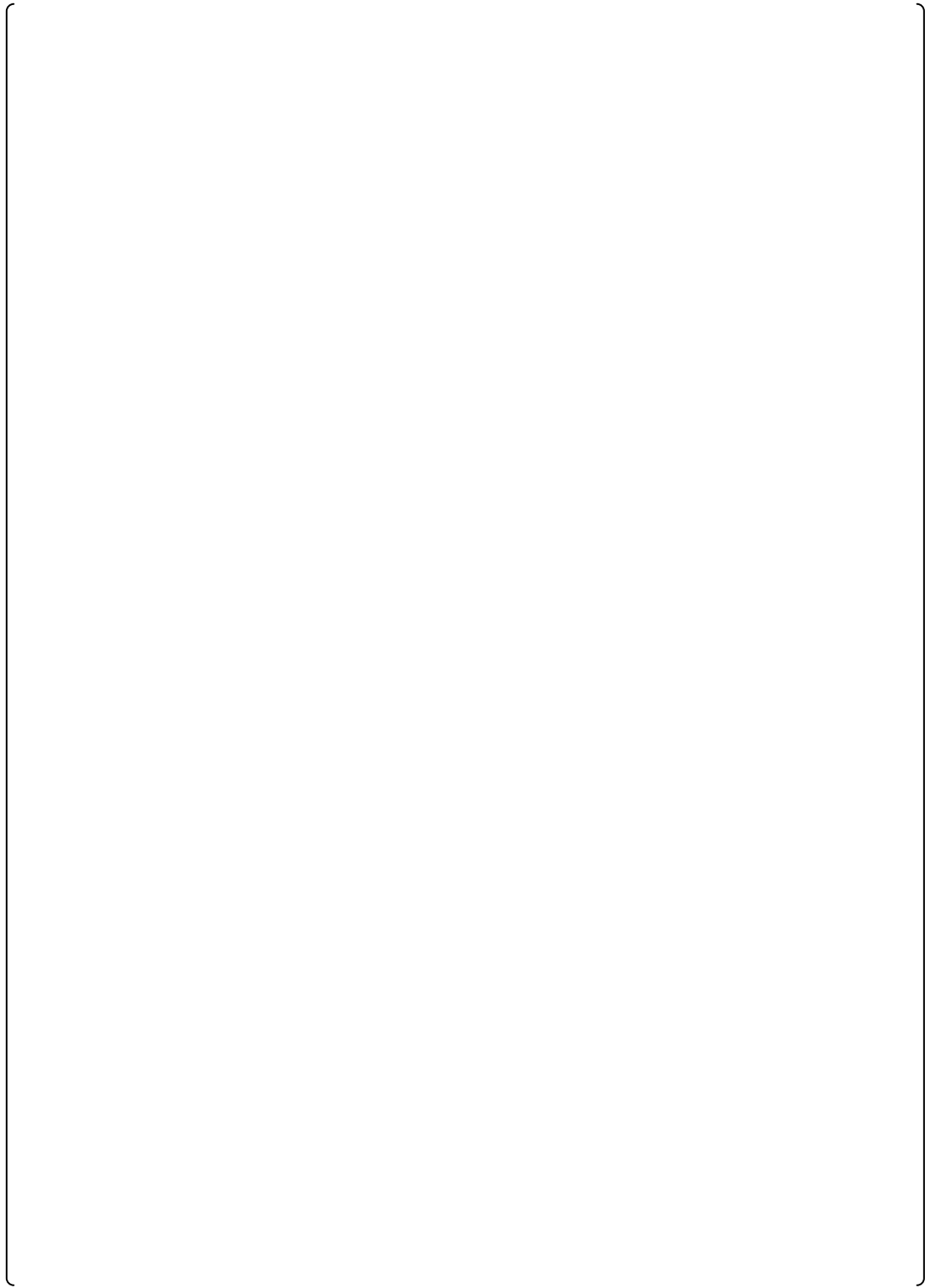


**Figure C-6 US-APWR Vessel Sections 7 to 8 (Horizontal View)**

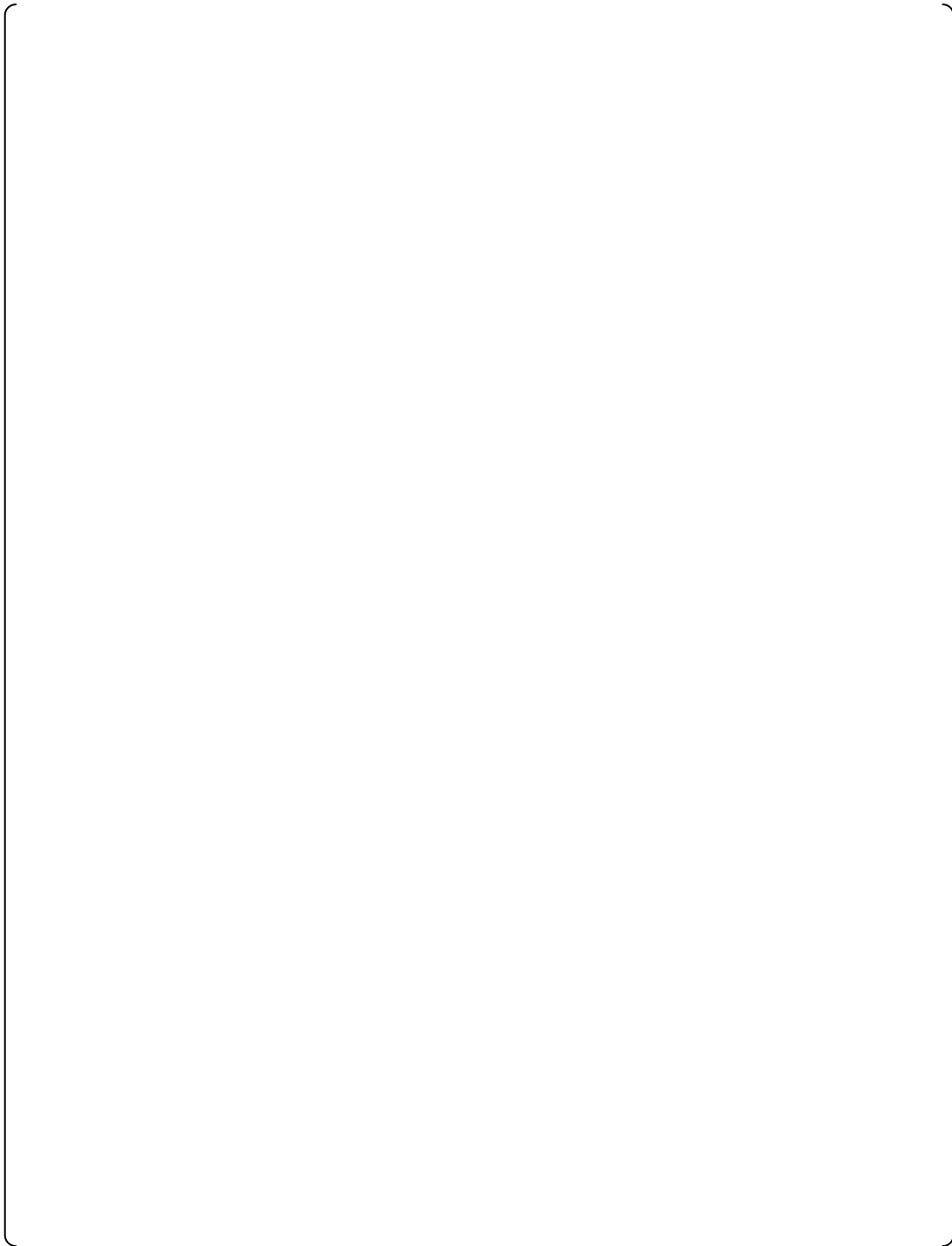


**Figure C-7 US-APWR Vessel Sections 9 to 10 (Horizontal View)**

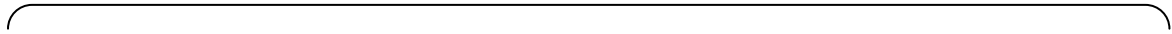


**Figure C-8 US-APWR WCOBRA/TRAC(M1.0) Model Vessel/Loop Layout**





**Figure C-9 Power Shape for Sensitivity Analysis**



**Figure C-10 Reflood PCT versus Equivalent Break Size**

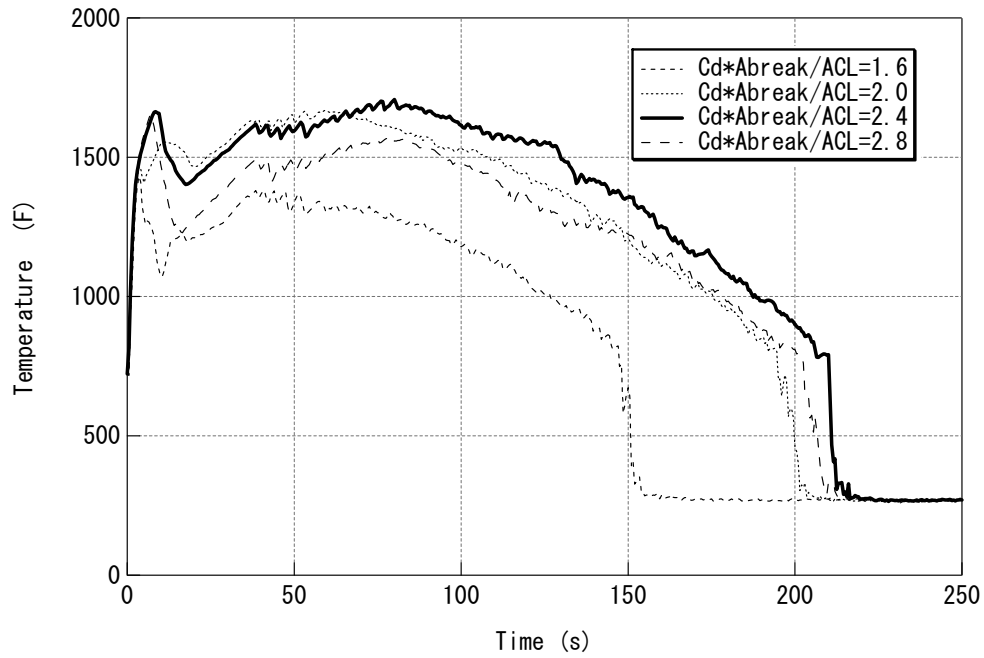


Figure C-11 Peak Cladding Temperature of Hot Rod (DECLG)

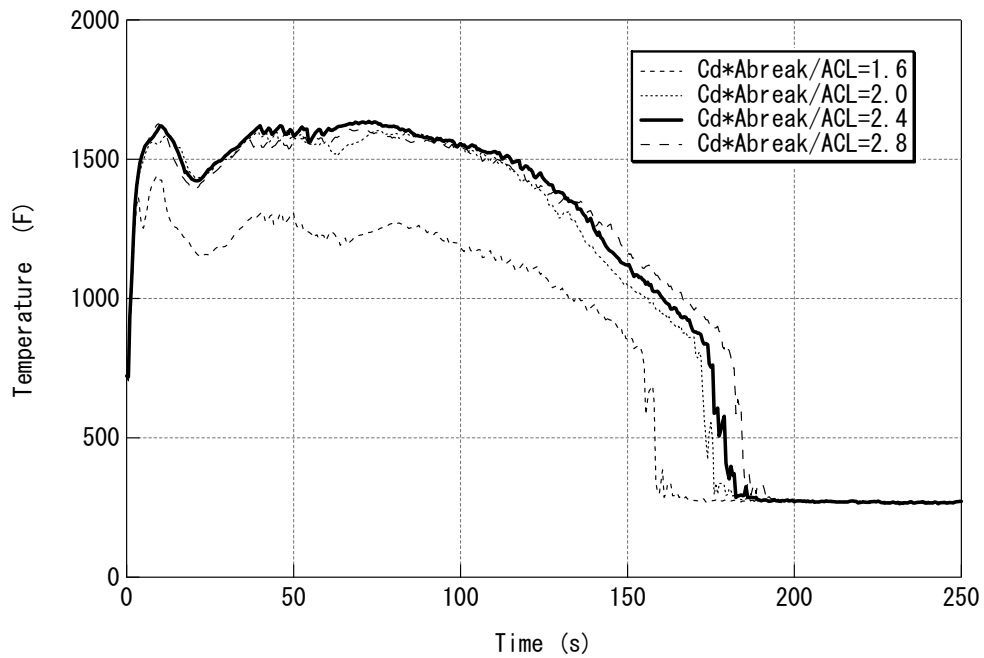
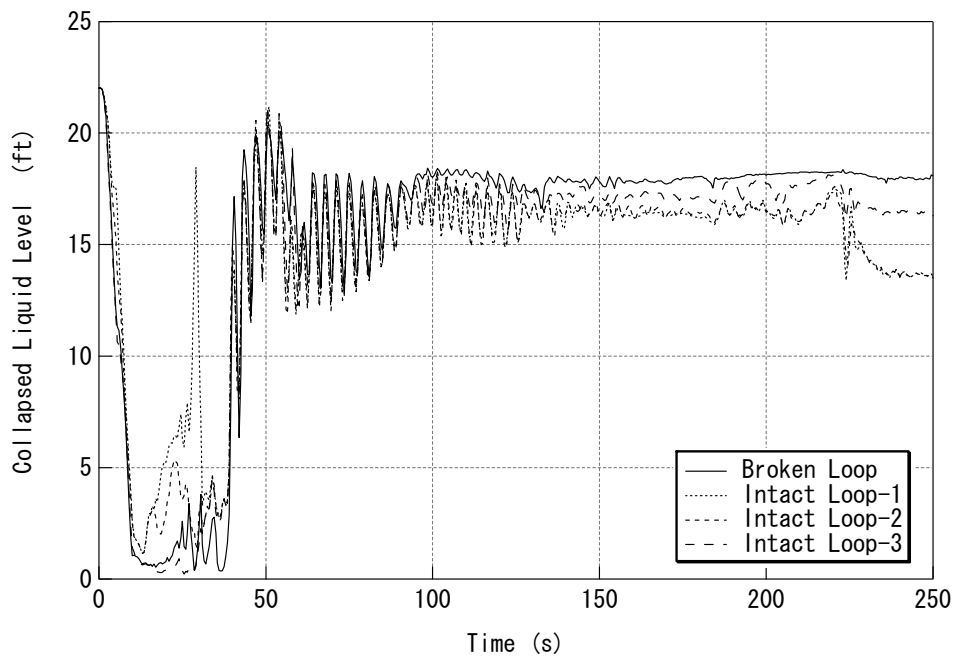


Figure C-12 Peak Cladding Temperature of Hot Rod (SPLIT)



**Figure C-13 Hot Assembly and NR Liquid Level ( $Cd \cdot A_{break} / ACL = 2.4$  DECLG)**



**Figure C-14 Downcomer Liquid Level ( $Cd \cdot A_{break} / ACL = 2.4$  DECLG)**



**Figure C-15 Integral of Vapor Mass Flow Rate at Core and NR Outlet  
(Cd\*Abreak/ACL=2.4 DECLG)**



**Figure C-16 Integral of Entrainment and Liquid Mass Flow Rate at Core and NR  
Outlet (Cd\*Abreak/ACL=2.4 DECLG)**



**Figure C-17 Integral of Velocity at Inlet of NR**

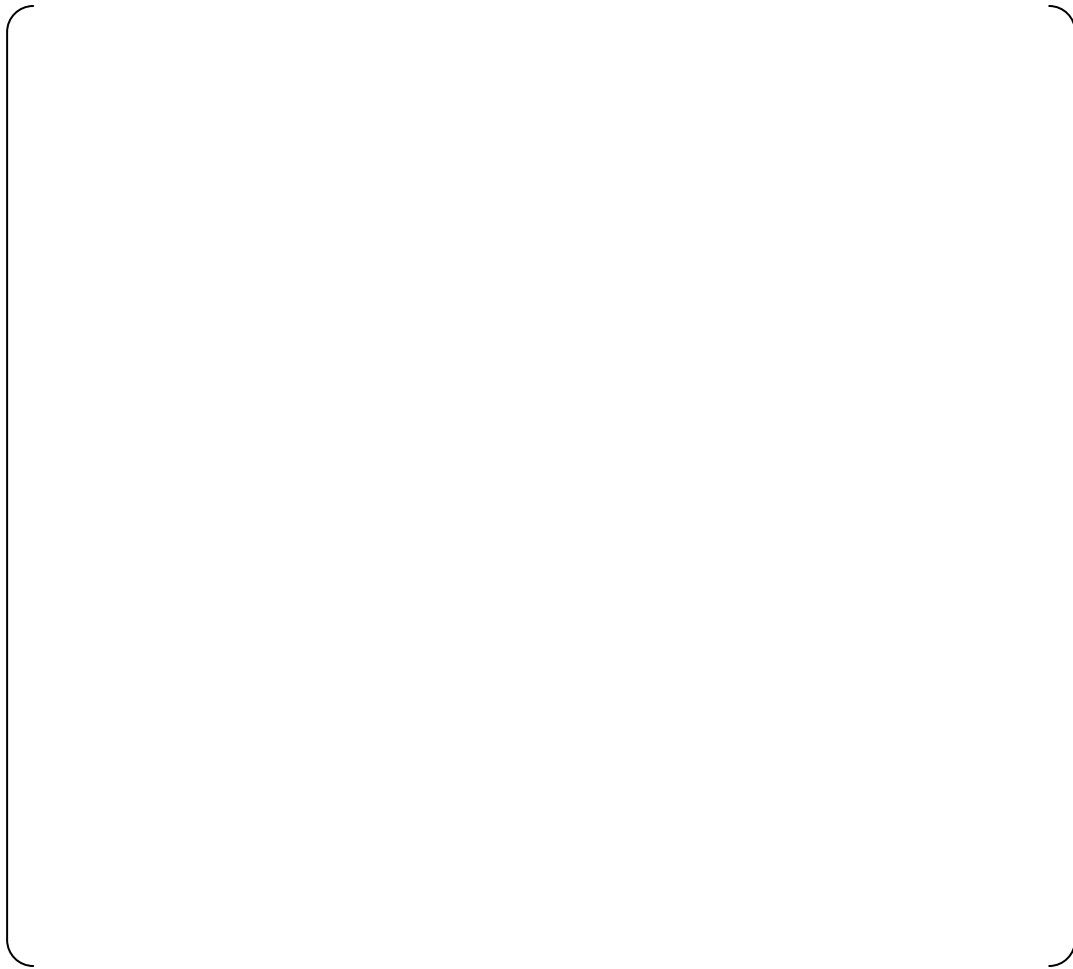


**Figure C-18 NR Wall Temperature**



**Figure C-19 Lower Plenum Water Temperature (DECLG)**



**Figure C-20 Lower Plenum Water Temperature (SPLIT)**



**Figure C-21 NR Outlet Pressure (DECLG)**



**Figure C-22 NR Outlet Pressure (SPLIT)**